Mechanistic Insight Into Replication Fork Reversal Under Genotoxic Stress.

Dissertation zur

Erlangung der naturwissenschaftlichen Doktorwürde

(Dr. sc. nat.)

vorgelegt der

Mathematisch-naturwissenschaftlichen Fakultät der

Universität Zürich von

Marko Vujanovic

aus Serbien

Promotionskomitee

Prof. Massimo Lopes (Vorsitz und Leitung der Dissertation)

Prof. Simon Boulton

Prof. Petr Cejka

Prof. Pietro Pichierri

Zürich, 2016

Table of Contents

Zusammenfassung **5**

Summary **7**

1. Introduction **8**

1.1 DNA replication **8**

1.1.1 General concepts of replication in eukaryotes 8

1.1.2 Initiation of DNA replication 8

1.1.3 Origin activation and chain elongation. 11

1.1.4 Termination of DNA replication 14

1.2 DNA damage and repair mechanisms. **16**

1.2.1 DNA damage and consequences. 16

1.2.2 DNA damage repair mechanisms. 17

1.2.3 DNA damage tolerance (DTT) pathways 19

1.2.3.1 Translesion synthesis (TLS) 21

1.2.3.2 Template switching mechanisms 25

1.3 Replication stress. **28**

1.3.1 Definition and detection of replication stress. 28

1.3.2 Sources of replication stress. 29

1.4 Replication fork reversal **31**

1.4.1 Definition. 31

1.4.2 Replication fork reversal - a friend or a foe? 36

1.4.3. Protein(s) potentially involved in replication fork reversal. 38

1.5 Proliferative Cell Nuclear Antigen (PCNA) and the role in DNA damage response. **42**

2. Results **46**

2.1 Downregulation of ZRANB3 rescues replication fork speed **46**

2.2 Downregulation of ZRANB3 leads to impaired replication fork formation **49**

2.3 ZRANB3 knock out cells **50**

2.3.1 ZRANB3 KO cells show no fork slowdown upon genotoxic treatment 50

2.3.2 ZRANB3 KO cells show impaired reversed fork formation 51

2.4 Generation of stable cell lines **53**

2.4.1. NZF, PIP&APIM and HD mutant show no fork slowdown upon genotoxic treatment. 56

2.4.2. NZF, PIP&APIM and HD mutant show no fork slowdown upon genotoxic treatment 57

2.5. PCNA and ubiquitin mutants **59**

2.5.1 PCNA 164K mutant mouse embryonic fibroblasts 59

2.5.2 Mutating K164 in PCNA abolishes replication fork slowing upon DNA damage. 60

2.5.3 PCNA K164 mutant shows defective replication fork reversal upon genotoxic treatments 61

2.5.4 Inducible replacement of endogenous ubiquitin with a K63 mutant 62

2.6 Ubc13 downregulation **64**

2.6.1 Upon UBC13 downregulation there is partial rescue of the replication fork speed 65

2.6.2 Ubc13 depletion leads to ineffective fork reversal induced by genotoxic agents 65

2.7 Ubc13 knock out cells **66**

2.7.1 Ubc13 KO cells have unrestrained replication fork progression upon low doses genotoxic treatment 67

2.7.2 Ubc13 KO cells fail to increase the frequency of reversed replication forks upon genotoxic treatments 68

2.8. Additional experiments **69**

2.8.1 Werner syndrome protein 69

2.8.2 HARP (SMARCAL1) 70

2.8.2.1. Depletion of Harp impairs reduction of replication fork speed upon mild CPT treatments. 71

2.8.2.2. Harp depletion leads to partial decrease in reversed fork frequency upon genotoxic treatment. 72

2.9. Following polyubiquitination of PCNA with Western Blot and Chromatin enrichment. **73**

2.10 Contribution to collaborative projects with the lab of Prof. Alessandro Vindigni (Department of Biochemistry and Molecular Biology, Edward A. Doisy Research Center, Saint Louis University School of Medicine, St. Louis, USA) **79**

2.10.1 RecQ1 involvement in reversed replication fork restart 79

2.10.2 DNA2 /WRN contribution to reversed replication fork restart, by regressed arm processing **90**

3. Discussion **108**

4. Materials and Methods. **114**

4. 1. Cell culture and cell lines. **114**

4.2. Transfections. **114**

4.3. Western blotting. **115**

4.4. Detection of chromatin-bound PCNA **116**

4.5. Immunoprecipitation. **117**

4.6. Antibodies. **118**

4.7. Pulse-field gel electrophoresis. **118**

4.8. DNA fiber spreading. **119**

4.9. Electron microscopic analysis of genomic DNA. **120**

4.10. Chromatin enrichment. **121**

4.11. Creation of stable cell lines. 122

5. References..... 124

Zusammenfassung

Die Standard-Konformation der Replikationsgabel ist eine dreiarmige DNS -Struktur. Die Transformation dieser dreiarmigen Struktur in eine vierarmige Struktur dient als physiologische Antwort von Zellen auf verschiedenste genotoxische Substanzen sowie auf die Aktivierung von Onkogenen und schwer replizierbare Regionen des Genoms. Dieser Prozess wird als "Umkehr der DNS Replikationsgabel" definiert. Die Umkehr der DNS Replikationsgabeln - die Transformation einer dreiarmigen DNS-Struktur (Standard-Konformation der Replikationsgabeln) in die vier-armige - ist die generelle physiologische Antwort auf verschiedenste genotoxische Substanzen, Aktivierung von Onkogenen und auf schwer replizierbare Regionen innerhalb des Genoms. Es ist jedoch noch nicht genau bekannt, welche Proteine für diese molekulare Transformation in vivo verantwortlich sind. Viele verschiedene Proteingruppen wurden für diese Rolle vorgeschlagen, allerdings hauptsächlich auf biochemischen Daten basierend, die die Komplexität dieser Transformation in vivo kaum wiedergeben können. Wir haben unsere Forschung auf zwei Proteingruppen konzentriert, nämlich auf Annealing-Helikasen und Faktoren der post-replikativen Reparatur (PRR). Die erste Proteingruppe (SMARCAL1 und ZRANB3) hat die einzigartige Fähigkeit RPA-gebundene einzelsträngige DNS zu doppelsträngiger DNS zusammenzufügen, was möglicherweise notwendig ist um Standard-Replikationsgabeln zu umgekehrten Replikationsgabeln umzuformen. Die zweite Proteingruppe (z. B. E2 Ubiquitin-konjugierendes Enzym UBC13 und poly-ubiquitiniertes PCNA) wurde ausgewählt, da frühere Studien gezeigt haben, dass der fehlerfreie Zweig der PRR durch "Template switching" Mechanismen abläuft und möglicherweise die Umkehr der DNS Replikationsgabel beinhaltet. Wir konnten in der Tat zeigen, das ZRANB3 für das effiziente Verlangsamen und Umkehren der Replikationsgabeln nach genotoxischem Stress benötigt wird. Im Moment sind wir dabei herauszufinden, welche Domänen des ZRANB3 Proteins für diese Funktion verantwortlich sind. Weiterhin haben wir den Beitrag von UBC13 und ubiquitiniertem PCNA zur aktiven Verlangsamung und zur Umkehr der Replikationsgabeln nach genotoxischem Stress definiert.

Summary

Replication fork reversal - the transaction from a three-way junction (the usual conformation of replication forks) to a four-way junction - has been reported as a general response in face of a wide variety of genotoxic agents, oncogene activation and difficult-to-replicate regions of the genome. Proteins mediating this molecular transaction in vivo are still elusive. Many different groups of proteins have been proposed to execute this operation, yet most of the data come from biochemical experiments that may hardly recapitulate the complexity of this transaction in vivo. We focused our research on two groups of proteins, such as annealing helicases and post replicative repair (PRR) factors. The first group of proteins (SMARCAL1 and ZRANB3) have the unique ability to re-anneal RPA coated single stranded DNA (ssDNA), which may be necessary to convert standard replication forks to reversed forks. The second group of proteins (e.g. the E2 ubiquitin-conjugating enzyme UBC13 and polyubiquitinated PCNA) was selected as previous studies suggested the error-free branch of PRR to operate via template switching mechanisms, possibly entailing replication fork reversal. We could indeed determine that ZRANB3 is required for efficient fork slowing and reversal upon genotoxic stress and we are currently uncovering which domains are crucial for this function. We also uncovered the contribution of UBC13 and PCNA ubiquitination to active fork slowing and replication fork reversal upon genotoxic stress.

1. Introduction.

1.1 DNA replication.

1.1.1 General concepts of replication in eukaryotes.

Genomes of the eukaryotes are large, ranging from 107 to >109 base pairs (bp) and are organized into chromosome(s). In a replicating eukaryotic cell, genome must be duplicated every cell cycle, more precisely in the S phase of the cell cycle. In order to maintain the fidelity of the genome, and therefore of the information stored in it, the process of replication has to be complete and precise. Errors in the process of replication can lead to variety of different malfunctions, both at cellular level (under- or over-replication, gene mutations, gene loss, expansions of repetitive sequences etc.), and at the organismal level (genetic diseases, cancer, birth defects etc.). To ensure the precise process of replication, the coordinated action of many different proteins, forming the "replisome", is required. Different proteins are sequentially assembled and recruited to efficiently execute initiation, elongation and termination of replication. Each of these phases is strictly controlled to ensure exact, timely and complete replication.

Eukaryotic cells have evolved checkpoint signaling as an additional mechanism of control, which regulates the cell cycle progression in case of DNA damage or perturbation of DNA synthesis (Thomas J. Kelly, 2000).

1.1.2 Initiation of DNA replication.

In eukaryotic cells, DNA replication is initiated from multiple sites on chromosomes, called "origins". In *Saccharomyces cerevisiae* the origins are short, well-defined sequences of about 150 bp. These origins, termed autonomously replicating sequences (ARS) for their ability to confer autonomous replication to plasmids, fire asynchronously during S-phase in order to

ensure efficient replication of the chromosomes (Friedman KL, 1996). However, in higher eukaryotes

origins are not well characterized, and in metazoans origins of replication seem to vary in size. It seems that in mammalian cells replication initiation requires AT rich sequences (Paixao S, 2004; Wang L, 2004), dinucleotide repeats and asymmetrical purine-pyrimidine sequences (Wang L, 2004). Even though the origins of replication are difficult to define in metazoans, mechanisms driving the initiation of DNA replication are conserved in all eukaryotes.

DNA replication is initiated by binding of the multi-subunit (heterohexameric) protein called origin recognition complex (ORC) – to the origins of replication (Bell S.P., 1992). In mammals, ORC binding does not show any sequence specificity (Vashee, 2003) and the access of initiation factors to the origins is regulated by chromatin structure (Cayrou C, 2010). Binding of ORC to the origin persists during the entire cell cycle, dissociating only briefly after replication. The next step in the process is loading the ring-shaped heterohexameric minichromosome maintenance protein (MCM) complex MCM2-7 to the replication origin (Remus D, 2009). This is brought about by at least two proteins, Cdc6 and Cdt1. This process is like a "clamp loading" procedure in which a clamp loader loads a ring shaped molecule onto the DNA by opening the ring. MCM 2-7 complex possesses an ATPase dependent DNA helicase activity and its recruitment to the origin is restricted to late mitosis and G1 phase, before initiation of DNA replication. Mcm10, a chromatin-binding protein, is required for the association of the MCM2–7 complex with replication origins (Homesley L1, 2000). The recruitment of all these factors on chromatin occurs during late mitosis (M) and early G1 phase, generating the pre-replication complex (pre-RC) (Fig. 1.1). In order to initiate replication, DNA at the origin must unwind, generating single stranded DNA (ssDNA) to which the replicative polymerases can be loaded (Takeda DY, 2005).

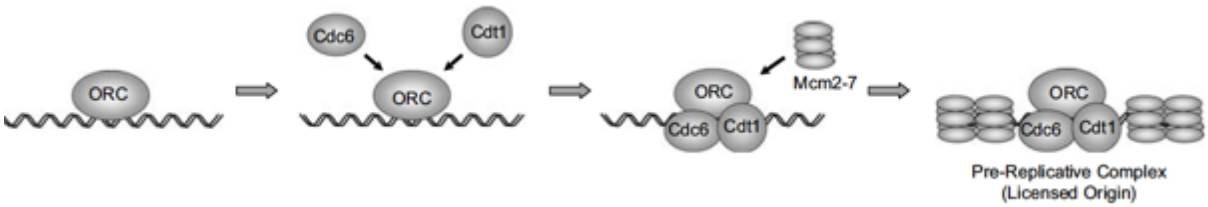

Figure 1.1 Assembly of pre-replicative complex. Different steps of eukaryotic assembly of pre-replicative complex. DNA replication is initiated by recruitment of Pre-RC components to the origin. ORC recruits Cdc6 and Cdt1, required for the subsequent loading of the Mcm2−7 complex. Many Mcm2−7 complexes are loaded at each origin and Pre-RC formation occurs during late M and early G1 phases of the cell cycle, licensing DNA for replication during S phase (Takeda DY, 2005).

The transition from G1 to S phase requires the conversion of pre-RCs into active replication forks. Initiation requires origin unwinding, stabilization of single stranded DNA, and loading of the replicative polymerases. This requires action of at least two kinases: S-phase cyclin dependent kinases (S-CDKs) and Dbf4-dependent Cdc7 kinase (DDK) (Thomas J. Kelly, 2000). These factors are temporally regulated throughout S phase, being associated with origins at the time of activation, suggesting that mechanisms influencing origin choice and timing probably regulate the targeting of these factors to origins (Takeda DY, 2005). CDKs are required to dissociate helicase-loading proteins Cdc6 and Cdt1, unwind the origin DNA and load DNA polymerases. In yeast Cdc6 is degraded, while in mammals Cdc6 is exported from the nucleus after CDK phosphorylation (Delmolino LM, 2001; Drury LS, 2000). Replication licensing shall occur only once per cell cycle, therefore initiation factors are regulated at different and redundant levels, comprising delocalization and degradation of some components upon entry in S-phase. These regulations are mostly mediated by CDK activity, which is required to activate the initiation complex and subsequently block re-initiation of DNA replication (Thomas J. Kelly, 2000). Protein kinases trigger DNA replication and at the same time prevent the assembly of new pre-replicative complex until the onset of new cell cycle.

1.1.3 Origin activation and chain elongation.

Initiation of DNA replication requires transition from pre-RC into replication fork, and this depends on CDK and DDK activity. The activity of these kinases causes disassembly of pre-RC and binding of factors like Cdc45, GINS, Sld3, Sld2 and Dpb11 to replication origins, as well as Mcm10, the loading of which is required for the recruitment of Cdc45 (Gregan J 2003; Sawyer et al., 2004). Cdc45 loading on the origin is one of the crucial steps to form an initiation complex and to load many other replication proteins such as DNA polymerase α and DNA polymerase ε. Mcm10 facilitates DDK phosphorylation of Mcm2–7 by physically interacting with both complexes (Lee et al., 2003). Mcm10's function in elongation may be related to its ability to retain Cdc45 on elongating forks. Mcm10 also interacts with the elongation factors DNA polymerase δ, DNA polymerase δ and DNA2 (Yasuo Kawasaki, 2001), and has been shown to activate the primase activity of DNA polymerase α *in vitro* (Fien, 2004). GINS complex is a stable, four-factor complex comprising Sld5, Psf1, Psf2 and Psf3, which is essential for DNA replication in both yeast and Xenopus egg extracts (Kubota and Takisawa, 2003). GINS is prerequisite for the engagement of Cdc45 with the nascent replisome and is necessary to regulate association of Cdc45 with MCM subunits (Gambus et al., 2006; Takayama Y, 2003). It is also required for continued association between Cdc45 and MCM complex during S-phase progression (Kanemaki M, 2006; Labib, 2007). The GINS complex may be involved in coordinating the progression of the MCM helicase and priming events at the replication fork (Marinsek, 2006). The association of MCM, GINS and Cdc45 forms the CMG complex (Ilves et al., 2010). Replisome is believed to harbor factors that are not only essential for replication, but also involved in other chromosome transactions and chromatin regulation. These are referred to as "replisome progression complexes" (RPC), which are

composed of more than 20 replication related proteins (Gambus et al., 2006). In addition to Cdc45, MCM complex and GINS, the RPC contains MRC1, Tof1 and Csm3 (Claspin, Timeless and Tipin in mammalian cells), that are considered fork stabilization factors (Calzada et al., 2005). In eukaryotes, the full CMG complex is the functional helicase machinery required for DNA unwinding (Hashimoto et al., 2012). Interaction of Ctf4, a polymerase accessory factor, with Mcm10 is required for the loading of DNA pol α on a chromatin (Zhu Z, 2008). Once CMG complex is formed, the helicase activity can facilitate DNA unwinding, generating ssDNA, subsequently stabilized by RPA (Fig. 1.2).

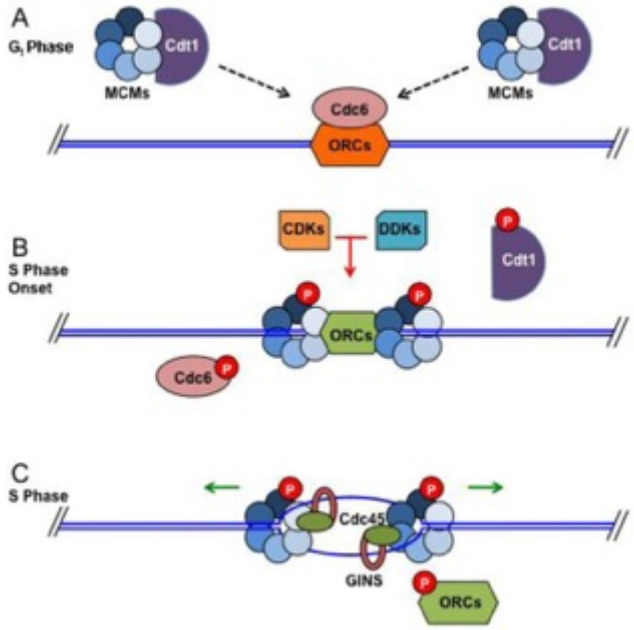

Figure 1.2 Activation of pre-RC. Step wise demonstration of eukaryotic DNA replication. The formation of pre-RC complex comprises binding of ORC to DNA and loading of Mcm2-7 helicase complex by Cdc6 and Cdt1. CDK/DDK-dependent phosphorylation of pre-RC components leads to Cdc45 loading, resulting in origin firing. MCMs and associated proteins unwind DNA to initiate replication (Noguchi, 2013).

The leading strand is synthesized in a continuous way, while the lagging strand is copied in a discontinuous manner, generating short stretches of DNA: the Okazaki fragments (approximately 200 bp long). However, DNA polymerases are not able to initiate DNA synthesis *de novo* but they require a primer with a free 3'-OH. Therefore, both the leading strand and every Okazaki fragment on the lagging strand are primed by a short RNA that is synthesized *de novo* by a specialized RNA polymerase called primase, which in eukaryotes is part of the Pol α polymerase complex, known as Pol α–primase (Stillman, 2008). The primase initiates DNA synthesis, starting with a short RNA primer (approximately 10 nt), which is subsequently extended by DNA polymerase α forming a RNA-DNA primer of about 30 nucleotides. This priming process takes place at the origin of replication of the leading strand and at the 5'end of each Okazaki fragment on the lagging strand. The leading strand is synthesized by polymerase ε in a continuous way, while the lagging strand is copied in a discontinuous manner by polymerase δ, generating short stretches of DNA: the Okazaki fragments, which are joined postreplicatively. After this initiation event, the clamp loader complex replication factor C (RFC) loads the sliding clamp proliferating cell nuclear antigen (PCNA) onto double-stranded DNA (Garg P, 2005). The sliding clamp encircles the double-stranded DNA and tethers two polymerases - Pol δ and Pol ε to the template to increase enzyme processivity, although the mechanism by which this occurs is not clear. PCNA, a ring-shaped homotrimer, is able to slide along double-stranded DNA, acting as processivity factor for DNA polymerases (Prelich et al., 1987). The PCNA complex keeps polymerases on DNA, ensuring high-processivity of DNA replication. In addition to its function in replication, PCNA plays an essential role in regulating repair processes at the replication fork, acting as an interaction platform for repair factors (Moldovan et al., 2007). Pol ε has been shown to be the polymerase responsible for leading strand synthesis (Pursell et al., 2007) (Fig.1.3). It is a highly processive enzyme. Lagging strand synthesis on the other hand requires Pol δ (Fig.1.3). It is thought to

proceed in several discrete stages, *i.e.*, initiation by DNA primase, limited elongation of the RNA primer by Pol α, a switch of the primer terminus from Pol α to Pol δ proposed to be brought about by RFC, elongation by Pol δ, and maturation of the completed Okazaki fragment in conjunction with Fen1 and DNA ligase1. Each transition is believed to be mediated by a specific protein or protein complex and has to occur with very high efficiency (Garg and Burgers, 2005).

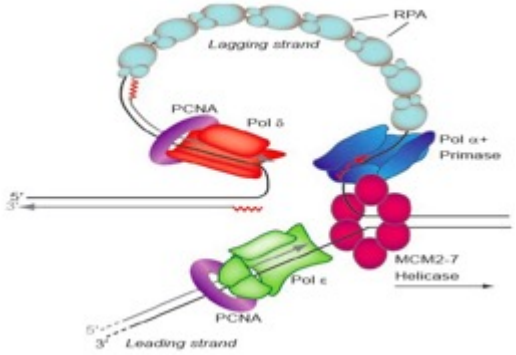

Figure 1.3 Model of an eukaryotic replication fork (McCulloch SD, 2008).

The extensive unwinding of the DNA during replication generates topological stress which would slow down, and eventually stop, replication fork progression unless there were enzymes that are relieving it. DNA topoisomerases are enzymes that control and modify the topological state of DNA. Topoisomerases can be divided in two classes, type I and type II). Type I topoisomerases operate by transiently breaking a DNA strand and passing the other strand through the transient break. Type II topoisomerases operate by transiently breaking a pair of complementary strands and passing another double-stranded segment.

1.1.4 Termination of DNA replication.

Eukaryotic genomes have multiple origins of replication, which, when activated, enable start of replication bi-directionally, meaning that every origin produces two replication forks moving in

opposite direction. Termination of replication occurs when two replication forks, coming from adjacent active origins of replication, meet (Edenberg HJ, 1975). Termination of replication is often occurring at replication fork barriers (RFB) or replication termination sites. In these regions, termination is achieved by arresting the first fork that enters the termination region, forcing it to wait there for the inevitable convergence with the fork coming from the opposite direction. Specific termination sites (TERs) containing fork pausing elements such as RFBs have been characterized in eukaryotes (Fachinetti et al., 2010). Much is still unknown about the exact mechanism of fork fusion, but it seems possible that the presence of polar RFBs at TERs leads to the non-simultaneously converging of the two forks (Fig. 1.4). This process implies that at least one of the two forks would exit from the pause region with asymmetric leading and lagging strands before converging with the other fork. Topoisomerase II enzyme seems to be required to facilitate replication termination, resolving catenated junctions formed after fork fusion, and thus, preventing genome rearrangements. Rrm3 DNA helicase is also required for fork s.

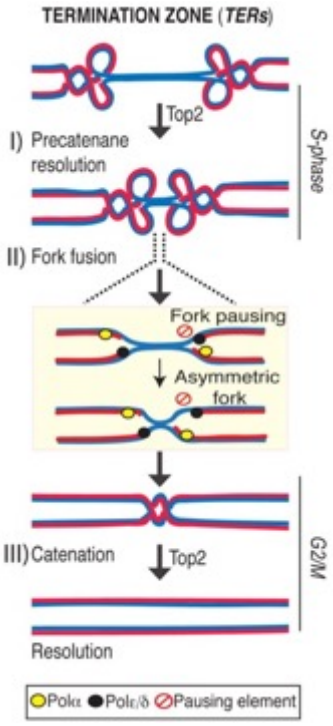

Figure 1.4 Model for replication termination. One of the two converging forks stalls at a polar pausing site (red symbol) emerging with an asymmetric conformation. This process leads to non-simultaneously converging of the two forks. Top2 enzymes resolves catenated junctions formed after fork fusion, allowing chromosome resolution (Fachinetti et al., 2010).

1.2 DNA damage and repair mechanisms.

1.2.1 DNA damage and consequences.

Integrity of eukaryotic genome is constantly being under threat due to numerous endogenous and exogenous agents that are damaging the DNA, and this can lead to compromised cell survival and proliferation (Figure 1.5). Endogenous sources of DNA damage could be spontaneous reactions intrinsic to the chemical nature of DNA in an aqueous solution (mostly hydrolysis), that lead to creation of abasic sites and cause deamination (Lindahl, 1993). The other sources of endogenous DNA damage are reactive oxygen and nitrogen species, lipid peroxidation products, endogenous alkylating agents, estrogen and cholesterol metabolites, and reactive carbonyl species generated by cellular metabolism (De Bont R, 2004). Exogenous sources include physical and chemical agents like UV radiation, ionizing radiation and carcinogens present in different chemicals. Different sources of damage can cause very different types of damage. For instance, 8-oxoguanine, an oxidative lesion that on DNA replication pairs equally well with the cytosine (normal pairing) and adenine (abnormal pairing), causing GC→TA transversions (Akbari, 2008). Conversely, ionizing radiation or processing of interstrand cross-links causes double strand breaks (DSBs), which is one of the most serious lesions, as only one can be sufficient for cell death. Mutations arise from inaccurate processing of the lesions, and the genome is especially susceptible to such damage during the S-phase. Various types of repair mechanisms and checkpoints signaling pathways have evolved in order to ensure genome integrity in response to DNA damage. Deregulation of DNA damage repair and checkpoint signaling is associated with predisposition to many types of cancer. In some cases, replication may stall or arrest when encountering a base damage or strand break. Cells have also evolved mechanisms to bypass such damages before being repaired, ensuring the completion of the cell cycle. This strategy relies on specialized mechanisms, which are collectively named DNA damage tolerance mechanisms (DDT), and are sometimes referred as

post-replication repair (PRR). PRR can be divided in two branches: an error-free pathway named “template switching” (TS) and error-prone pathways known as translesion synthesis (TLS).

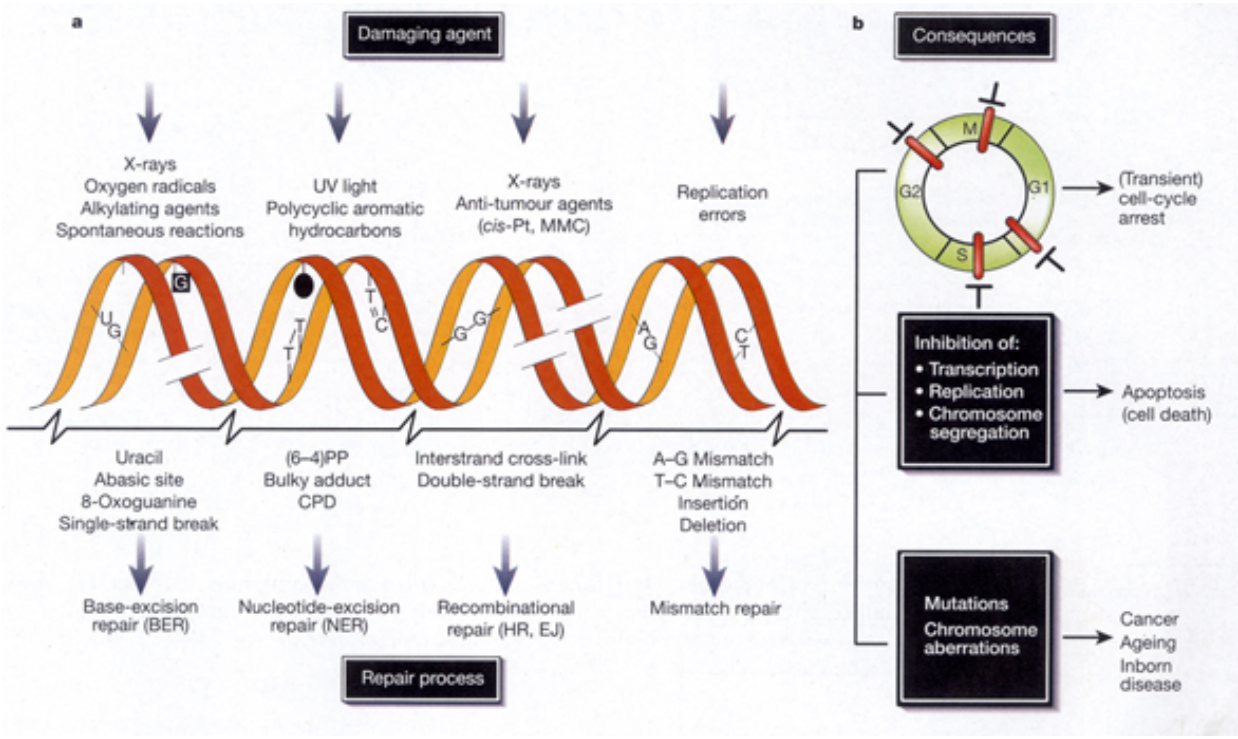

Figure 1.5 Different sources of DNA damage and repair pathways (a) and possible outcomes (b) (Hoeijmakers, 2009).

1.2.2 DNA damage repair mechanisms.

Base excision repair (BER) is the primary pathway responsible for repairing base damage generated by ROS, ionizing radiation or chemical agents like chemotherapeutic drugs. These damages arise through the processes of oxidation, alkylation, deamination and depurination/depyrimidination. This pathway is subdivided into short patch BER (a single damaged nucleotide is replaced) or long patch BER (repair between 2 and 13 nucleotides). The main components facilitating this process are specific enzymes, including DNA glycosylases, AP endonucleases, DNA polymerases and ligases (Houtgraaf et al., 2006).

Nucleotide Excision repair (NER) pathway repairs helix-distorting DNA lesions such as 6-4 photoproducts (6-4 PPs) and cyclobutane pyrimidine dimers (CPDs). These lesions are caused by UV radiation, ROS or chemical agents. NER also contributes to the repair of intrastrand and interstrand crosslinks (ICLs). Hereditary deficiency in NER pathway leads to UV sensitivity and skin cancer development (Andressoo et al., 2005). Human diseases Xeroderma Pigmentosum and Cockayne's syndrome are known (Lehmann, 2003). Individuals diagnosed with Xeroderma Pigmentosum suffer from extreme sensitivity to UV light, increased cancer predisposition and in some cases problems with the nervous system (Brooks PJ, 2014). Cockayne syndrome patients suffer from impaired development of nervous system, short stature, extreme sensitivity to sunlight and microcephaly, but without apparent increased cancer development risk (Bender M, et al., 2003(Hoeijmakers, 2009). There are two modes of action for NER: the global genome NER (GG-NER), responsible for monitoring and repairing constantly the whole genome, and the transcription-coupled NER (TC-NER), activated in presence of transcription blocking lesions.

Mismatch Repair (MMR) pathway corrects replication errors that can result in mismatched bases due to the wrong nucleotide incorporation (A-G or C-T). MMR can also recognize lesions resulting from cellular metabolisms and physical or chemical agents, such as chemotherapeutics. Defective MMR increases mutation rates and results in microsatellite instability (MSI), associated with cancer development (Umar, 2004).

Homologous Recombination Repair (HR) repair pathway of double-strand breaks takes place during S and G2 phases of the cell cycle and is essential for the maintenance of genome stability. The extreme cytotoxic nature of DSBs requires fast and accurate repair, otherwise chromosomal rearrangements, translocations and deletions can easily occur. DSBs arise by ionizing radiations, ROS, chemotherapeutic drugs or can be formed by replication of a single-

strand break. This pathway requires extensive sister chromatid homology and needs to be precise. HR is mediated

by the Rad52 epistasis group, including Rad51 protein. Rad51 is a strand-exchange protein, which searches for an undamaged copy of the broken DNA on the sister chromatid to be used as DNA template. This way, the damage can be repaired without loss of genetic information (San Filippo J, 2006).

Non Homologous End joining (NHEJ) another mechanism for repairing DSB, does not require homology, since the two ends of broken DNA are directly ligated together by DNA ligase/Xrcc4 complex. NHEJ is less accurate than HR, but is active in all phases of the cell cycle, mainly during G0 and G1 and early S-phase (Shrivastav M, 2008)

1.2.3 DNA damage tolerance (DTT) pathways.

Cells possess multiple DNA repair mechanisms to counteract DNA damage and remove lesions on the DNA in timely and accurate manner. However, some DNA damage can remain unrepaired for prolonged time and/or not be recognized by the functionally adequate repair mechanism. If the damage persists, and cells need to go through S phase of the cell cycle, some of this damage has to be tolerated and repaired later on. In this way a mechanism is provided for cells to finish replication and move to the next cell phase, increasing the chances of survival and preventing genome instability. Interestingly, mechanisms in DTT are associated with increased mutagenesis, which can lead to various outcomes, from cell death to cancerogenesis (Ghosal G, 2013). The DTT mechanism is also known as post replication repair (PRR). Studies in yeast and mammalian cells have marked two major pathways for PRR: translesion synthesis (TLS) and damage avoidance by template switching (TS) (Branzei D, 2010; Chang DJ, 2009; Lee KY, 2008). A critical step for both pathways is monoubiquitination of PCNA – following DNA damage and/or replication stress PCNA gets mono- or polyubiquitinated on lysine 164 (K164) (Hoege C, 2002; Parker JL, 2009; Stelter P1, 2003). It was demonstrated in various systems that

monoubiquitination of PCNA promotes TLS (Bienko M, 2005; Kannouche, 2003; Kannouche, 2004), while polyubiquitination of PCNA promotes damage avoidance through template switching (Daigaku Y, 2010; Parker JL, 2009). (Figure 1.6)

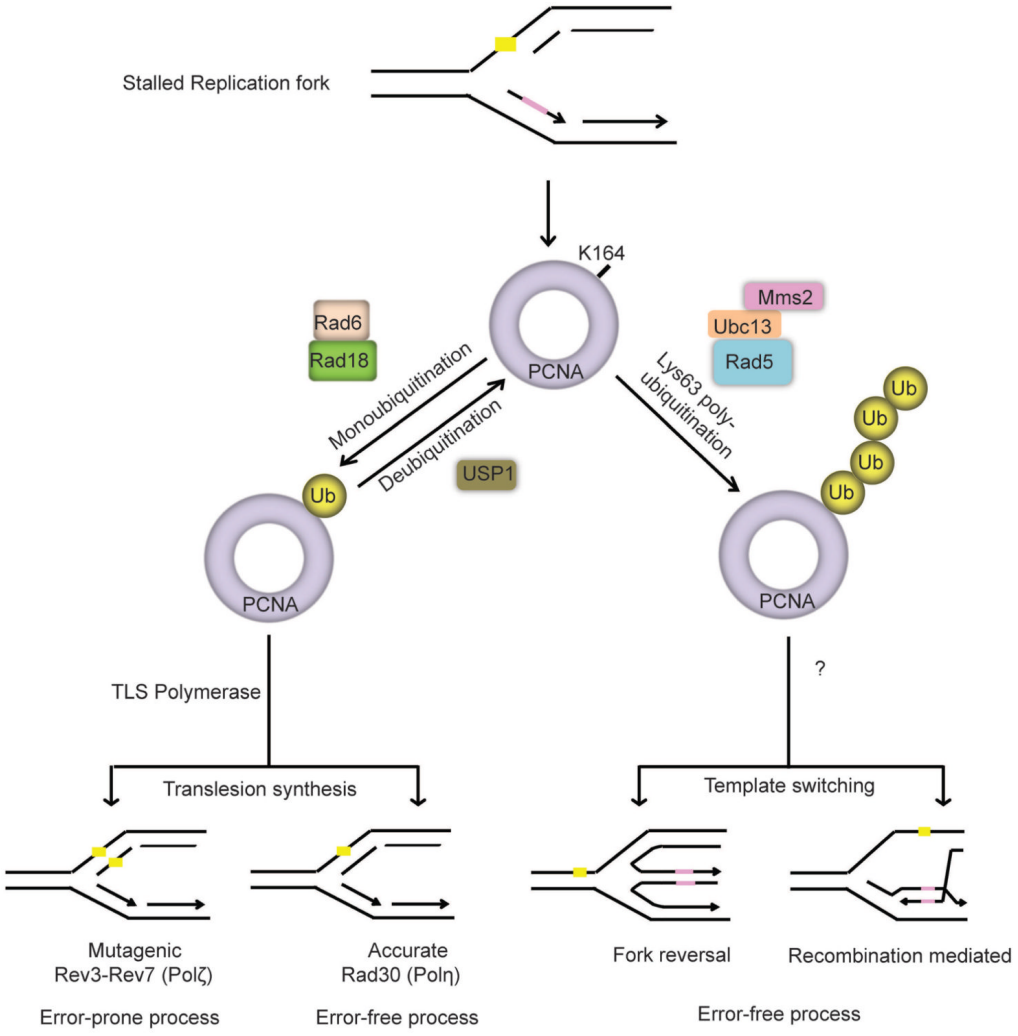

Figure 1.6 Post replicative repair pathways. Two major pathways of postreplicative repair (PRR) – the translesion synthesis (TLS) on the left, and template switching (TS) on the right (Ghosal G, 2013).

In both yeast and human, monoubiquitination is mediated by Rad6/Rad18 complex (Broomfield S, 2001). Polyubiquitination in yeast is mediated by Mms2/Ubc13 and Rad5 (Broomfield S, 2001; Kannouche, 2004; Karras GI, 2010) and in human by Mms2/Ubc13 and Rad 5 orthologs, supposedly HLTF and SHPRH (Motegi A, 2008; Unk I, 2010).

1.2.3.1 Translesion synthesis (TLS).

It is generally not possible for the replicative polymerases to accommodate damaged base in their active site due to high stringency and fidelity. For this reason, replication past lesions requires the use of specialized DNA polymerases which have been adapted for this specific function. These polymerases have lower stringency than the replicative polymerase and their active sites are more open and can therefore accommodate damaged bases. There is a growing number of DNA polymerases recently found to mediate DNA synthesis across specific damages. In eukaryotic cells, five translesion polymerases have been identified: polη, polι, polκ and Rev1, belonging to the Y-family, and Polζ, belonging to B-family of DNA polymerases. Each of these polymerases shows specificity for different types of damages; some are able to bypass a specific DNA lesion, while others are only efficient in insertion or extension step of lesion bypass.

Interferon-stimulated gene 15 (ISG15) modification, also named ISGylation, is involved in termination of error-prone TLS (Park et al., 2014). The deubiquitinating enzyme ubiquitin specific protease 1 (USP1) was found to deubiquitinate PCNA, inhibiting error-prone TLS (Huang TT, 2006). In response to cellular stress, such as UV irradiation, USP1 is auto-cleaved, allowing monoubiquitinated PCNA to accumulate and translesion synthesis to start.

Even though PCNA is crucial for regulation of PRR, there are two new recently discovered factors – Spartan (C1orf124/DVC1) and PCNA – associated factor PAF15 (KIAA0101) (Centore R.C., 2012; Ghosal G., 2012; Mosbech A., 2012; Povlsen L.K., 2012). Spartan co localizes with PCNA and ub PCNA at damage sites and stabilizes Rad18 and ub PCNA at sites of damage. It preferentially binds to polη upon damage by UV, and to POLD3 in non-treated

conditions (Ghosal G., 2012). Upon depletion of Spartan POLD3 binds to error-prone TLS polymerase polζ and this leads to increased mutagenesis.

In unperturbed S phase PAF15 is monoubiquitinated on two lysine residue (15 and 24) and is tightly bound to PCNA on chromatin. Upon DNA damage, it gets deubiquitinated and quickly removed from the chromatin. This allows for lesion bypass by means of polη recruitment (Povlsen LK, et al., 2012).

It was proposed that for UV induced lesions like CPDs, translesion synthesis (TLS) with polη is most efficient, inserting the correct nucleotide opposite the damaged base (Chikahide Masutani, 2000). In its absence, a less efficient and more error- prone pathway is brought into play leading to UV induced hypermutations in the DNA. A study has shown that polη localizes to the nucleus, and that during S phase it accumulates in nuclear foci at sites of DNA synthesis (Kannouche, 2001). In humans, the inactivation of polη causes cancer-prone syndrome, known as the variant form of xeroderma pigmentosum (XP-V) (Chikahide Masutani, 2000). The mechanism by which polη is thought to be recruited to the replication forks upon UV damage is by monoubiquitination of PCNA by Rad6 and Rad18 (Kannouche, 2004) which increases the affinity of PCNA for polη. This increased affinity for polη brings about the " polymerase switch" where polδ is replaced by polη at the damaged replication fork. polη then carries out replication past the CPD. After the lesion is bypassed, polη dissociates and chain extension is taken over by the more processive polδ. New evidence suggests that the PIP domain, rather than the direct binding of K164-linked ubiquitin moiety on PCNA, is required for polη accumulation at the site of damage (Narottam Acharyaa and Jerard Hurwitzc, 2008). Recent data indicated that Rad18 might be targeted to PCNA at the site of stalled replication fork by polη (Durando, 2013) and this new role for polη in stimulation of PCNA monoubiquitination seems to be uncoupled from its DNA polymerase activity.

Polι, physically interacting with polη (Patricia Kannouche, 2003) is able to insert the correct base opposite many types of lesions, but cannot further synthesize from the inserted bases, so that another polymerase is required to complete the lesion bypass.

Polκ can carry out TLS past benzo[a]pyrene-guanine both in vivo and in vitro (T. Ogi, 2002). UV sensitivity, showed by polκ-deficient cells, seems to imply a role for this polymerase in the repair synthesis step of NER (Lehmann, 2006).

Rev1, even if is structurally a member of the Y-family, is a dCMP transferase rather than a DNA polymerase. Rev1 is able to insert dCMP opposite Gs or abasic sites. This polymerase plays a role in prevention of mutagenesis in yeast (Gibbs et al., 2000), but little is known about humans. Unlike the other Y-family polymerases, Rev1 is found at the site of DNA synthesis in only a small proportion of S-phase cells (Ogi et al., 2004), possibly because of the short time of residence in replication foci. The C-terminal of mammalian Rev1 can interact with the other three Y-family polymerases and with Rev7 subunit of polζ (Guo C, 2003), indicating that Rev1 might act as a platform in switching between TLS and replicative polymerases.

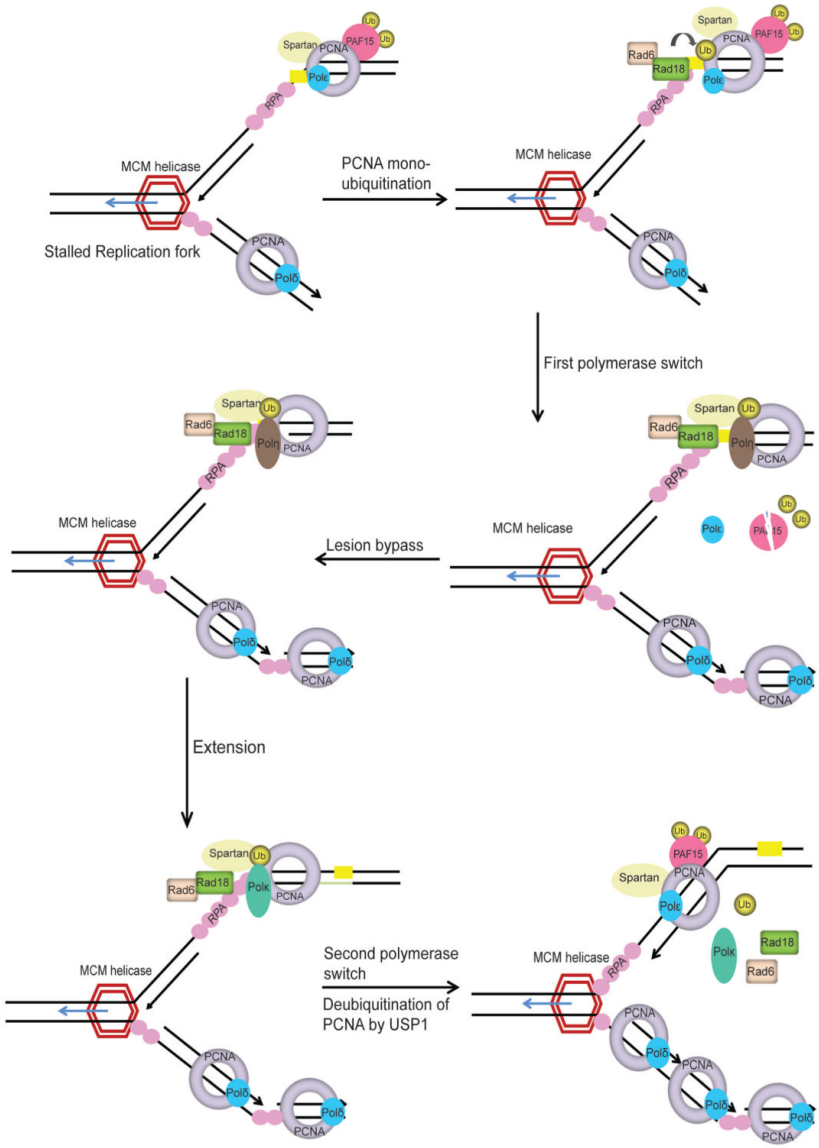

Figure 1.7 Proposed model of translesion synthesis (TLS). Replication fork stalling uncouples the replicative helicase from normal high-fidelity DNA polymerases resulting in DNA unwinding and generation of tracts of ssDNA, which is coated by RPA. RPA-ssDNA also recruits RAD18 E3-ligase to activate DNA damage tolerance pathway. PCNA monoubiquitinated at K164 (ub-PCNA) by RAD18-RAD6 operates as a molecular switch from normal DNA replication to the TLS. Under normal conditions ubiquitinated PAF15 is bound to PCNA. Upon DNA damage PAF15 is degraded by the proteasome and this facilitates the binding of TLS polymerase to ub-PCNA. Additionally, Spartan is recruited to DNA damage sites by ub-PCNA and is required to stabilize RAD18 and ub-PCNA on the chromatin. TLS polymerase Polη bound to ub-PCNA, inserts a nucleotide directly opposite the lesion and requires an additional TLS polymerase, such as Polζ (Pol zeta), to extend beyond the insertion. Following extension, the second polymerase switch is initiated where the TLS polymerase is replaced by high fidelity replicative DNA polymerase. USP1 deubiquitinates PCNA and DNA synthesis is resumed by high-fidelity replicative DNA polymerase. The precise mechanism of polymerase switching and regulation of TLS by Spartan, PAF15 and USP1 is still unclear (modified from (Ghosal G, 2013).

1.2.3.2 Template switching mechanisms.

Template switching has evolved as a mechanism to promote DNA damage bypass by the replication fork and/or DNA damage tolerance followed by gap filling. In yeast, Rad5-Mms2-Ubc13 genes, encoding ubiquitin ligases and ubiquitin conjugating enzymes, control this pathway and mediate PCNA polyubiquitination, acting as a signal for error-free bypass mechanisms. The pathway is still mechanistically unclear and subjected to intense studies in higher eukaryotes. This process was proposed to involve a switch of template and, in fact, the blocked nascent strand might use the undamaged newly synthesized strand of the sister chromatin as a template (Xiao W, 2000).

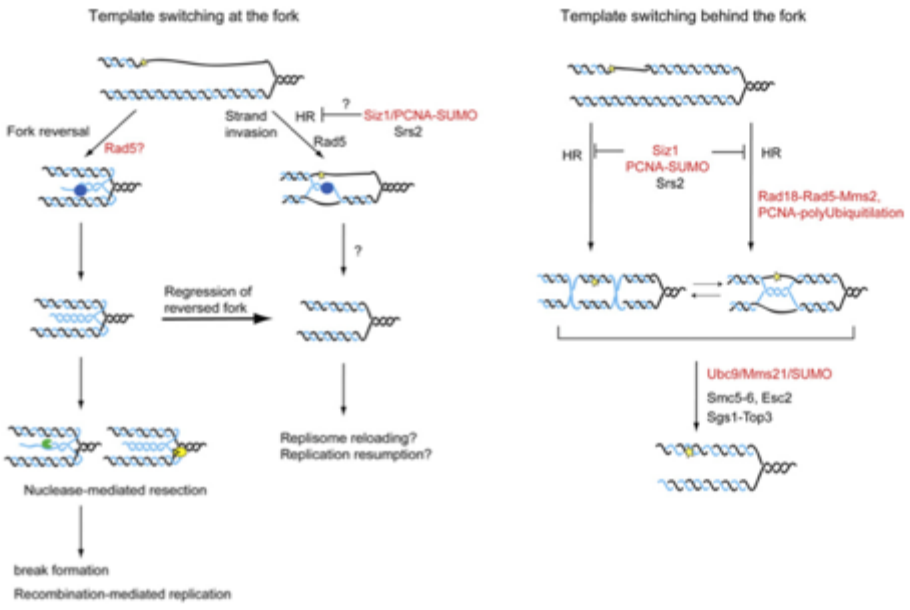

Figure 1.8 Model for template switching mechanisms. Representation of mechanisms promoting template switching events at the fork or behind the fork (Branzei D, 2004).

Two models describing template-switching mechanism, at and behind the fork, have been proposed (Branzei D, 2004) (Fig. 1.8). In the first model, the lesion is bypassed through the formation of a regressed fork intermediate and would not invoke the role of recombination proteins. In this fork reversal model, also known as "chicken foot" model, the newly synthesized strands are displaced and the parental and daughter strands annealed, regressing the replication fork and creating an alternative template for DNA synthesis. It was demonstrated that Rad5 ATPase and helicase activities promote fork reversal *in vitro* (Blastyak A., 2007), and human HLTF protein exhibits the same fork remodelling activity, being able to regress replication-fork like DNA structures in an ATP-dependent manner (Blaystak et al., 2009). Nevertheless, it still needs to be clarified whether reversed fork intermediates can promote error-free DNA damage tolerance in vivo. Findings from the recent study showed that HIRAN domain of the HLTF protein is necessary for replication fork slow down upon nucleotide depletion, presumably through promoting replication fork reversal (Kile AC, 2015). Additional observations, mostly collected in yeast, led to the postulation of a second model of template switching that involves recombination-like invasion mechanisms and might occur behind the fork. In this model, the blocked nascent strand invades the opposite homologous duplex, utilizing the undamaged sister chromatid as a template. Template switching behind the fork leads to the formation of X-shaped structures (Minca et al., 2010; Branzei et al., 2008) containing linked sister chromatids (Branzei et al., 2011). These template-switch intermediates may also contain Holliday Junctions (HJs) (Ashton et al., 2011) and need to be resolved to restore normal replication. Recent work in yeast has demonstrated that upon damage and activation of TLS the gap region on the parental strand that resulted from fork stalling at the lesion, actually becomes paired with the newly created duplex, creating three stranded DNA region. The pairing of parental strands leads to displacement of the newly synthetized strand which now can serve as a template for extension of the 3' end of the strand that was stalled at

the lesion. This would result in Holliday Junction like structures that are resolved by highly regulated "resolvases" (Giannattasio M, 2014). Many resolvases have been identified in eukaryotes (Wyatt and West, 2014). Enzymes identified so far, which are required for the resolution of damage-induced template-switch intermediates, are RecQ helicase Sgs1 (BLM in human) or topoisomerase III. Therefore, cells in which these enzymes are not functional accumulate sister chromatid junctions (SCJs) near the replication fork (Hickson and Mankouri, 2006). PCNA polyubiquitination and error-free PRR factors are required for both gap-filling damage tolerance and for template switching-mediated SCJ formation behind the fork.

Recent findings indicated that Rad18-Rad5 play a role not only in gap-filling by template switching (Minca et al., 2010), but also in DBS repair by HR (Szuts et al., 2006). This complex may act with recombination factors to join sister chromatids and promote damage bypass by template switching (Branzei et al., 2008). While in the reversed fork model these events must occur at the fork, in recombination-like invasion mechanisms they can take place either at the fork or behind.

Besides being ubiquitynated, PCNA can also be sumoylated at two lysine residues, K164 and K127 (Hoege et al., 2002). PCNA sumoylation favours damage bypass of the lesion utilizing factors acting in the error-free branch of PRR. In *S.cerevisiae*, during unperturbed DNA replication, PCNA is SUMOylated at Lys164 to recruit Srs2 helicase. This helicase negatively regulates recombination by disrupting Rad51 nucleoprotein filament (Esta et al., 2013). (Hoege et al., 2002) (Fig 1.10). Relatively recently it was shown that even in human cells PCNA can get SUMOylated, and that this modification may serve to prevent replication fork collapse upon DSBs, and therefore promote genome stability (Gali H, et al., 2012).

1.3 Replication stress.

1.3.1 Definition and detection of replication stress.

Replication stress has been a well-known phenomenon for many years, however a consensus over the exact definition was difficult to reach. Reasons for this are that replication stress has many different sources, with many different outcomes in the cells. Nevertheless, one unifying definition has emerged stating that replication stress identifies a high number of different circumstances slowing or stalling of replication fork progression and/or DNA synthesis (Zeman MK, 2014).

Different sources of replication stress usually lead to single-stranded DNA stretches (ssDNA) created as the replicative helicase continues to unwind the parental DNA after the polymerase has stalled (Pacek M et al., 2004). These ssDNA stretches are coated by RPA and this serves as a signal for activation of the replication stress kinase ATM-Rad3-related (ATR) (Zou L, et al., 2003, MacDougal C, et al., 2007, Nam E, et al., 2011). This leads to cell cycle arrest and inhibition of late origin firing by phosphorylation of many downstream targets. Phosphorylation of histone variant H2AX was proposed to be one of the markers of replication stress. However, later on was discovered that this modification can be induced by several kinases and that those can reflect different types of damage throughout the cell cycle. More reliable marks of replication stress would be ATR-dependent phosphorylation of RPA (Ser33) or Chk1 (Ser345), or detection of ssDNA, directly using native BrdU immunofluorescence or indirectly through formation of RPA foci (Nam E, et al., 2011, Marechal A, et al 2013). The most reliable readout of replication stress is probably direct measurement of DNA synthesis using DNA fiber or DNA combing assays, which rely on the incorporation of nucleotide analogues (Bianco J, et al., 2012).

1.3.2 Sources of replication stress.

There are a number of recognized sources of replication stress, to name just a few (for schematic overview see Figure 1.9):

1) Nicks, gaps, and ssDNA – can be both sources and symptoms of replication stress.

   DNA lesions – probably the most-studied source of replication stress. Lesions could be caused by UV light, chemical mutagens, byproducts of cellular metabolism, etc. (Ciccia A, et al., 2010).

2) Misincorporation of ribonucleotides - polymerase ε and polymerase δ are very specific enzymes in terms of base pairing, however they are less specific when it comes to distinction between deoxyribonucleotides (dNTPs) and ribonucleotides (rNTPs). This is usually dealt with by RNase H2, FEN1 and EXO1 (Sparks J, et al., 2012).

3) Unusual DNA structures – trinucleotide repeats leading to formation of hairpins triplexes etc. (Mcurray C, et al., 2010, Kim J, et al., 2013), and as of recently G – quadruplexes that form in GC – rich regions (Paeschke K, et al., 2013, Bochman M, et al., 2012).

4) Conflict between replication and transcription – since both replication and transcription are occurring on the DNA molecule, collisions are almost inevitable. Recent studies identified a class of fragile sites ("early replicating fragile sites") that lie within highly replicated genes in early S phase (Barlow J, et al., 2013). Formation of R – loops was also widely implicated in replication stress (Aguilera A, et al., 2012).

5) Limiting levels of "building blocks" or essential replication factors – e.g. insufficiency of nucleotides, replication factors, histone and histone chaperones (Poli

J, et al., 2012, Bester A, et al., 2011, Anglana M, et al., 2003, Aguilera A, et al., 2013; Toledo LI, et al., 2013).

6) Common fragile sites – genomic regions prone to replication stress-induced DSBs, which are usually prevented by ATR activity (Debatisse M, et al., 2012, Casper A, et a., 2002). The molecular determinants of fragility in these regions are less clear and more heterogenous – including collision of replication machinery with transcription of very long genes (Bochman M, et al., 2012) and lack of replication origins in these regions (Letessier A. et al., 2011).
7) Oncogene induced replication stress – overexpression or constitutive expression of several different oncogenes (w.g. H-RAS, MYC and cyclin E) leads to replication stress probably because of depletion of nucleotide pools and/or increased collisions with transcription (Bester A, et al., 2011, Srinivasan S., et al., 2013, Jones R, et al., 2012, Halazonetis T, et al., 2008).
8) Chromatin inaccessibility – the chromatin status seems to play a role in replication stress. Compacted chromatin may pose an obstacle for the replication machinery. Studies show that chromatin relaxation can reduce common fragile sites breakage (Jiang Y, et al., 2009).

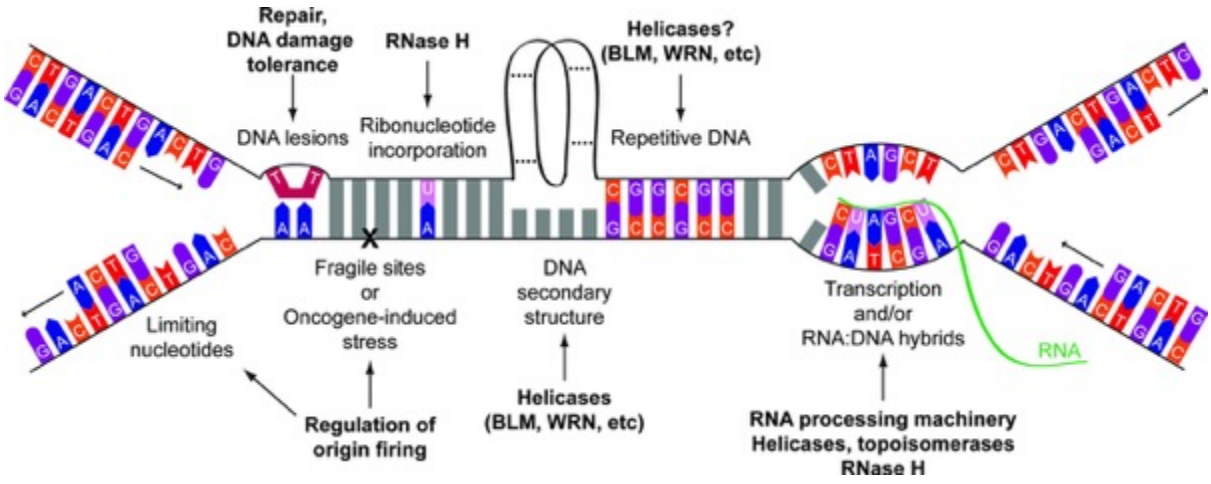

Figure 1.9 Different sources of replication stress (Zeman MK, 2014).

Recent reports have identified replication fork reversal as a cellular response to different types of replication stress, namely replication through trinucleotide repeats, oncogene overexpression and different genotoxic agents (Follonier C, et al., 2013, Neelsen K.J, et al 2013, Zellweger R, et al., 2015). The process and benefits of fork reversal are discussed in details in the next chapter.

1.4 Replication fork reversal.

1.4.1 Definition.

Replication fork reversal identifies the process of transition of a normal replication fork (three-way junction) into a four-way junction, where the two nascent strands are unwound from their parental partners and annealed with each other, while the parental strands are also reannealed, leading to back-tracking of the replication fork (Neelsen and Lopes, 2015) (see figure 1.10 for clarification). Although a transaction of this kind was suggested 4 decades ago, it was not widely accepted due to technical concerns of the method used to obtain results.

Replication fork reversal in prokaryotes is well characterized: key findings are published in high-profile papers (Manosas M, et al., 2012, De Septenville A.L, et al., 2012, Nelson S.W.&BenkovicD.J., 2010) and have been summarized in a recent review (Atkinson and McGlynn, NAR 2009). However, in eukaryotic cells remained elusive until recently.

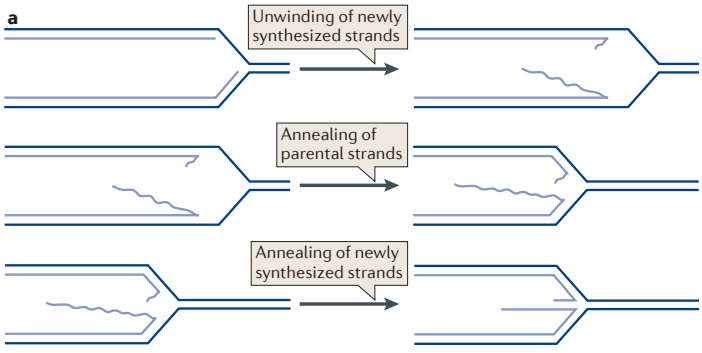

Figure 1.10 Process of replication fork reversal– Fork reversal might occur through stepwise strand exchange, as shown in the scheme, or through simultaneous re-annealing of the parental strands with the annealing of the nascent strands. (Neelsen KJ, 2015).

In eukaryotes replication fork was a matter of substantial debate among opposing groups of thinking. On one side, it was considered pathological. The proof of this was the notion that in yeast (*Saccharomyces cerevisiae*) these structures could only be observed in checkpoint defective upon treatment with various genotoxic agents (UV irradiation, methyl methanesulfonate – MMS and ribonucleotidereductase inhibitor hydroxyurea –HU), (Sogo J.M, et al., 2001, Lopes M, et al., 2006, Mojas N, et al., 2007). However, using topoisomerase inhibitors in checkpoint proficient *S. cerevisiae* cells, frequent fork reversal was observed (Ray Chaudhuri A, et al., 2012). Importantly, in yeast cells TopI inhibition is known to be checkpoint-blind (Radon C, et al., 2003), and the checkpoints are responsible for checkpoint-mediated phosphorylation of DNA replication ATP-dependent helicase-nuclease 2 (Dna2), which is processing reversed replication forks (Hu J, et al., 2012).

DNA topoisomerases solve the topological problems associated with DNA replication, transcription, recombination, and chromatin remodeling by introducing temporary single- or double-strand breaks in the DNA. In addition, these enzymes fine-tune the steady-state level of DNA supercoiling both to facilitate protein interactions with the DNA and to prevent deleterious excessive supercoiling (Champoux, 2001).

Camptothecin (CPT), or its clinically relevant derivatives irinotecan and topotecan, inhibit TopI action by trapping it in a covalent complex with DNA after its cleavage (TopI cleavage complexes; TopIccs). Replication fork collision with the TopIccs was proposed as the primary cytotoxic mechanism for TopI inhibitors in dividing cells (Holm et al., 1989). This hypothesis is known as ‘’Replication run-off’’ theory. In this scenario collision of the replication forks with the TopIccs results in double strand breaks (DSBs). This hypothesis was supported by data implicating the role of DNA damage markers like H2AX phosphorylation and homologous recombination factors in CPT induced cytotoxicity

(Pommier, 2006). Indeed, CPT is commonly used in many basic research laboratories as agent of choice to induce DSBs.

Some reports have recently challenged this theory, by showing that TopI inhibitors also prevent relaxation activity of TopI, leading to accumulation of positive supercoils, potentially contributing to TopI inhibitors-mediated cytotoxicity (Koster et al., 2010).

Recent work investigated the cellular response to TopI poisoning by CPT or its derivatives in more detail. It was shown in several different eukaryotic systems (*S. cerevisiae*, *Xenopus laevis* egg extracts, cultured mouse embryonic fibroblasts and human cells) that, upon treatment with low doses of TopI inhibitors, replication forks undergo rapid slowdown and frequent reversal, uncoupled from DSB formation (Ray Chaudhuri et al., 2012). Replication fork reversal was proven to be a global, evolutionary conserved response to replication stress induced by TopI inhibitors. These observations were made upon treatment with low (25nM), but clinically relevant doses of CPT, uncovering potential drug resistance mechanisms in cancer chemotherapy.

Another study identified replication fork reversal as a general response to replication stress induced by chemotherapeutic treatment. The genotoxic agents used in the research belong to four different groups: Topoisomerase inhibitors (etoposide - ETO, and doxorubicin - DOXO), base damaging agents (UV-C irradiation, MMS, and hydrogen peroxide H2O2), DNA crosslinking agents (mitomycin C - MMC and cis-diamminedichloroplatinum - CDDP) and antimetabolites that inhibit nucleotide biosynthesis (HU) or DNA polymerases (aphidicolin - APH) (Zellweger R, 2015).

Thorough analysis of the replication intermediates isolated from non-treated (NT) or treated cells revealed accumulation of short (40nt) ssDNA at the junctions, presumably identifying lagging strand synthesis. All treatments led to extended (1.5-2 fold) ssDNA at the junctions, reflecting uncoupling of DNA synthesis at the fork. The extent of fork uncoupling upon

different treatments is strictly correlated with the frequency of reversed replication forks - i.e. the more uncoupling, the higher reversed replication fork frequency. Having in mind that RAD51 binds to long stretches of ssDNA to drive homology directed strand invasion during homologous recombination (Symington and Gautier, 2011), its potential role in the process of fork reversal was investigated. Strikingly, upon downregulation of RAD51, reversed replication fork frequency in CPT, MMC and HU treated dramatically dropped compared to mock transfected cells. Interestingly, upon all tested treatments, reduction in reversed fork frequency was accompanied by an increase in the length of the ssDNA at the junction, suggesting that uncoupled forks are precursors of RAD51-mediated fork reversal.

Poly (ADP-ribose) polymerase (PARP) activity is required to observe CPT, MMC and HU-induced replication fork slowing and reversal. Its activity was shown to limit the activity of the RECQ1 helicase - which in turn drives reversed fork restart upon CPT (Berti M, et al., 2013) (see figure 1.11) as well as MMC and HU treatments (Zellweger R, et al., 2015) - thus allowing stabilization and accumulation of reversed forks. The dependency of efficient fork reversal on PARP activity may contribute to explain the promising synergistic effect of TopI and PARP inhibitors and opens new synthetic lethality treatment concepts, especially considering that MMC- and HU-induced fork slowing and reversal are also, at least partially, PARP dependent.

Another recent study revealed that, besides RECQ1, DNA2 and WRN proteins have also a role in the restart of the reversed replication forks (Thangavel S, et al., 2015) (see figure 1.11). Co-depletion of RECQ1 and DNA2 leads to a more marked accumulation of reversed replication forks compared to single RECQ1 or DNA2 depletion, suggesting two possibilities: either these proteins are involved in distinct mechanisms of replication fork restart, or that RECQ1 acts downstream of DNA2. The study also shows that nuclease

activity of DNA2 and the ATPase activity of WRN are crucial for processing of stalled forks, and that REQ1 regulates fork processing activity of DNA2.

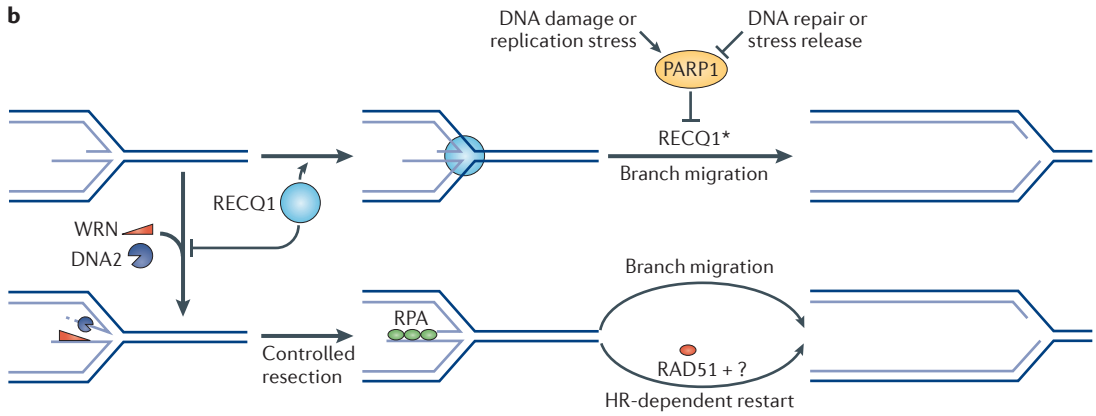

Figure 1.11 Processing of reversed replication forks – restart of the reversed replication forks goes through action of RecQ1, WRN and DNA2 proteins. (Neelsen and Lopes, 2015).

Other recent publications documented the detection of reversed replication forks in vivo in yet different situations associated with replication stress – namely trinucleotide repeats and oncogene overexpression. It was shown, by using plasmid based system, that the reversed forks frequency was very high upon replication through trinucleotide repeats of different length (Follonier C, et al., 2013), possibly contributing to the inherent instability of these repeats (Mirkin, Nature 2007; Neelsen and Lopes, 2015). Upon overexpression of different oncogenes (CyclinE and CDC25A overexpression), reversed forks were identified among the most prominent structures observed under these conditions and, in the case of CDC25A overexpression, were shown to be processed into DSB by the deregulated action of structure-specific nucleases (Neelsen K.J, et al., 2013). Thus overall, albeit contributing to a physiological and protective response to genotoxic stress, reversed forks may also contribute to genome rearrangements. Overall, we believe that fork reversal should be seen as a "double-edged sword", with physiological and pathological outcomes that depending on the cellular context and on the specific condition of replication stress, as discussed in the next chapter.

1.4.2 Replication fork reversal - a friend or a foe?

The situations in which fork reversal could be beneficial for maintenance of genomic stability are lesions on the template strand, lack of nucleotides, discontinuities on the template strand and possibly interstrand crosslinks. Reversing the fork could prevent the excessive accumulation of single-stranded DNA (ssDNA), allow more time for repair of DNA lesions and enable excision repair by repositioning a lesion in double stranded DNA (Figure 1.12a)
Conversely, the situations in which fork reversal would lead to increase in genomic instability are replication through trinucleotide repeats and oncogene overexpression. In replication through trinucleotide repeats there could be misalignment of the repeats on the regressed arm, so when the fork is restarted potential deletions or insertions of repeats could be provoked in the next round of replication. As mentioned above emergence of replication forks was observed even upon oncogene overexpression. These structures were cleaved by methanesulfonate UV-sensitive clone 81 (MUS81) and synthetic lethal of unknown function 4 (SLX4) endonucleases, leading to double strand breaks in checkpoint deregulated systems (Figure 1.12b).
Having in mind all this, it is difficult to make a definite statement what is direct role of replication fork reversal in human health, other than that is a mechanism primarily designed to prevent genetic instability. Healthy cells would probably benefit of fork reversal – genome stability is prerequisite for normal divisions and unperturbed transcription, in one-word viability. But, cancer cells can also exploit this role of fork reversal and thus use it as a mechanism to tolerate drugs, i.e. to develop resistance (example of TopI inhibitor). So the

role in maintaining genome stability can have positive and negative outcomes. Conversely, as discussed, promoting instability of trinucleotide repeats could have deleterious effects on individual's health in some conditions.

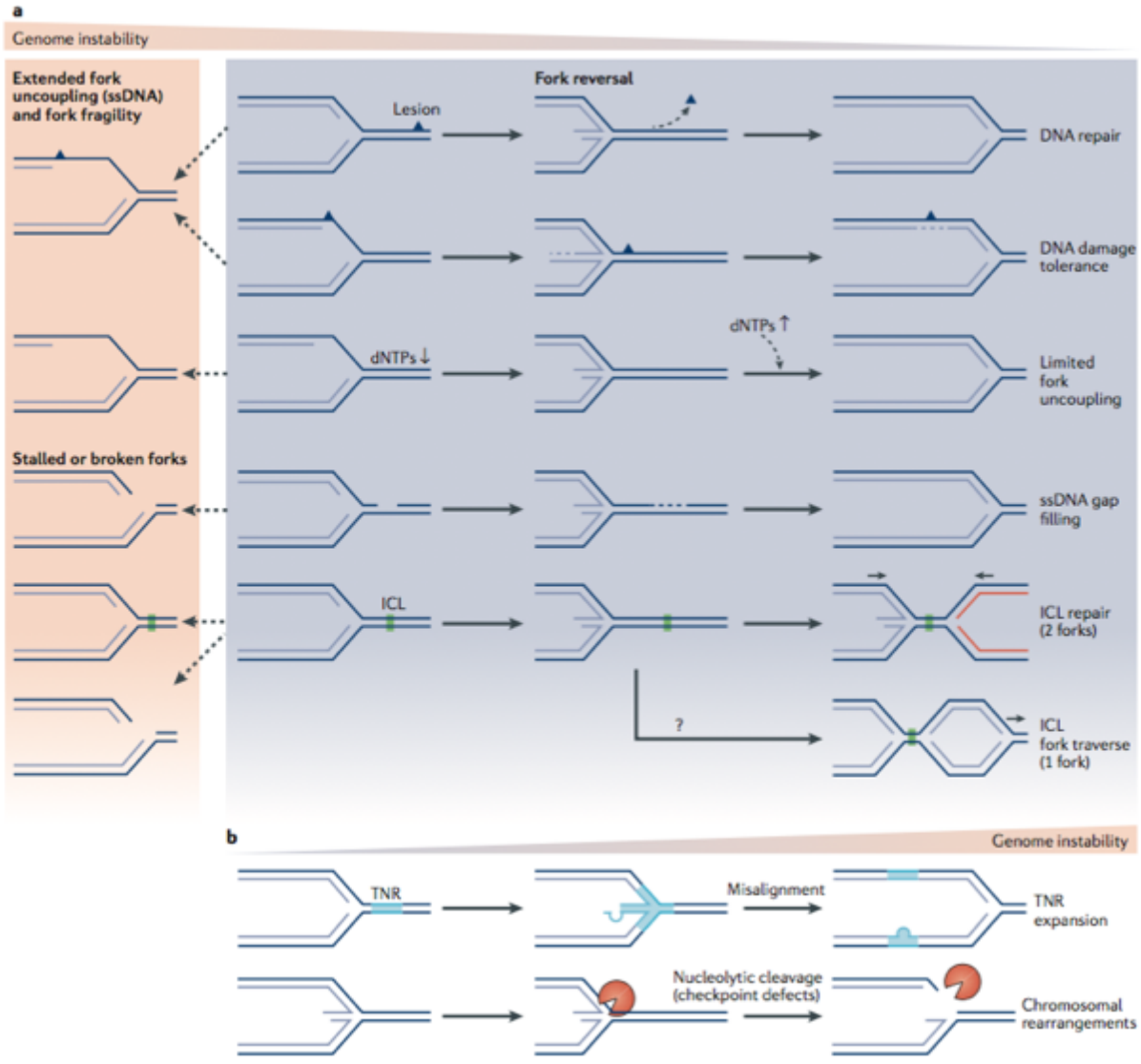

Figure 1.12. Different roles of fork reversal. a) Roles in maintaining genomic stability. b) Roles in destabilization of genomic integrity (Neelsen and Lopes, 2015).

Numerous questions remain open on the process of fork reversal and its cellular role (Neelsen and Lopes, 2015). Most notably, it is still elusive what is(are) cellular factor(s) responsible for replication fork reversal upon replication stress induced by chemotherapeutics treatment. Extensive literature analysis has resulted in a few promising candidates.

1.4.3. Protein(s) potentially involved in replication fork reversal.

Annealing DNA helicases–HARP (SMARCAL1) and ZRANB3 (AH2) - The term ‘’annealing helicase’’ was created upon discovery of helicase domain-containing proteins that had annealing and no unwinding activity. The first to be discovered was HARP (HepA related protein), also referred to as SMARCAL1 (SWI/SNF-related, matrix associated, actin-dependent regulator of chromatin, subfamily a-like 1), which is member of the SWI/SNF family. Mutations in HARP are associated with Schimke Immuno-Osseous Dysplasia (SIOD), a multisystem autosomal recessive disorder characterized by short stature, kidney disease and a weakened immune system (Boerkoel et al., 2000). HARP has ability to catalyze the ATP-dependent reannealing of ssDNA bubbles coated with RPA (Yusufzai, 2008). In vitro data also show that HARP can catalyze branch migration of Holliday junctions (HJs) and regression of replication forks (Wu, 2012). Upon DNA damage, HARP co-localizes with RPA and γH2AX foci, and the interaction with RPA is required for localization to the sites of DNA damage (Yusufzai, 2009). HARP is phosphorylated in response to replication stress and DNA damage. It can be phosphorylated by ATM, ATR and DNA-PK, yet significance of these phosphorylations is unclear, as some promote and some inhibit it's function (Bansbach et al., 2009; Carroll et al., 2013; Couch et al., 2013; Postow et al., 2009).

Recently, it was shown that HARP can promote both fork reversal and reversed fork restart, depending on where the ssDNA gap is located (i.e. leading or lagging strand) and on the presence or absence of RPA (Betous et al., 2013). This study showed that in presence of RPA, HARP is preferentially reversing model replication forks if the gap is on the leading

strand (Figure 1.13), presumably to allow for the bypass of the damage. Conversely, if the gap is on the lagging strand and the RPA is present (Figure 1.14), HARP is preferentially restarting reversed forks. This may suggest that HARP is necessary for keeping replication process unperturbed, as having replication forks reversed upon gap formation on the lagging strand would not be beneficial, but rather unnecessarily energy and time consuming, as these gaps are physiologically formed during the replication process. Interestingly, the preference for replication fork reversal, or reversed fork restart changes completely in the absence of RPA, although the physiological significance of this observation is debatable.

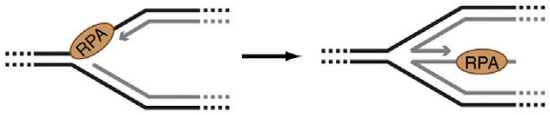

Figure 1.13. HARP promotes replication fork reversal in the presence of RPA if the gap is on the leading strand. (Betous R, et al., 2013)

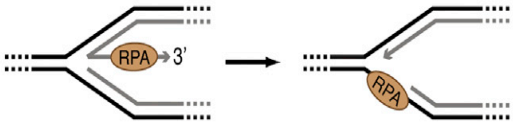

Figure 1.14. In the presence of RPA HARP promotes reversed fork restart if the gap is on the lagging strand. (Betous R, et al., 2013)

After HARP, another annealing helicase was discovered – ZRANB3 (zinc-finger, RAN-binding domain containing 3) also known as AH2 (annealing helicase 2) (Yusufzai and Kadonaga, 2010) (Figure 1.15).

Figure 1.15. ZRANB3 domains. Red coloured domains are necessary for annealing activity, green (PIP and APIM) for interaction with PCNA, purple (NZF) for interaction with polyubiquitinated PCNA, and grey (HNH) for endonuclease activity (Ciccia A, et al., 2012).

Similar to HARP, ZRANB3 displays DNA-dependent ATP-ase activity and ATP-dependent rewinding activity. *In vivo* data suggest that, unlike HARP, ZRANB3 does not interact with RPA, but it is recruited to the sites of DNA damage via interaction with PCNA. ZRANB3 possesses three domains for interaction with PCNA, two of which (PIP box and APIM) are required for direct

interaction with PCNA, and the third, called NZF (NPL4 zinc finger) recognize K63-linked ubiquitin chains. This motif is required for specific interaction with the K63-linked polyubiquitinated form of PCNA in vitro and for retention of ZRANB3 at damage sites in vivo (Ciccia et al., 2012). As mentioned above, the polyubiquitinated form of PCNA is involved in error-free PRR in the template switching process, so - taking all these data together - it was tempting to suggest that fork regression is executed by ZRANB3, which is recruited via polyubiqinated PCNA (this working hypothesis essentially represents the rationale of this PhD thesis). Apart from being able to reanneal ssDNA bubbles, it was reported from biochemical experiments that ZRANB3 can exhibit its activity on some additional substrates – it can regress stalled forks and can disrupt D-structures (Ciccia et al., 2012). Additionally, a novel biochemical activity was reported for ZRANB3, as structure specific, ATP-dependent endonuclease (Weston et al., 2012). Latest reports suggest additional members of the ‘’annealing helicases’’ family – such as Rad54L and SMARCA1 (Yuan et al., 2012).

Factors involved in error free post-replicative repair (PRR) – As described before, upon DNA damage the Rad6-Rad18 complex monoubiquitinates PCNA, and this action can be followed by either error-prone TLS, error-free TLS, or error-free PRR controlled by Rad5 and Mms2-Ubc13 proteins. Mms2-Ubc13 compose an ubiquitin conjugating complex,

whereas Rad5 has ubiquitin ligase and DNA dependent ATP-ase activity. In the error-free PRR Rad5 and Mms2-Ubc13 promote K63 linked polyubiquitination of the PCNA. In this pathway the damage is bypassed by template switching using the newly synthesized DNA strand of the sister duplex as the template. For this process to occur, a new primer-template junction needs to be formed, for which two mechanisms are proposed – one is post-replicative strand invasion, the other is replication fork regression (Figure 1.16). Both X-shaped sister chromatid junctions

and regressed replication forks can be detected at damaged replication forks by electron microscopy, supporting the existence of the proposed intermediate DNA structures, although their relative abundance is quite different in lower and higher eukaryotes (Giannattasio et al., 2014; Zellweger et al., 2015). Furthermore, double-

stranded DNA containing only newly synthesized strands can also be detected by sedimentation analysis (Unk et al., 2010).

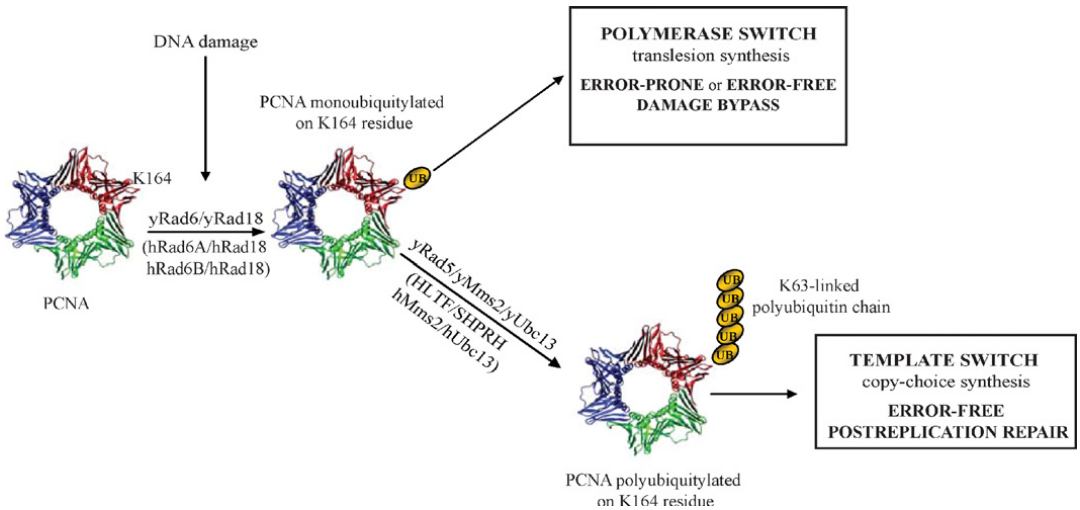

Figure 1.16. Control of Rad6-Rad18 dependent damage tolerance by PCNA ubiquitination (y and h prefixes marking yeast and human proteins, respectively) (Unk et al., DNA Repair 9 (2010) 257-267).

Humans possess two RAD6 homologs – HHR6A and HHR6B and corresponding proteins show 70% identity with yeast Rad6. Human Rad18 has 62% similarity with yeast Rad18, and can interact with both HHR6 proteins in vivo. Also, human Mms2 and Ubc13 have been identified. Concerning Rad5, there are two human orthologues – HLTF and SHPRH. In vitro data suggests that both Rad5 and HLTF possess fork regression activity, while this remains to be determined for SHPRH (Unk et al., 2010). It was shown that HLTF and SHPRH act in a damage-specific manner – HLTF prevents mutations induced by UV, and SHPRH prevents mutations induced by MMS (Lin J.R, et al., 2011). As mentioned above, recent study revealed that HIRAN domain of the HLTF protein is prerequisite for replication fork slow down upon nucleotide depletion. Additionally, in vitro data from the same study revealed that HIRAN domain of the HLTF is necessary for replication fork reversal through recognition of the 3' DNA ends (Kile AC, et al., 2015). A novel E3 ligase, TRAIP (RNF206), was implicated as an important factor associated with replication fork with a role in facilitating response to replication stress. It was shown that it interacts with unperturbed and stalled replication forks, and promotes ssDNA formation and checkpoint signaling at the stalled forks. Findings from this study also suggest that TRAIP's PIP box, necessary for interaction with PCNA, and its E3 ligase activity are necessary for this protein's function (Hoffmann S, et al., 2015).

1.5 Proliferative Cell Nuclear Antigen (PCNA) and the role in DNA damage response.

PCNA is a DNA polymerase processivity factor. It functions as a loading scaffold for the replication machinery through association with various replication-related factors (Moldovan G.L, et al., 2007). During DNA replication, the chaperonin-like replication factor C (RFC) binds to the RNA primer-DNA template junction and loads PCNA onto DNA (Bowman G.D, et al., 2004; Majka J, et al., 2004). Upon PCNA loading, Polα is released and Polε is loaded

to mediate leading-strand elongation (Kunkel T.A, et al., 2000). For the discontinuous lagging strand, firstly the short Okazaki fragments have to be produced by Polα and Polδ (Nick McElhinny S.A, et al., 2008). PCNA is characterized by its trimeric ring-shaped structure. Three PCNA monomers are associated to form a closed ring consisting of two sides. The topologically identical N and C termini of PCNA monomer are connected on one side while the other side contains several β sheets linked by loops (Krishna T.S, et al., 1994). The ring-shaped structure of PCNA is evolutionarily conserved and belongs to the family of β-clamps and (Schurtenberger P, et al., 1998). Rich in lysine and arginine residues, the inner ring of PCNA is positively charged, which allows for the effective encircling around the negatively charged duplex DNA. Recent studies reveal that PCNA is not only essential for replication in eukaryotes, but also plays critical roles in several DNA damage-responsive pathways (Moldovan G.L, eta al., 2007). Living organisms are constantly challenged by various sources of DNA damage. Environmental agents including radiation and chemical mutagens, and endogenous cellular metabolites can cause DNA damage (Friedberg E.C, et al., 2006). Under normal conditions, most DNA lesions can be removed by DNA repair pathways such as nucleotide excision repair and base excision repair. However, failure in lesion correction by these pathways prior to S phase in the cell cycle could pose severe consequences leading to genome instability or even cell death. Cells have evolved sophisticated lesion-bypass mechanisms to deal with this threat and ensure survival by allowing DNA synthesis in the presence of replication-blocking lesions. These lesion-bypass pathways in the budding yeast Saccharomyces cerevisiae are driven by factors belong to the RAD6 epistasis group (Prakash S, et al., 1993; Friedberg E.C, et al., 1988 and Broomfield S, et al., 2001) and have been classified as error-prone translesion synthesis (TLS), error-free TLS and error-free postreplication repair (Xiao W, et al 2000) or DNA damage tolerance (DDT). Interestingly, as briefly discussed above, all three bypass pathways require PCNA,

and different covalent modifications of PCNA by ubiquitin (Ub) or a small Ub-like modifier (SUMO) determine which tolerance pathway will be utilized in the face of unrepaired lesions (Andersen P.L, et al., 2008). Ubiquitination is a chemical process by which Ub is covalently attached to the Lys residue of a target protein by three enzymes: Ub-activating enzyme (Uba or E1), Ub-conjugating enzyme (Ubc or E2) and Ub ligase (E3) (Hershko and Ciechanover, 1998). Substrate proteins can be modified by a Ub monomer either at one Lys residue (monoubiquitination) or multiple Lys residues (multi-monoubiquitination). Proteins can also be modified by a Ub chain where Ub moieties sequentially link to a previous Ub (polyubiquitination) (Hochstrasser M, 1996). Although all 7 Lys residues (K6, K11, K27, K29, K33, K48 and K63) in Ub have been shown capable of forming poly-Ub chains (Peng J, et al., 2003; Xu and Peng, 2003), the physiological significance of some poly-Ub chains in living cells is not fully understood. The most characterized function of Ub modification is the K48-linked poly-Ub chain that targets proteins for degradation by the 26S proteasome (Hochstrasser M, 1996). On the other hand, K63-linked poly-Ub chain plays a role in regulating various signaling pathways largely in a proteolysis-independent manner (Pickart and Fushman, 2004). A paradigm of DNA-damage response through covalent modifications of PCNA was discovered by Stefan Jentsch and his colleagues (Hoege C, et al, 2002), in which PCNA can be either monoubiquitinated by the E2-E3 complex Rad6–Rad18 at the K164 residue or further modified with K63-linked Ub chain by another E2-E3 complex, Mms2-Ubc13-Rad5. Recently, the stepwise PCNA monoubiquitination and polyubiquitination by the two complexes was reconstituted in vitro (Parker and Ulrich, 2009), further confirming the above genetic model. In addition, the same K164 residue of PCNA can also be SUMOylated by yet another E2-E3 complex, Ubc9-Siz1 (Hoege C, et al., 2002; Stelter and Ulrich, 2003).

In mammalian cells, PCNA can also get mono- or poly-ubiquitinated. Mammalian homologues of Rad6/Rad18 complex, responsible for monoubiquitination of PCNA at K164 residue have been identified. Also, mammalian homologues of Mms2/Ubc13 have been identified, while for the Rad5 homologues there are few candidates. Some reports suggest that damage induced PCNA polyubiquitination in mammalian cells is not entirely dependent on Mms2, suggesting some redundant mechnisms for execution of this action (Brun J, et al., 2008). As mentioned, for the Rad5 homologues, there are few candidates, namely HLTF and SHPRH, which seem to work in a damage dependent manner (Lin JR, et al., 2012). TRAIP, a third E3 ligase associated with PCNA polyubiquitination, was recently discovered and implicated in maintainance of replication fork stability upon genotoxic stress (Hoffmann S, et al., 2015; Soo Lee N, et al., 2016). It is obvious that this pathway in mammalian cells is far more complex than in yeast and further research is needed to elucidate it completely.

2. Results.

2.1 Downregulation of ZRANB3 rescues replication fork speed.

Replication fork progression in vivo in cultured cells can be assessed by DNA fiber spreading, a technique based on pulse-labeling with halogenated nucleotides, cell lysis and DNA spreading over microscopy slides. When replication fork progression is analyzed this way in mock transfected cells treated with low doses of CPT (50nM), significant fork slowdown is rapidly observed upon treatment. In cells depleted of particular candidate factor with a potential role in fork reversal, we expected to observe impaired or no fork slowing upon CPT treatment. As a proof-of-principle, this result was obtained in cells treated with CPT and PARP inhibitor at the same time (Ray Chaudhury A, et al., 2012). In this case, as now clarified mechanistically (Berti et al., 2013), PARP inhibition ‘’unleashes’’ the activity of RecQ1 helicase, leading to untimely fork restart and impairing accumulation of forks arrested in the reversed conformation. We thus expected depletion of cellular factors driving fork reversal in response to mild CPT treatment to give very similar results to those observed

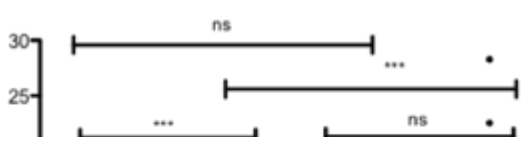

upon PARP inhibition. Indeed, after siRNA mediated knock down of ZRANB3 we could observe completely defective slowing of the replication fork progression (Figure 2.1).

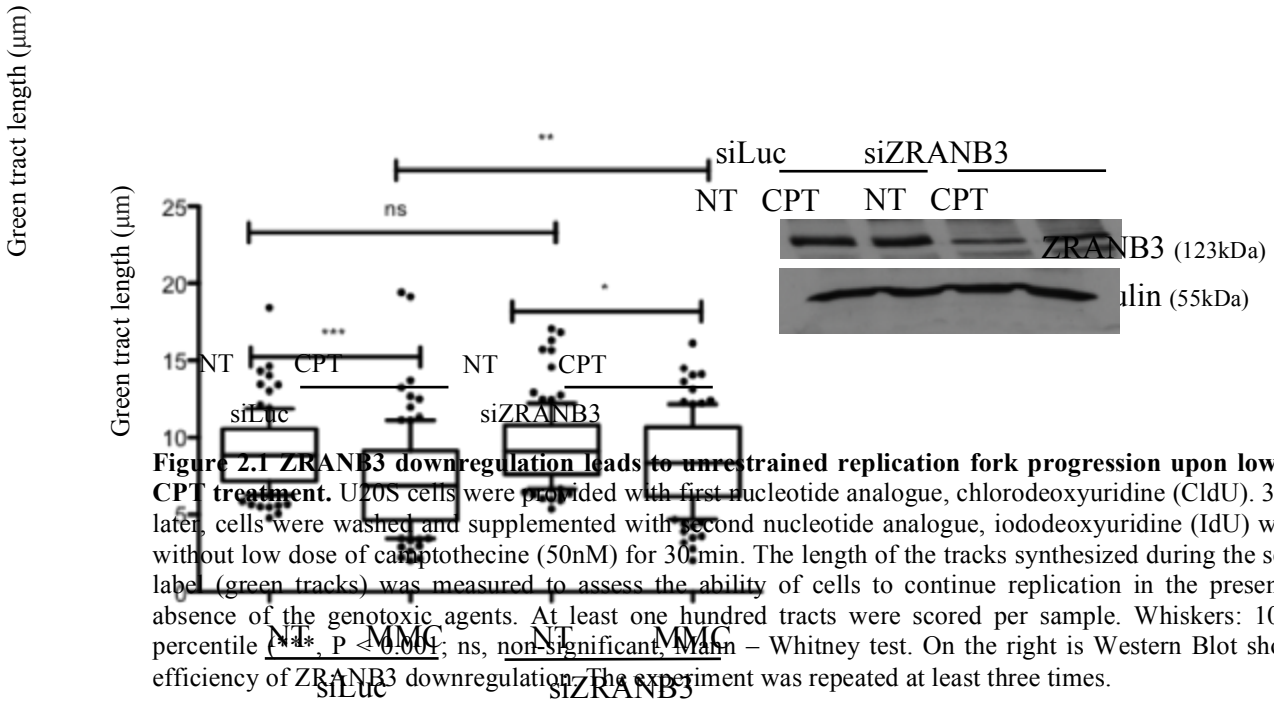

Figure 2.1 ZRANB3 downregulation leads to unrestrained replication fork progression upon low dose CPT treatment. U2OS cells were provided with first nucleotide analogue, chlorodeoxyuridine (CldU). 30 min later, cells were washed and supplemented with second nucleotide analogue, iododeoxyuridine (IdU) with or without low dose of camptothecine (50nM) for 30 min. The length of the tracks synthesized during the second label (green tracks) was measured to assess the ability of cells to continue replication in the presence or absence of the genotoxic agents. At least one hundred tracts were scored per sample. Whiskers: 10-90th percentile (***, P < 0.001; ns, non-significant, Mann – Whitney test. On the right is Western Blot showing efficiency of ZRANB3 downregulation. The experiment was repeated at least three times.

Figure 2.2 ZRANB3 downregulation leads to unrestrained replication fork progression upon MMC treatment. The experimental setting was the same as in Figure 2.1, except that 200nM mytomicin C (MMC) was used instead of CPT. At least one hundred tracts were scored per sample. Whiskers: 10-90th percentile (***, P < 0.0001; **, P < 0.01; *, P < 0.05 ns, non-significant, Mann – Whitney test. The experiment was repeated at least two times.

We decided to test the another genotoxic agent, mitomycin C (MMC), in low doses of 200nM, in the same experimental setting. We could still observe at least partial rescue of replication fork speed in MMC-treated ZRANB3 downregulated cells (Figure 2.2).

Having established that downregulation of ZRANB3 leads to complete (CPT treatment), or partial (MMC treatment) rescue of replication fork speed, we tested whether this could be an off-target effect of the siRNA. For this reason, we compared results obtained by two different oligonucleotides upon low dose CPT treatment, i.e. the condition that gave us clear cut results in this assay. Even though with the second oligo we didn't observe complete rescue of fork speed upon CPT treatment, we could see that forks were indeed moving faster in downregulated cells compared to mock transfected, treated cells. Of note, the downregulation of the protein achieved by the second oligo was much less efficient, thus reinforcing the link between effective ZRANB3 depletion and unrestrained fork progression (Figure 2.3).

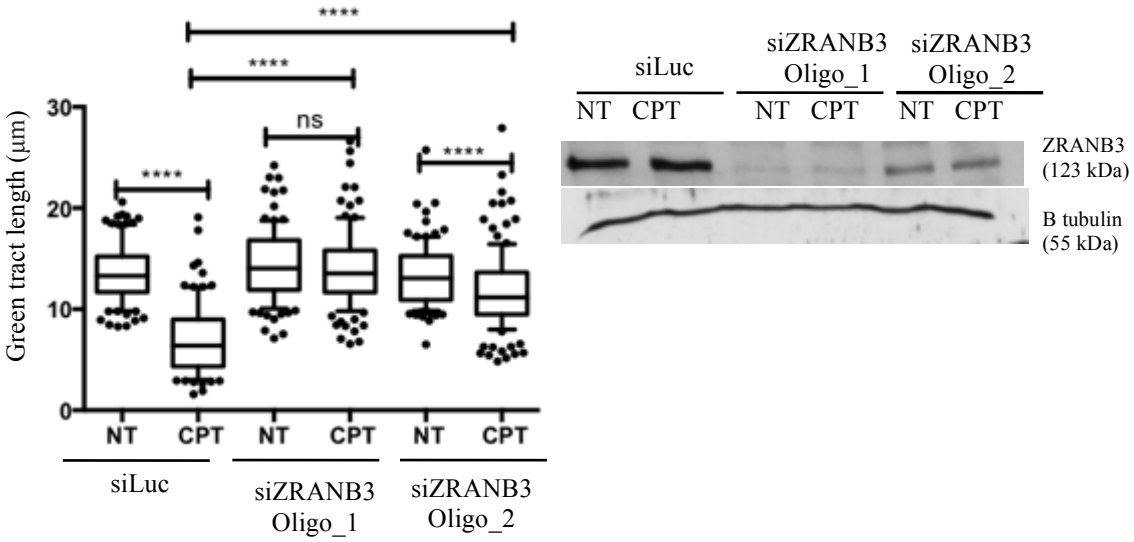

Figure 2.3 Testing additional siRNA for ZRANB3 downregulation. DNA fibers technique was again used to assess replication fork progression in the presence of genotoxic agent. Now, two different oligos for downregulation of ZRANB3 were used. U20S cells were provided with first nucleotide analogue, chlorodeoxyuridine (CldU). 30 min later, cells were washed and supplemented with second nucleotide analogue, iododeoxyuridine (IdU) with or without low dose of camptothecine (50nM) for 30 min. The length of the tracks synthesized during the second label (green tracks) was measured to assess the ability of cells to continue replication in the presence or absence of the genotoxic agents. At least one hundred tracts were scored per sample. Whiskers: 10-90th percentile (****, $P < 0.0001$; ns, non-significant, Mann – Whitney test. On the right is Western Blot showing efficiency of ZRANB3 downregulation. The experiment with Oligo_2 was done once.

2.2 Downregulation of ZRANB3 leads to impaired replication fork formation.

In light of the promising DNA fiber results we were encouraged proceed with direct visualization of replication intermediates, namely by electron microscopy (EM).

Firstly, we downregulated ZRANB3 protein by means of siRNA, and assessed reversed fork frequency upon genotoxic treatment. We could observe slightly elevated levels of reversed replication forks in ZRANB3-downregulated untreated cells (ca. 10% vs 3-5% of reversed replication forks usually observed in mock-transfected U2OS cells), possibly reflecting specific problems of the replication machinery to deal with some intrinsically difficult-to-replicate regions even, where fork reversal may provide additional time for replication machinery to solve replication interference. Interestingly, upon genotoxic treatments, the level of fork reversal in ZRANB3-depleted cells did not further increase (in the case of CPT where the frequency was around 11%), or increased only marginally (Figure 2.4), nicely reflecting our DNA fiber results (Fig. 2.1-2.2) and implicating ZRANB3 in the process of drug-induced replication fork reversal. As already mentioned, ZRANB3 was reported as capable of regressing stalled forks in vitro (Ciccia A, et al., 2012). To our knowledge, this is the first evidence *in vivo* that this protein plays a crucial role on the formation of reversed replication forks upon genotoxic treatment.

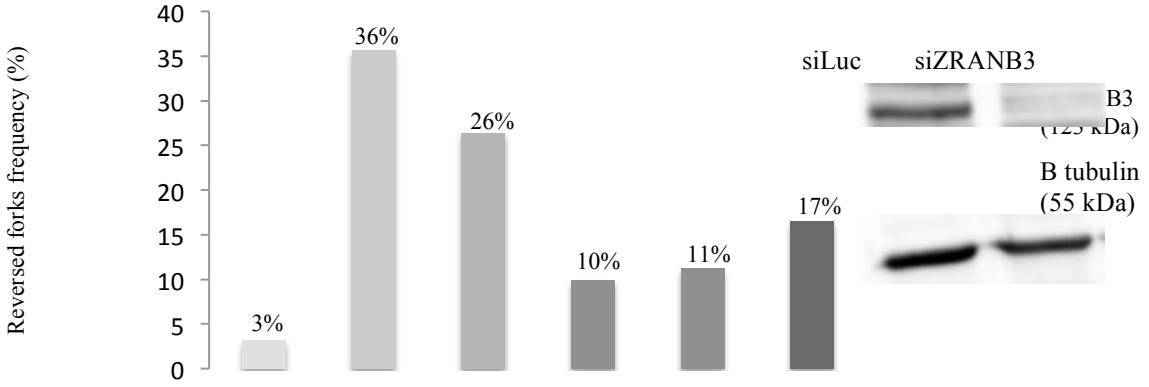

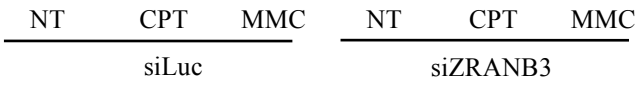

Figure 2.4 Cells with ZRANB3 downregulation show elevated levels of endogenous fork reversal, but no, or marginal reversed fork induction upon genotoxic treatments. Cells were depleted of ZRANB3 protein by means of siRNA interference, as done in fibers experiments (Fig. 2.1-2.3). Then the cells were treated with either CPT (50nM) or MMC (200nM) for one hour. Afterwards, cells were crosslinked in order to preserve replication intermediates, the DNA was extracted, spread on carbon-coated copper grids, and analyzed by transmission electron microscope (TEM) (more on the technique details in Neelsen K.J, et al., 2014). On the right part of the figure is Western Blot showing downregulation efficiency. Experiment was repeated twice.

2.3 ZRANB3 knock out cells.

To further exclude off-target effects and possibly strengthen our point that ZRANB3 is indeed involved in fork slowing and remodeling in vivo upon genotoxic stress, we decided to use ZRANB3 knock out (ZRANB3 KO) cells in our assays. The ZRANB3 KO cells were generated by the Crispr-Cas9 system and were a generous gift from David Cortez (Vanderbilt-Ingram Cancer Center, Vanderbilt University School of Medicine, Nashville, TN 37232, USA). Firstly, we decided to perform fiber assays, as it is fast assay usually predictive of a possible role in replication fork reversal.

2.3.1 ZRANB3 KO cells show no fork slowdown upon genotoxic treatment.

The results of the fiber experiments nicely matched our previous results obtained by means of siRNA downregulation.

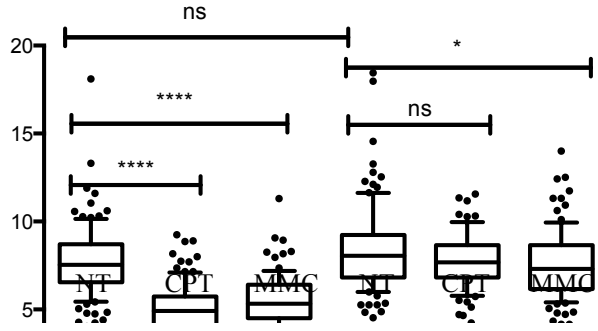

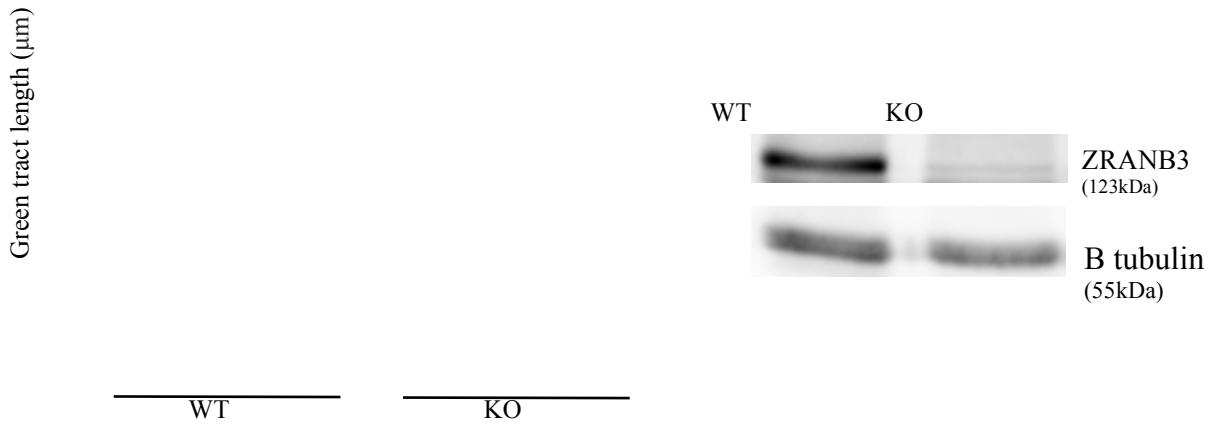

Figure 2.5 ZRANB3 Wild Type (WT) and Knock Out (KO) cells. DNA fibers technique was used to assess replication fork progression in presence of genotoxic agents. WT or ZRANB3 KO U2OS cells cells were provided with first nucleotide analogue, chlorodeoxyuridine (CldU). 30 min later, cells were washed and supplemented with second nucleotide analogue, iododeoxyuridine (IdU) with or without low dose of camptothecine (50nM) or mitomycin C (MMC) for 30 min. The length of the tracks synthesized during the second label (green tracks) was measured to assess the ability of cells to continue replication in the presence or absence of the genotoxic agents. At least one hundred tracts were scored per sample. Whiskers: 10-90th percentile (****, $P < 0.0001$; *, $P < 0.05$; ns, non-significant, Mann – Whitney test. On the right is Western Blot as an evidence that ZRANB3 is not present in KO cells. The experiment was repeated twice.

We used the same genotoxic treatments – CPT and MMC in low concentrations, treat the cells for 30 min, and assessed the lengths of the second label (green tracks). In WT cells the green labels upon treatments were significantly shorter than in non-treated cells, while in KO cells the green labels were approximately the same length in treated and non-treated cells, indicating the strict requirement of ZRANB3 for active fork slowing upon genotoxic stress (Figure 2.5).

2.3.2 ZRANB3 KO cells show impaired reversed fork formation.

In light of these promising DNA fiber data, we decided to use same knock out cells for EM experiments, using the same conditions as in knock down cells, i.e. low CPT and MMC treatment for 1h. In this experiment the results for reversed fork frequencies mirrored the data obtained by downregulation of the protein: there was initially a slightly elevated level of reversed forks in non-treated knock out cells (around 7%). However, there was only a marginal further induction of fork reversal after both treatments (13%) (Figure 2.6). These EM results prompted us to proceed with the experiments described below, aimed to dissect the role of different protein domains in fork slowing and remodeling.

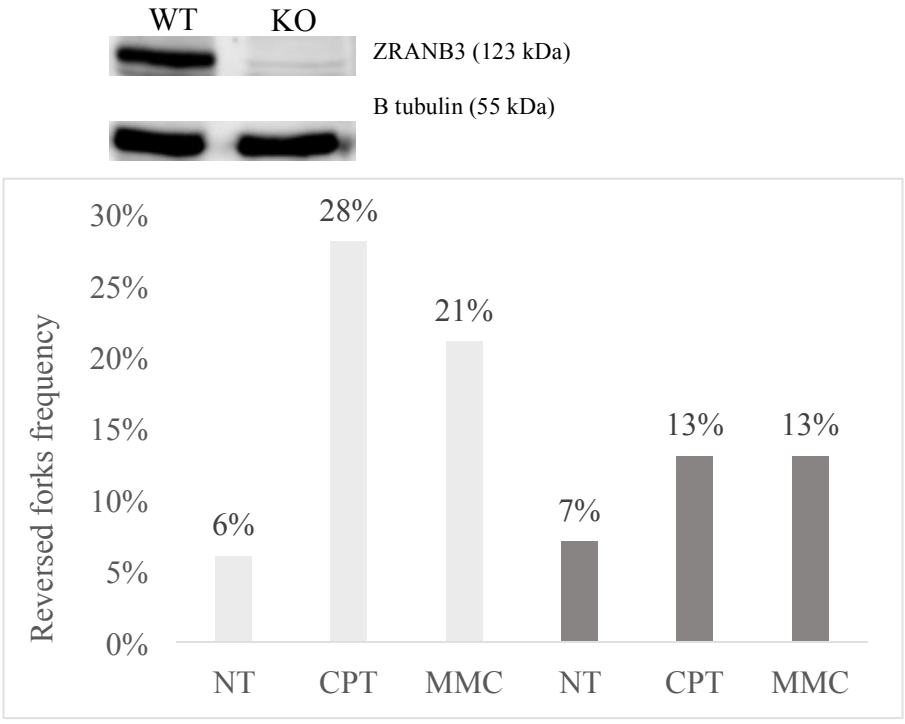

Figure 2.6 ZRANB3 KO cells show marginal reversed fork induction upon genotoxic treatment. WT or ZRANB3 KO U2OS cells treated with either CPT (50nM) or MMC (200nM) for one hour. Afterwards, cells were crosslinked in order to preserve replication intermediates, the DNA was extracted, spread on carbon-coated copper grids, and analyzed by transmission electron microscope (TEM) (more on the technique details in Neelsen K.J, et al., 2014). On the right part of the figure is Western Blot showing downregulation efficiency. Experiment was repeated twice. Western Blot confirming knock out cells have no traces of ZRANB3 is above the graph.

2.4 Generation of stable cell lines.

ZRANB3 protein has several domains, as described previously (Ciccia A, et al., 2012).

We thus aimed to assess the contribution of individual domains of the ZRANB3 protein in the process of fork slowing and reversal. To this aim, we decided to generate stable cell lines expressing different mutants of the protein. In order to achieve this, we decided to use ZRANB3 knock out cells, where we introduced retrovirus-based constructs harboring a selectable resistance to puromycin and genes encoding the FLAG-tagged wild type ZRANB3 protein or different mutants. The mutants that were produced had mutations in following domains: mutants in annealing helicase domain (HD, aspartic acid at position 157 and glutamic acid at position 158 changed to alanine), in endonuclease domain (ND, histidine at position 1045 changed to leucine in the domain responsible for interaction with polyubiquitinated PCNA (NZF, threonine at position 631 changed to leucine, and tyrosine at position 632 changed to valine), and domains responsible for interaction with PCNA (PIP, where glutamine at position 519 was changed to alanine, and isoleucine at position 522 was changed to alanine; APIM, where phenylalanines at position 525 and 526 were changed to alanines, and a stop codon was introduced instead of threonine at position 1073). I succeeded in generating all expressing stable cell lines, by the following procedure. I transfected Phoenix retrovirus producer cells with plasmids that were carrying the corresponding retroviruses. Afterwards, the media in which the cells were grown was collected and used for

the infection of the target cells, in this case ZRANB3 knock out cells. Cells were kept in selection media containing this antibiotic for few days until cells from control group (that were not infected, and are sensitive to puromycin), died out. If the integration took place in the infected cells, they were supposed to survive, while the cells with no integration should die, as control uninfected cells. At this point we decided to pursue two different strategies for collecting surviving cells expressing the protein. The first strategy was to collect all the surviving cells from particular mutant and check for the expression level. The second strategy was to have different dilutions of particular mutant cell lines and to try to obtain individual colonies, which were then further propagated. The ratio behind choosing the two different approaches was as follows: with the collection of all surviving (puromycin-resistant) cells we obtained mixed population of cells with virus being integrated at various places in genome, yielding an heterogeneous population in terms of transgene expression, but minimizing the risk of biological effects. Conversely, selection of individual clones enables to select cells expressing the trasngene at the same level, but bear the risk of positional effects of construct integration. Therefore, we decided to use both strategies in parallel, and identify cell populations and/or clones with similar levels of transgene expression and no obvious integration effect. Following these two strategies, we managed to create mutants in all relevant ZRANB3 domains, and also to re-introduce the wild type protein in the ZRANB3-KO cells. We used collection of the mixed population (the first strategy) for WT, NZF and PIP&APIM mutant. By means of Western Blot we showed that the expression level was similar to re-introduced wild type protein, and also to the endogenous wild type protein, detectable in the isogenic cell-line U2OS (Figure 2.7).

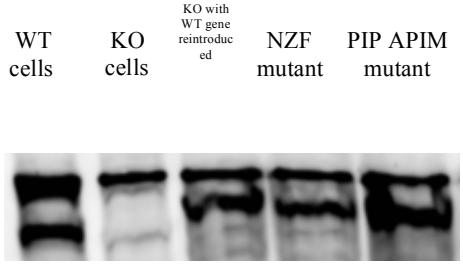

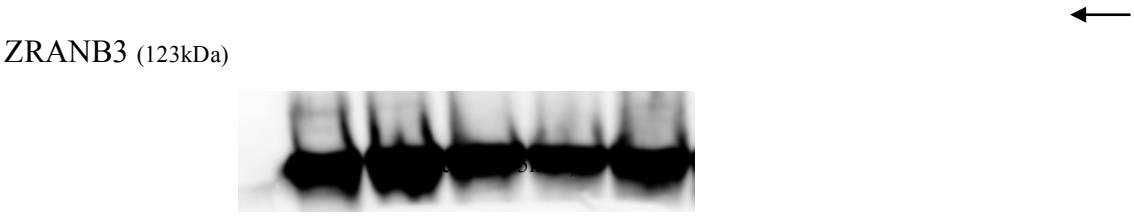

Figure 2.7 Generation of mutant cell lines – NZF and PIP APIM mutants. As described, these mutants were created by collecting the mixed population of cells from particular mutant. Nevertheless, for the two above mentioned mutants this approach could mimic the expression level of the protein in wild type cells, which was confirmed by Western Blot. The protein runs at slightly higher molecular weight than the protein extracted from wild type cells as it is FLAG-tagged.

The second approach - selection of individual clones, was used for the HD and ND mutant. We had multiple clones for each mutant, and we selected for future experiments just the ones that were expressing the protein at similar levels as clones where the wild type protein was reintroduced. Also we compared all the expression levels with the level of the protein in wild type cells, and it was comfortingly comparable. There, too, we saw that expression levels of reintroduced wild type protein and mutants was similar to the parental U2OS cells (Figure 2.8).

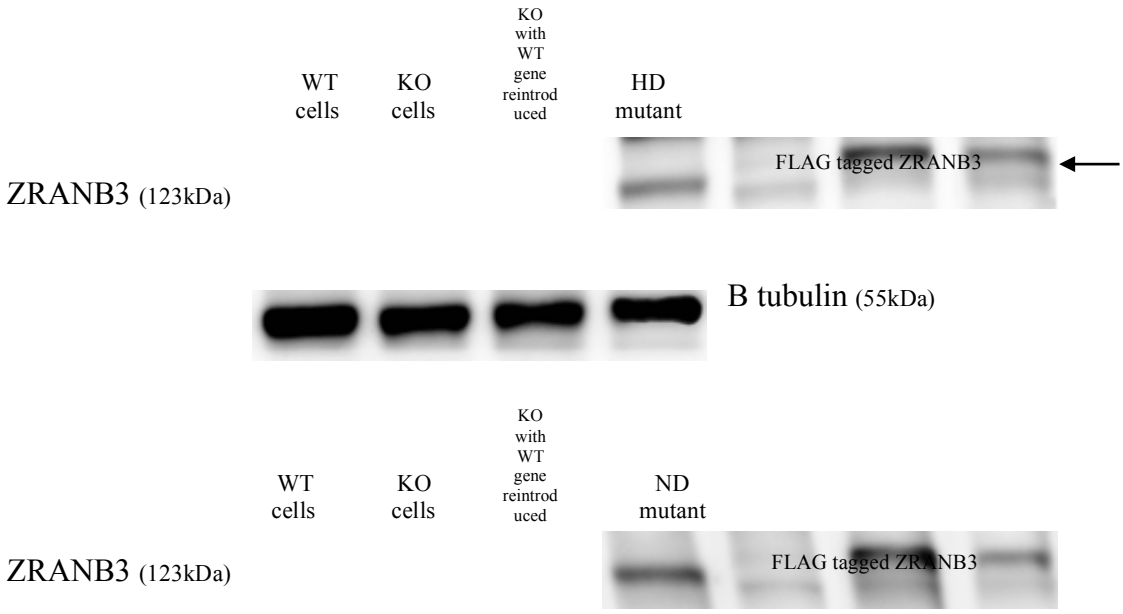

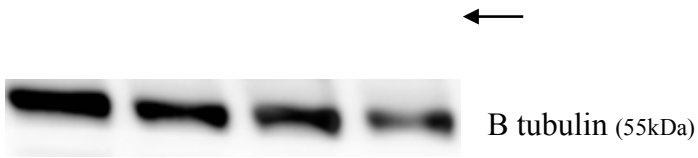

Figure 2.8 Generation of mutant cell lines – HD and ND mutants. As described, these mutants were created by selecting multiple clones. For the two above mentioned mutants this approach could mimic the expression level of the protein in wild type cells, which was confirmed by Western Blot. The protein runs at slightly higher molecular weight than the protein extracted from wild type cells as it is FLAG-tagged.

2.4.1 NZF, PIP&APIM and HD mutant show no fork slowdown upon genotoxic treatment.

Having obtained stable cell lines, we decided to explore the relative importance of individual domains in replication fork slowing and reversed fork formation, upon treatment with CPT (in light of the high number of cell lines, we limited this set of experiments to a single genotoxic agent). First we performed DNA fibers technique to assess the impact of the different mutations on replication speed. These results are preliminary, as these experiments were only performed once, but many of them are quite promising and in line with some other results within this thesis. The repetition is ongoing and will be completed after completion of this thesis, and prior to submission of the manuscript.

We could observe that reintroducing WT ZRANB3 in ZRANB3-KO cells restored CPT-induced replication fork slowing (compare Fig. 2.5 And Fig. 2.9). However, no significant fork slow down upon CPT treatment was observed reintroducing NZF, PIP&APIM and HD mutants, showing that all these domains are essential for active fork slow down upon genotoxic stress. Conversely, replication fork slowdown was restored in ZRANB3-KO cells even by reintroducing the ND mutant, suggesting that ZRANB3-nuclease activity is dispensable for active fork slowing. It should be noted that experiment with NZF and PIP&APIM mutant were done separately from that with HD and ND mutants, as the cell lines obtained came from different strategies of stable cell line production (pool of resistant cells

vs single clones, as described above (Figure 2.9). Accordingly, each set of mutants was compared to its own WT counterpart, obtained by the same strategy

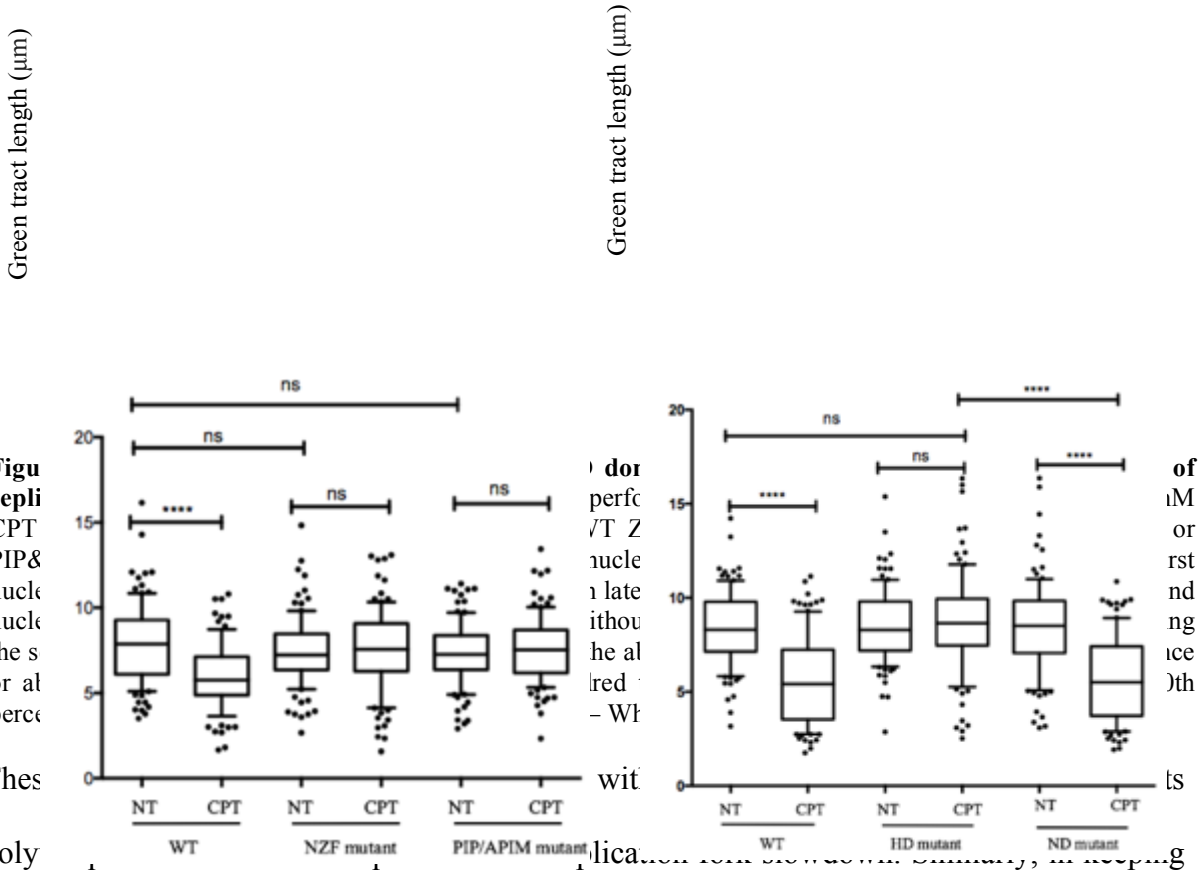

Figu **dor** **of**
repli perfo ıM
CPT /T Z or
PIP& ıucle rst
nucl ı late nd
nucl ithou ng
the s he al ıce
or al lred)th
perc – Wh

Thes wit ts

poly plica

with the published biochemical evidence on ZRANB3 fork regression activity, the helicase domain of ZRANB3 is required for fork slowdown upon damage. The only domain of ZRANB3 that seems dispensable for fork slowdown is the nuclease domain.

2.4.2 NZF, PIP&APIM and HD mutant show no fork slowdown upon genotoxic treatment

We next assessed the efficiency of replication fork reversal in vivo in all these cell lines. EM experiment showed that reintroducing the WT protein in ZRANB3-KO cells restored standard frequencies of fork reversal observed in the paternal cell line (ca. 3% in untreated, 25-30% in CPT-treated cells). Similar results were obtained reintroducing the NZF-mutant

protein, suggesting that, at least in these experimental conditions, the residual binding to PCNA and polyubiquitinated PCNA reported in this mutant (Ciccia et al., Mol Cell 2012) may be sufficient to induce fork reversal upon CPT treatment. Conversely, reintroduction of the PIP&APIM mutant, which displays fully defective PCNA-interaction (Ciccia et al., Mol Cell 2012), did not restore the original phenotype observed in ZRANB3-KO cells reintroduced with WT protein in terms of reversed fork frequency, both in both non-treated (higher basal level, around 9%) and CPT-treated cells (marginal induction, to about 13%) (Figure 2.10).

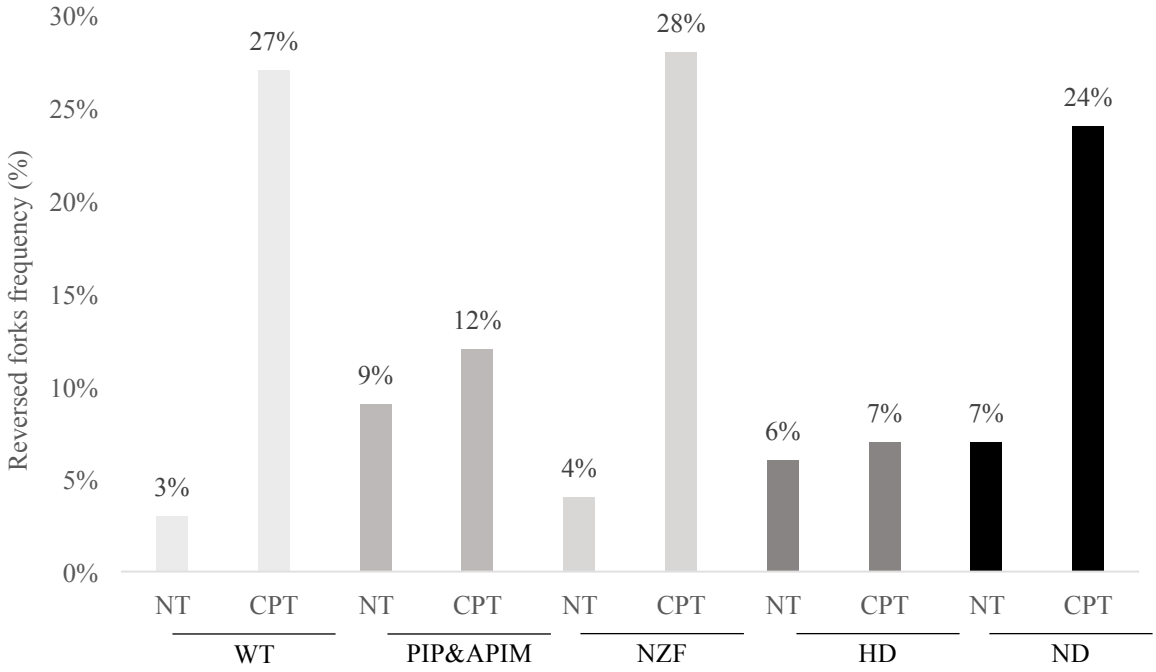

Figure 2.10 Mutations in PIP&APIM mutant lead to impaired reversed fork formation upon CPT treatment. U2OS cells expressing either WT or mutated versions of ZRANB3 protein were treated with CPT (50nM) for one hour. Afterwards, cells were crosslinked in order to preserve replication intermediates, the DNA was extracted, spread on carbon-coated copper grids, and analyzed by transmission electron microscope (TEM). Experiment was done once.

Interestingly, comparable results were obtained in the KO ZRANB3 cells with reintroduced helicase dead (HD) mutant of ZRANB3, both in untreated and treated conditions (6% of reversed replication forks in non-treated, and 7% in CPT treated cells). From these preliminary results we can conclude that the interaction with PCNA and annealing helicase activities of ZRANB3 are crucial for it to be able to efficiently reverse the forks. However, in our experimental conditions, full binding to polyubiquitinated PCNA (via a fully functional NZF domain - which is required for efficient fork slowing) and its nuclease domain, do not seem to be essential for fork reversal upon genotoxic stress.

2.5 PCNA and ubiquitin mutants

Upon damage PCNA gets monoubiquitinated at the lysine K164 (by Rad6-Rad18 complex) in the process of PRR, driving its error-prone branch by TLS. The error-free branch of this pathway requires polyubiqitination of the same PCNA residue, via formation of K63 linked ubiquitin chains by the E2 Mms2-Ubc13 and the E3 Rad5 in yeast (Rad5 has multiple putative orthologues in human cells, i.e. SHPRH, HLTF and TRAIP). This promotes template switching potentially and possibly entails the frequent fork reversal observed in human cells.
To test this possibility, we used two systems – the first one involved mouse embryonic fibroblasts (MEFs) that had PCNA mutated at lysine K164 to arginine, which cannot be ubiquitinated. The other system we used was tetracycline inducible replacement of endogenous ubiquitin with a specific mutant, that is defective in forming K63 polyubiquitin chains.

2.5.1 PCNA 164K mutant mouse embryonic fibroblasts

Mouse embryonic fibroblasts with a K164R mutation on PCNA were generously provided by Heinz Jacobs (Netherlands Cancer Institute, Amsterdam, The Netherlands), along with their WT counterpart. We wanted to determine whether inability to ubiquitinate PCNA at this particular site would prevent replication fork slowing and impair efficient fork reversal upon mild genotoxic treatments.

2.5.2 Mutating K164 in PCNA abolishes replication fork slowing upon DNA damage.

The DNA fiber assay was performed as in previous cases – cells were either non-treated or treated with low CPT and MMC doses for 30min during the second label. The length of this second label was measured and plotted.

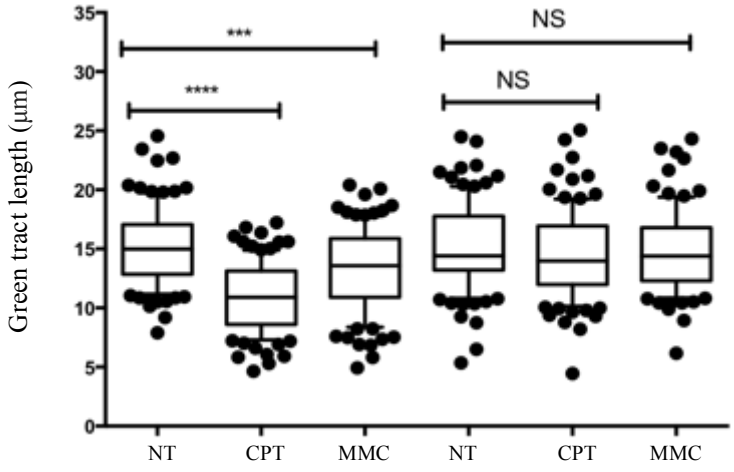

Figure 211. PCNA Wild Type (WT) and K164 mutant cells. Wild type or K164 mutant cells mouse embryonic fibroblasts (MEFs) were provided with first nucleotide analogue, chlorodeoxyuridine (CldU). 30 min later, cells were washed and supplemented with second nucleotide analogue, iododeoxyuridine (IdU) with or without low dose of camptothecine (50nM) or mitomycin C (MMC) for 30 min. The length of the tracks synthesized during the second label (green tracks) was measured to assess the ability of cells to continue replication in the presence or absence of the genotoxic agents. At least one hundred tracts were scored per sample. Whiskers: 10-90th percentile (****, P < 0.0001; ***, P < 0.001; ns, non-significant, Mann – Whitney test. The experiment was repeated twice.

Importantly, upon both CPT and MMC treatment, this single point mutation in PCNA abolished statistically significant replication fork slowing, while wild type MEFs displayed as expected significant reduction of fork speed. We therefore decided to investigate fork architecture in these cells by EM experiments (Figure 2.11).

WT K164 mutant

2.5.3 PCNA K164 mutant shows defective replication fork reversal upon genotoxic treatments.

Previous EM experiments published in our lab revealed that MEFs display a high basal level of reversed forks, probably resulting from replication stress associated with their immortalization procedure (Ahuja et al., 2016). However, fork reversal was further increased by both tested genotoxic treatments (Figure 2.12). MEFs bearing a K164 mutation in PCNA displayed a 2-fold reduction in the basal frequency of reversed forks, and only a marginal induction of fork reversal upon treatment (Figure 2.12).

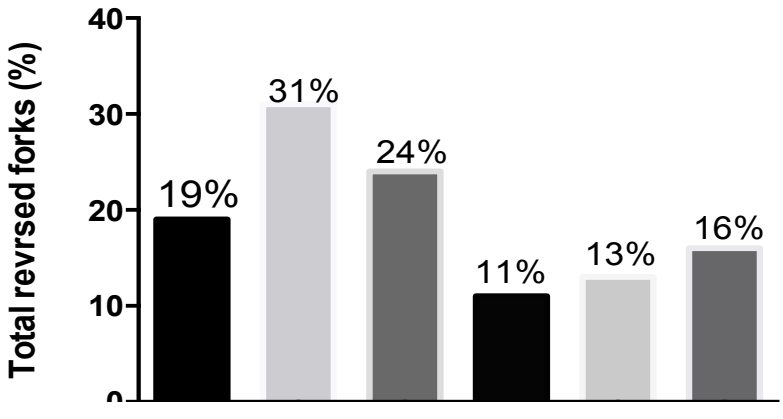

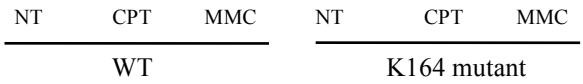

Figure 2.12 PCNA K164 mutant cells lines show no major induction of reversed replication forks upon genotoxic treatments. Mouse embryonic fibroblasts (MEFs) cells expressing either WT or K164R mutant PCNA protein were treated with either CPT (50nM) or MMC (200nM) for one hour. Afterwards, cells were crosslinked in order to preserve replication intermediates, the DNA was extracted, spread on carbon-coated copper grids, and analyzed by transmission electron microscope (TEM). Experiment was done twice.

2.5.4 Inducible replacement of endogenous ubiquitin with a K63 mutant.

Ubiquitin can form various types of chains (K6, K11, K27, K29, K33, K48, K63 and M1) linked at one of the seven different lysine residues on its N-terminus (Komander D, Rape M, 2012). We were interested in the ubiquitin mutant that cannot form K63-linked chains, as were shown to be formed on PCNA and involved in template switching events in the error-free PRR (refs?). We used a previously described U2OS-based cellular system (Xu et al., 2009), that enables tetracycline dependent downregulation of the endogenous ubiquitin (by

shRNA) and at the same time induces expression of exogenous (shRNA-resistant) ubiquitin, either WT or mutated at K63 (K63R).

The reason for choosing this system was that other available systems that enable, by transient transfection, downregulation of endogenous ubiquitin (by siRNA) and simultaneous overexpression of a specific mutant proved technically challenging. The main problem lays in the fact that cells need to be transfected twice, which in many cases is suboptimal in terms of cell survival. Also, from yeast to human, eukaryotic cells have 4 ubiquitin genes (UBC, UBA52, UBB and RPS27A), two of them encode linear polyubiquitin in which ubiquitin is linked to each other from ‘’head-tail’’, and the other two encode ubiquitin fused to ribosomal subunits (Finley et al., 1987). siRNA mediated depletion of the ubiquitin often leads to quite substantial left over of the endogenous protein, as it usually doesn’t lead to inactivation of expression from all ubiquitin genes.

In this system, the constructs have two expression cassettes, one was driven by tetracycline itself, and the other by IRES sequence (internal ribosome entry site – sequence that allows translation initiation in the middle of messenger RNA). Apart from ubiquitin genes, the constructs coded for HA tag and two ribosomal subunits (L40 and 27A), as their expression was also shut down together with endogenous ubiquitin (Figure 2.13)

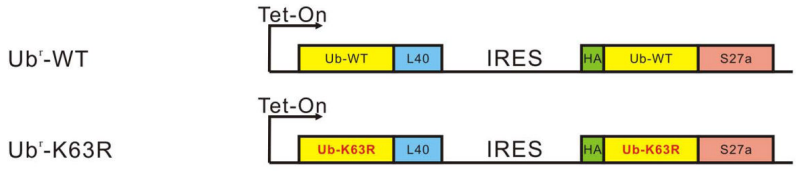

Figure 2.13 Scheme describing the two constructs used in ubiquitin replacement system. In yellow are depicted ubiquitin genes, in green HA, and red and blue are two different ribosomal subunits. Modified from Xu et al, 2009

The EM experiments performed using this system were performed upon doxycycline addition, comparing ubiquitin replacement with WT ubiquitin or with a K63R mutant. They showed that inability to form K63-linked chains leads to phenotypes similar to those observed in the PCNA-ubiquitination mutants and in ZRANB3-defective cells, i.e. there was only marginal reversed fork induction (13-14%) over background level (around 10%) following both CPT and MMC treatments (Figure 2.14).

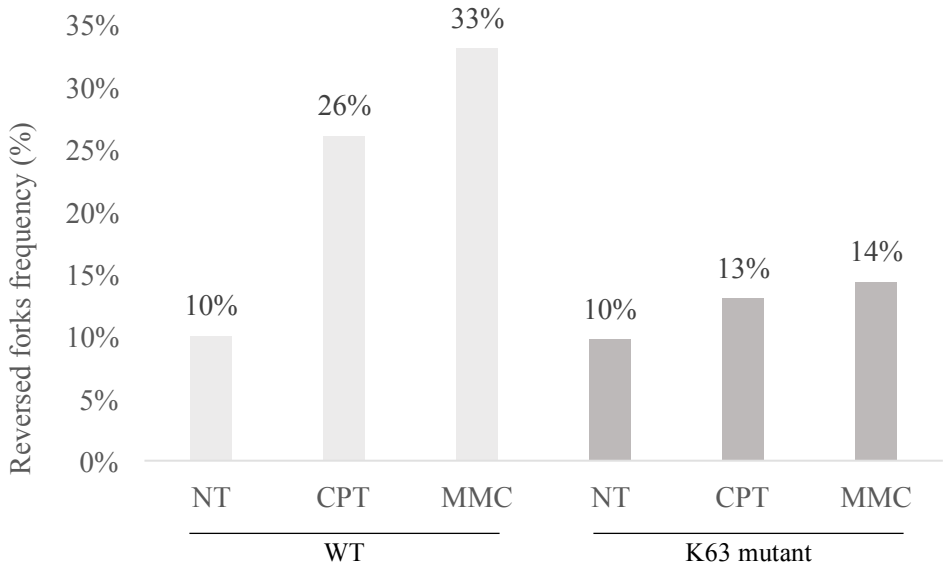

Figure 2.14 Cell lines expressing K63 mutant version of ubiquitin show no major induction of reversed replication forks upon genotoxic treatments. U2OS cells expressing either WT K63R mutant ubiquitin protein were treated with either CPT (50nM) or MMC (200nM) for one hour. Afterwards, cells were crosslinked in order to preserve replication intermediates, the DNA was extracted, spread on carbon-coated copper grids, and analyzed by transmission electron microscope (TEM). Experiment was done twice.

2.6 Ubc13 downregulation.

At least three different E3 ligases for PCNA polyubiquitination in human cells (SHPRH, HLTF, TRAIP; refs), making it difficult to effectively impair this PCNA modification by inactivation of the E3. However, Ubc13 was previously involved as the E2 in the process of polyubiqitination of PCNA at the K164 lysine and, more generally, in the formation of K63-linked ubiquitin chains (ref).Thus, to further test whether PCNA polyubiqutination is required

for fork reversal, we assessed whether inactivation of this E2 could lead to similar phenotypes as those described above for ZRANB3 defects, K164-PCNA mutant and ubiquitin K63 mutant. Again, replication fork speed and frequency of reversed replication forks were assessed upon CPT and MMC treatments.

2.6.1 Upon UBC13 downregulation there is partial rescue of the replication fork speed.

We used siRNA to deplete Ubc13 and then tested its effect in classical DNA fibers assay. Both mock transfected and downregulated cells were either treated or not with mild dose of MMC, then the fibers lengths were compared. As shown Figure 2.15, reduced UBC13 protein levels were associated with a partial defect in replication fork slowing upon MMC treatment (Figure 2.15).

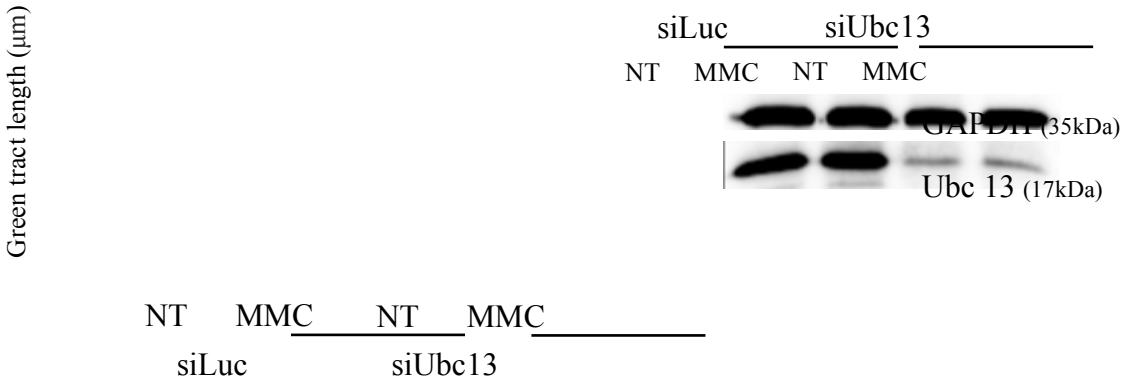

Figure 2.15 Ubc13 downregulation leads to rescue of replication fork speed upon genotoxic treatment. Ubc13 downregulated cells were provided with first nucleotide analogue, chlorodeoxyuridine (CldU). 30 min later, cells were washed and supplemented with second nucleotide analogue, iododeoxyuridine (IdU) with or without low dose mitomycin C (MMC) for 30 min. The length of the tracks synthesized during the second label (green tracks) was measured to assess the ability of cells to continue replication in the presence or absence of the genotoxic agent. At least one hundred tracts were scored per sample. Whiskers: 10-90th percentile (****, $P < 0.0001$; **, $P < 0.01$; ns, non-significant, Mann – Whitney test. The experiment was repeated at least twice.

In light o

cellular sy 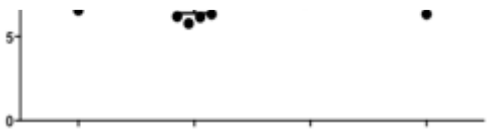 n of UBC13.

2.6.2 Ubc13 depletion leads to ineffective fork reversal induced by genotoxic agents.

Using optional siRNA-mediated downregulation of UBC13, we assessed the frequency of reversed forks in unperturbed cells or upon treatment with low doses of MMC and CPT for 1h.

The experiment revealed that downregulation of the Ubc13 protein lead to slightly increased basal levels of reversed forks, possibly indicative of accumulating replication stress, leading to UBC13-independent fork reversal. However, UBC13 downregulation drastically impaired genotoxin-dependent induction of reversed forks (Figure 2.16).

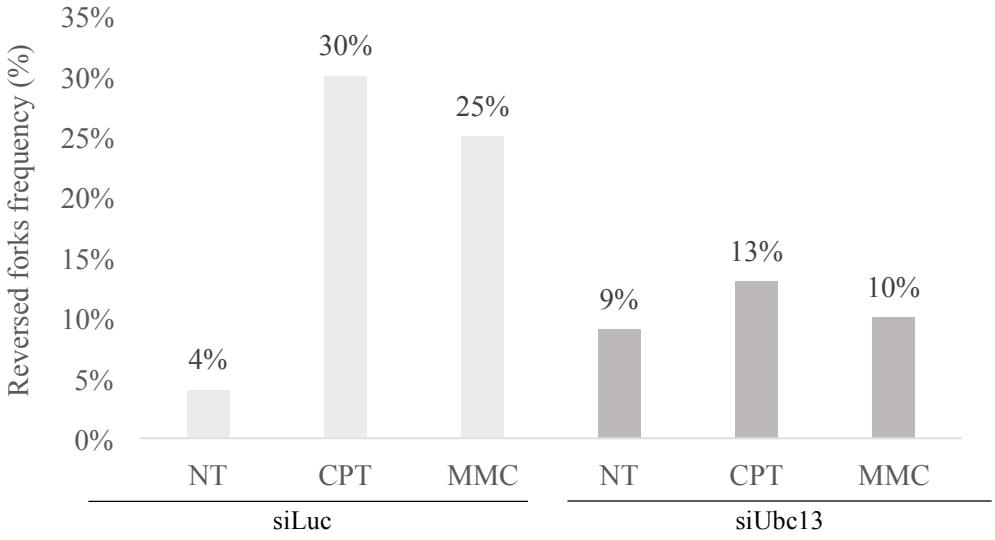

Figure 2.16 Cells with Ubc13 downregulation show no, or marginal reversed fork formation upon genotoxic treatment. U2OS cells were depleted of Ubc13 protein by means of siRNA interference, as in fibers experiments. Then the cells were treated with either CPT (50nM) or MMC (200nM) for one hour. Afterwards, cells were crosslinked in order to preserve replication intermediates, the DNA was extracted, spread on carbon-coated copper grids, and analyzed by transmission electron microscope (TEM). Experiment was done twice.

2.7 Ubc13 knock out cells.

To avoid potential off target effects of the siRNAs that we used and to assess whether partial effects reflected the residual levels of UBC13 protein, we decided to perform similar

experiments on a HCT116 UBC13 knock out cell line, obtained as a generous gift from Niels Meiland from University of Copenhagen (Copenhagen, Denmark).

2.7.1 Ubc13 KO cells have unrestrained replication fork progression upon low doses genotoxic treatment.

Since the KO cells were obtained relatively recently, these experiments were only performed once and the results should thus be considered as preliminary. The results we obtained to a great extent match the results from the knock-down cells. In the fibers assay, we decided to test both drugs we usually use, CPT and MMC. We treated the cells based on the usual labelling scheme and then assessed the replication fork progression during the second label (upon optional treatment with CPT or MMC). UBC13 KO cells are completely defective in active fork slowing upon both treatments (Fig. 2.17). This result confirms our initial observations obtained by siRNA in U2OS cells and strongly suggest that the partial effects observed upon downregulation result from residual UBC13 protein levels in those conditions.

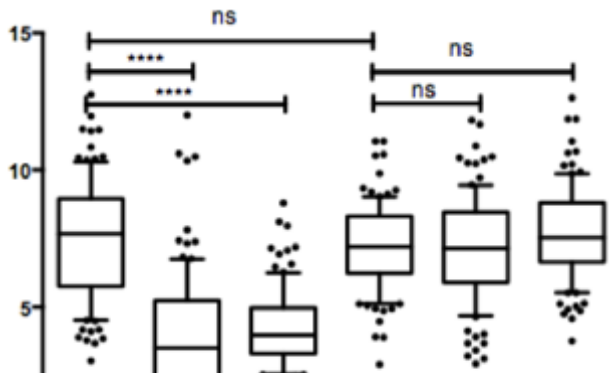

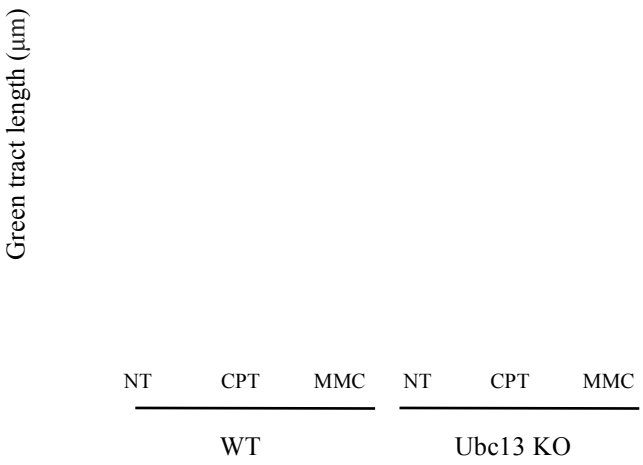

Figure 2.17 Ubc13 KO cells show complete rescue of replication fork speed upon genotoxic treatment. Ubc13 KO HCT116 cells were provided with first nucleotide analogue, chlorodeoxyuridine (CldU). 30 min later, cells were washed and supplemented with second nucleotide analogue, iododeoxyuridine (IdU) with or without low dose camptothecin (CPT, 50nM) or mitomycin C (MMC, 200nM) for 30 min. The length of the tracks synthesized during the second label (green tracks) was measured to assess the ability of cells to continue replication in the presence or absence of the genotoxic agent. At least one hundred tracts were scored per sample. Whiskers: 10-90th percentile (****, P < 0.0001; ns, non-significant, Mann – Whitney test. The experiment was done once.

2.7.2 Ubc13 KO cells fail to increase the frequency of reversed replication forks upon genotoxic treatments.

We next treated the both WT and KO cells with CPT and MMC for one hour, isolated DNA and assessed reversed fork frequency by our classical EM protocol. The results showed us that control HCT116 cells react to treatments as observed in numerous other cell lines, i.e. by a substantial accumulation of reversed forks upon both CPT and MMC treatments (27% and 21%. respectively). However, as already observed upon ubiquitin replacement with the K63R mutant, UBC13 KO cells, displayed elevated basal levels of reversed forks, but no further significant induction of fork reversal after either CPT or MMC (11% and 12% respectively) (Figure 2.18). Overall, the data in Figs. 2.11-2.18 strongly suggest that PCNA polyubiquitination is required for replication fork reversal in vivo. As every other lab attempting this to date, we have been so far unsuccessful in directly revealing endogenous levels of PCNA polyubiquitination upon conditions of mild replication stress. A few

unsuccessful attempts are described below (see 2.9), but a new set of experiments is currently ongoing, using different strategies for the enrichment of this rare modification.

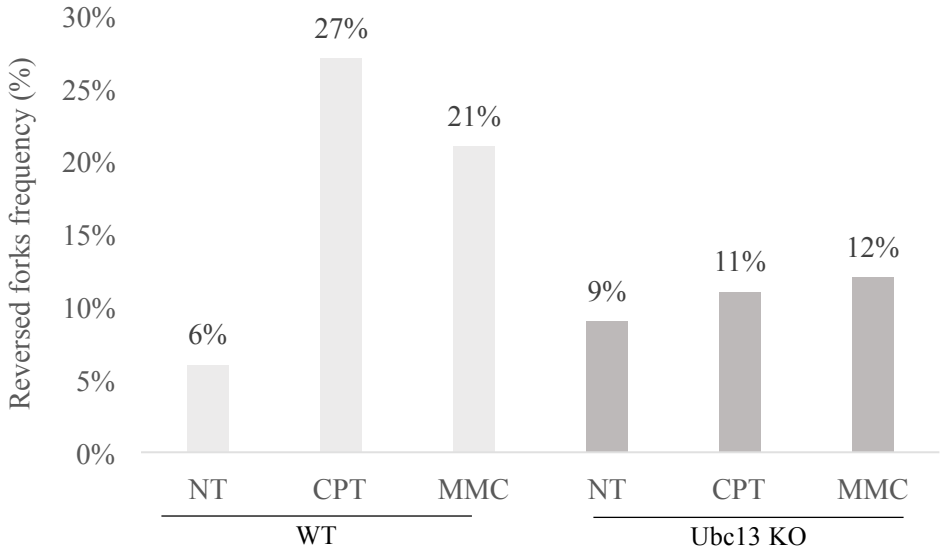

Figure 2.18 Ubc13 KO cells show no, or marginal reversed fork formation upon genotoxic treatment. The HCT116 WT or Ubc13 KO cells were treated with either CPT (50nM) or MMC (200nM) for one hour. Afterwards, cells were crosslinked in order to preserve replication intermediates, the DNA was extracted, spread on carbon-coated copper grids, and analyzed by transmission electron microscope (TEM). Experiment was done once.

2.8 Additional experiments.

2.8.1 Werner syndrome protein.

Previous studies used oligonucleotide based substrates and could show that Werner syndrome protein (WRN) has an ability to both form and restore reversed replication forks (Kangaraj R, et al., 2006; Machwe A, et al., 2006; Machwe A, et al., 2007). Mutations in this protein lead to Werner syndrome, mostly known for the accelerated aging in affected individuals. We thus reckoned that WRN could be a potentially interesting candidate to assess fork slowing and reversal in vivo. We performed initial fibers experiments, but - despite effective WRN downregulation - we failed to observe defective replication fork slowing upon mild CPT treatment (Figure 2.19), which is usually a predictive phenotype for defective fork reversal.

The next section includes the results of additional experiments performed on WRN, as part of a collaborative effort with the lab of A. Vindigni in St. Louis, USA (see 2.10).

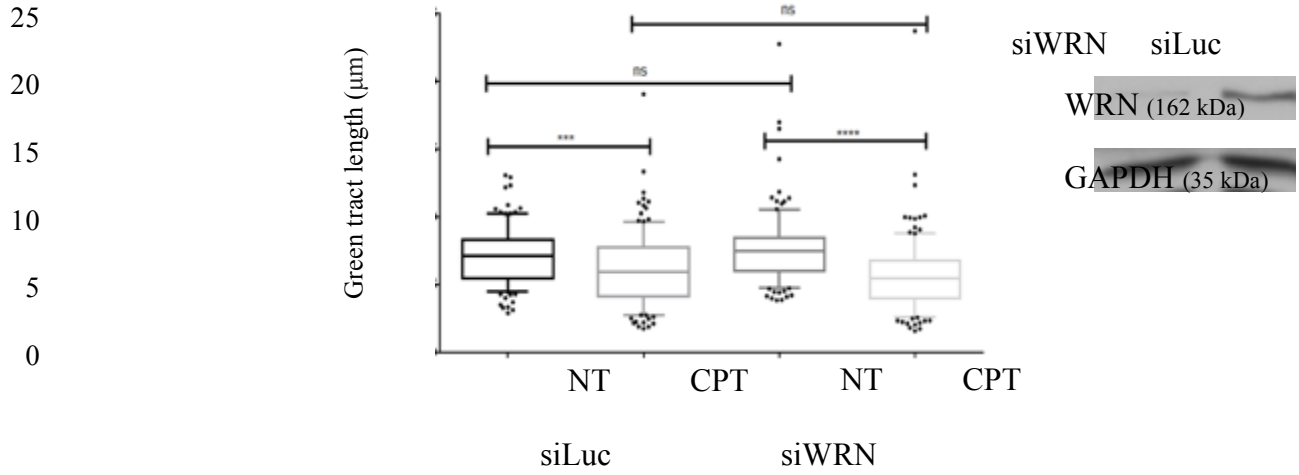

Figure 2.19 Downregulation of WRN showed no influence on replication fork progression upon mild CPT treatment. Cells were either mock transfected or depleted of WRN protein using siRNA. Afterwards, cells were provided with first nucleotide analogue, chlorodeoxyuridine (CldU). 30 min later, cells were washed and supplemented with second nucleotide analogue, iododeoxyuridine (IdU) with or without low dose (50nM) camptothecin (CPT) for 30 min. The length of the tracks synthesized during the second label (green tracks) was measured to assess the ability of cells to continue replication in the presence or absence of the genotoxic agent. At least one hundred tracts were scored per sample. Whiskers: 10-90th percentile (****, $P < 0.0001$; ***, $P < 0.001$; ns, non-significant, Mann – Whitney test. The experiment was done twice.

2.8.2 HARP (SMARCAL1).

As explained in detail in the introduction, HARP was the first annealing helicase to be described (Yusufzai and Kadonaga, 2009). It also has both fork regression (oligonucleotide and plasmid based assays) and fork restoration activity (only oligonucleotide based). RPA addition to these biochemical reactions, which contributes to having these biochemical assays in more physiological conditions, has a strong influence on HARP enzymatic activity and substrate specificity (Betous R, et al., 2013). For these reasons, we tested its requirement for replication fork slowing and reversal in vivo.

2.8.2.1 Depletion of Harp impairs reduction of replication fork speed upon mild CPT treatments.

As in the case of WRN, we started by testing whether HARP depletion by siRNA could affect in any way replication fork progression in the conditions of mild replication stress induced by mild CPT treatment. We observed that HARP depletion leads to a complete defect in reducing replication fork speed upon CPT treatment.

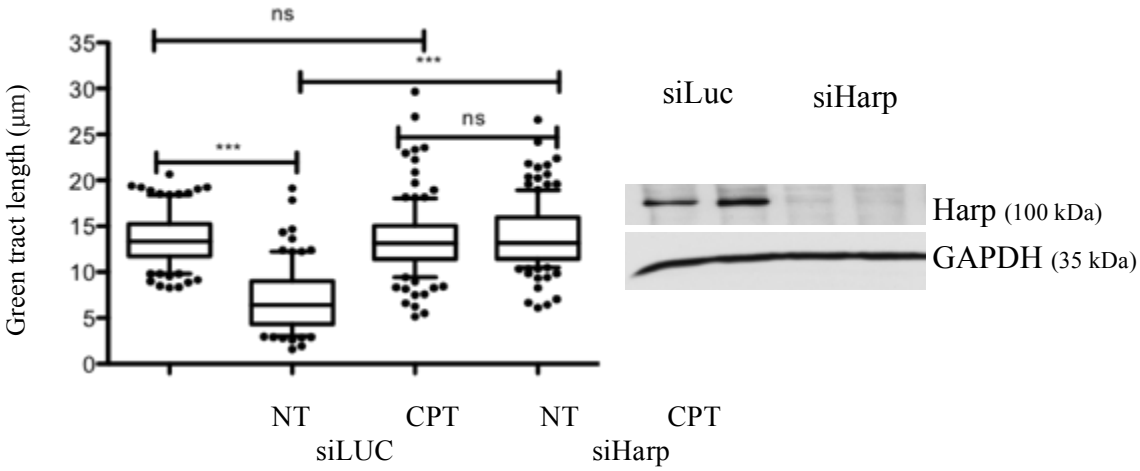

Figure 2.20 Harp depletion leads to complete replication fork speed rescue. Cells were either mock transfected or depleted of HARP protein using siRNA. Afterwards, cells were provided with first nucleotide analogue, chlorodeoxyuridine (CldU). 30 min later, cells were washed and supplemented with second nucleotide analogue, iododeoxyuridine (IdU) with or without low dose (50nM) camptothecin (CPT) for 30 min. The length of the tracks synthesized during the second label (green tracks) was measured to assess the ability of cells to continue replication in the presence or absence of the genotoxic agent. At least one hundred tracts were scored per sample. Whiskers: 10-90th percentile (***, $P < 0.001$; ns, non-significant, Mann – Whitney test). The experiment was done at least twice. On the right is Western Blot showing downregulation efficiency.

We also perform simultaneous knock down of Harp and ZRANB3 together. In light of the results obtained with individual downregulations (Figs. 2.1 and 2.20), it was not surprising to observe a complete defect in CPT-induced fork slowing also simultaneous downregulation of both cellular factors in U2OS cells (Fig. 2.21).

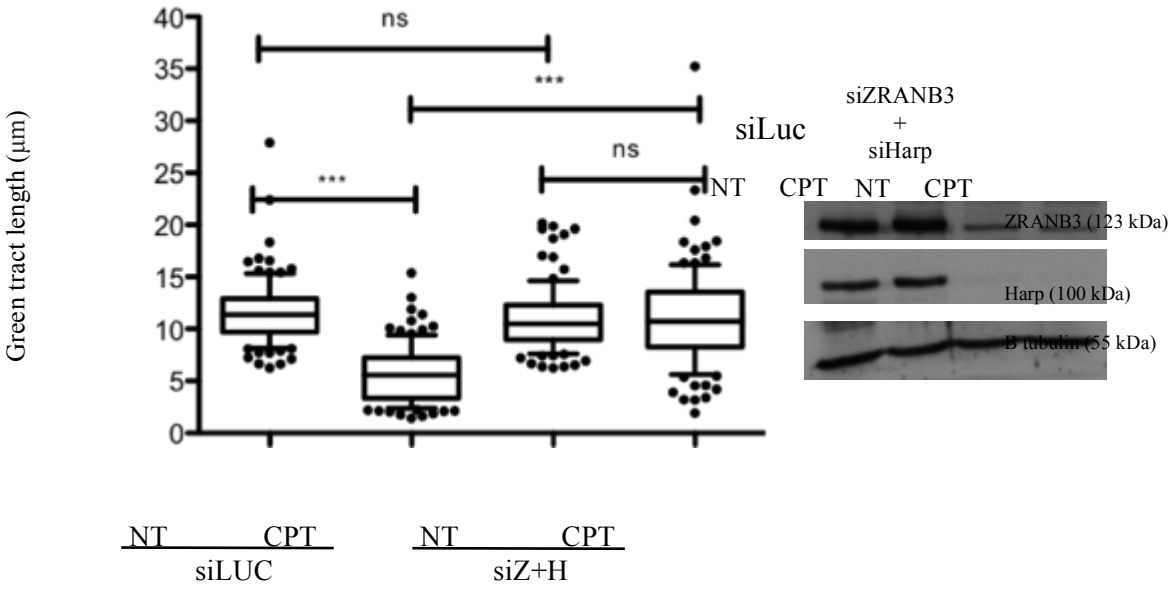

Figure 2.21 Double Harp and ZRANB3 depletion leads to complete replication fork speed rescue. Cells were either mock transfected, depleted of both HARP and ZRANB3 proteins using siRNA. Afterwards, cells were provided with first nucleotide analogue, chlorodeoxyuridine (CldU). 30 min later, cells were washed and supplemented with second nucleotide analogue, iododeoxyuridine (IdU) with or without low dose (50nM) camptothecin (CPT) for 30 min. The length of the tracks synthesized during the second label (green tracks) was measured to assess the ability of cells to continue replication in the presence or absence of the genotoxic agent. At least one hundred tracts were scored per sample. Whiskers: 10-90th percentile (***, $P < 0.001$; ns, non-significant, Mann – Whitney test). The experiment was done once. On the right is Western Blot showing downregulation efficiency.

2.8.2.2 Harp depletion leads to partial decrease in reversed fork frequency upon genotoxic treatment.

Following the logic that replication fork slowdown is usually coupled to reversed fork accumulation, we were expecting that defective replication fork slowdown would be accompanied by a drastic reduction in the frequency of reversed forks.

However, despite the complete defect in fork slowing observed upon HARP downregulation, when we assessed by EM fork reversal in U2OS upon downregulation of Harp following 1h low dose CPT treatment, we only found a 2-fold reduction in reversed fork frequency (from around 36% in mock transfected to around 18% in downregulated cells; Fig. 2.22). As already observed for other defects in drug-induced reversal (e.g. ZRANB3 or UBC13 inactivation) the basal levels of reversed forks were found to be slightly increased, likely resulting from accumulated replication stress, leading to HARP-independent fork reversal.

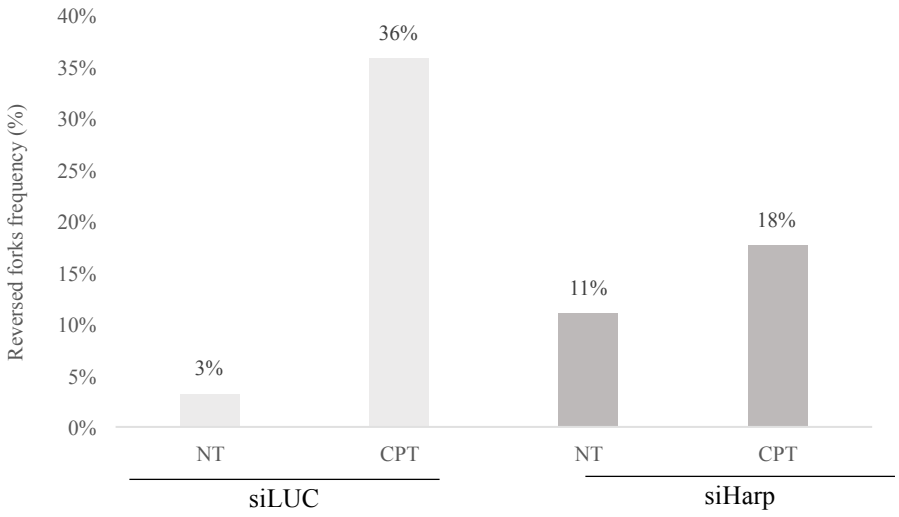

Figure 2.22 Cells with Harp downregulation show no, or marginal reversed fork formation upon genotoxic treatment. U2OS cells were depleted of Harp protein by means of siRNA interference, as in fibers experiments. Then the cells were cells were treated with CPT (50nM) for one hour. Afterwards, cells were crosslinked in order to preserve replication intermediates, the DNA was extracted, spread on carbon-coated copper grids, and analyzed by transmission electron microscope (TEM). Experiment was done once.

In light of the less striking results obtained with HARP, we decided to focus our investigation on PRR and ZRANB3, and we plan to continue our investigations on HARP once a first research manuscript will be submitted on PRR/ZRANB3, containing most of the data described above.

2.9 Following polyubiquitination of PCNA with Western Blot and Chromatin enrichment.

In parallel to our efforts to elucidate the contribution of mono- and poly-ubiquitination (via K63 ubiquitin chains) of PCNA to the process of fork reversal by means of DNA fibers and EM technique, we invested considerable effort in the attempt to directly observe endogenous PCNA polyubiqutination and thereby to identify its genetic dependencies upon conditions of mild replication stress.

We initially tried to use whole cell extracts in classical Western Blotting to detect mono- and poly- ubiquitination of PCNA, after very harsh treatment of the cells (30-40 J/m2 of UV

irradiation with 4h recovery, or 30 μM MMC treatment for 24 hours), using a total PCNA antibody. Although in certain conditions the antibody did recognize monoubiquitinated PCNA, we failed to reproducibly observe additional retarded bands, expected to represent polyubiquitinated PCNA (data not shown).

We next decided to use chromatin extracts, designed to eliminate all cytoplasmic and nucleoplasmid proteins and enrich for those stably bound to chromatin, where PCNA is expected to reside while performing its function. Furthermore, upon western blotting, we used a specific antibody raised against PCNA ubiquitinated at the K164 residue, reckoning that this antibody may also specifically detect polyubiqitinated forms of PCNA.

Somehow promisingly, following 40 J/m2 of UV irradiation with 4h or 12h recovery, by this approach we could clearly detect bands appearing above monoubiquitinated PCNA, which were not detected in the same samples by the total anti-PCNA antibody (Figure 2.23).

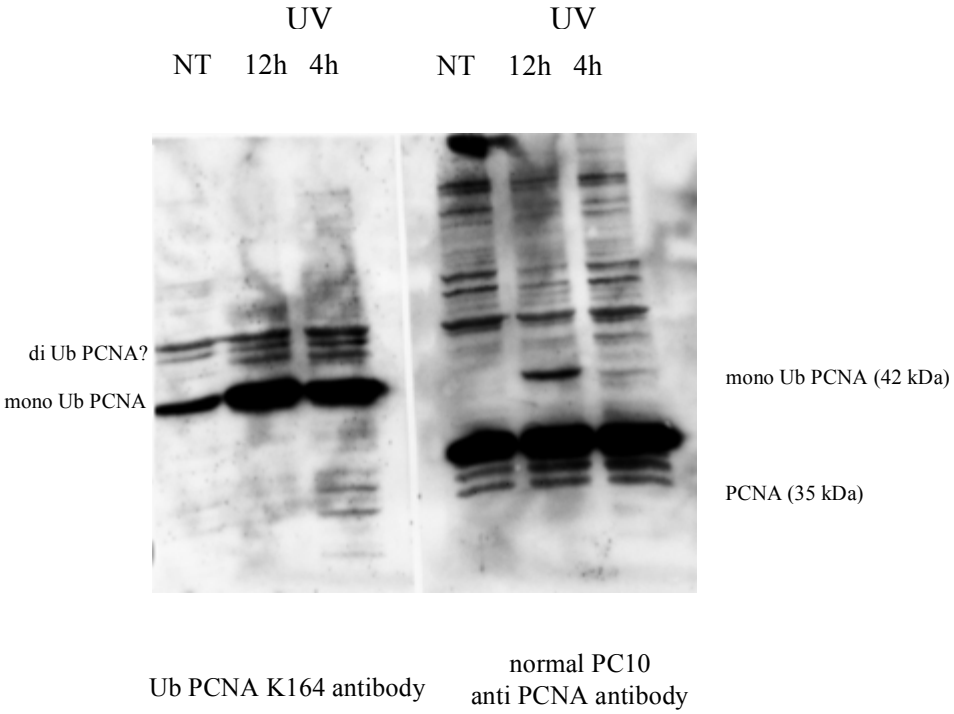

Figure 2.23. **Mono and potential polyubiquitination of PCNA following 40 J/m^2 of UV irradiation with 4 or 12h recovery.** Cells were irradiated, then the chromatin was enriched and run on Western Blot gel. For blotting we used specific antibody recognizing monoubiquitination of PCNA at specific residue – K164 and also standard PCNA antibody on the side to compare results.

Inspired by the detection of these upper bands, we assessed whether they showed the expected genetic dependencies for PCNA polyubiquitination, upon downregulation of factors that should either abrogate them – namely Rad18 and Ubc13 - or enhance them, as for downregulation of PCNA deubiquitinating enzyme USP1. Therefore, we performed experiments where we had combinations of these proteins depleted by siRNA and collected protein samples 12h after optional 40 J/m2 UV irradiation following. Unfortunately, we could not confirm any of the expected genetic dependencies, by intensification or disappearance of the bands detected above monoubiquitinated PCNA (Fig. 2.24). We only confirmed the expected effect of RAD18 depletion on PCNA mono-ubiquitination, which confirmed sufficient downregulation of this protein (Figure 2.23-2.24). These results suggest that the retarded bands observed above mono-ubiquitinated PCNA are unlikely to represent poly-ubiquitinated PCNA.

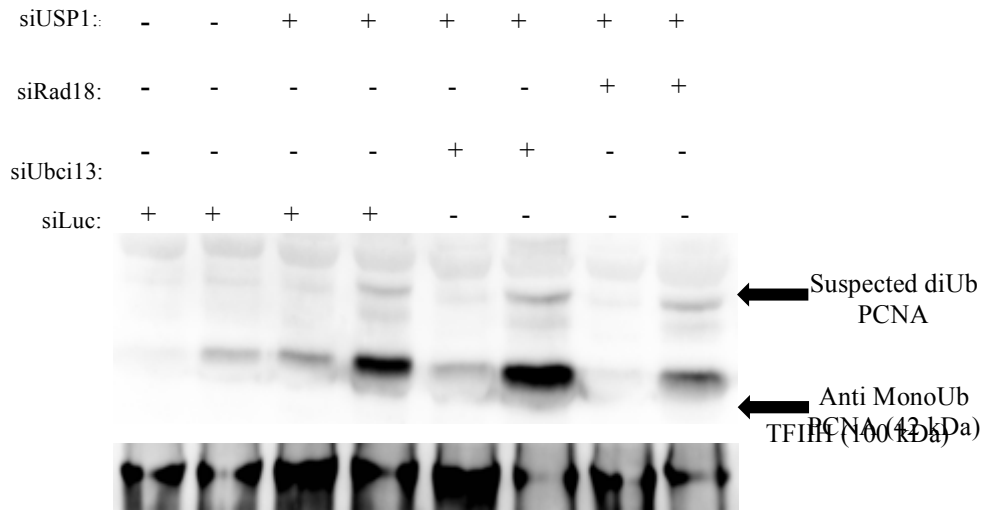

Figure 2.23. **Suspected diUb PCNA band does not seem to show genetic dependencies.** Cells were downregulated, and then treated with **40** J/m^2 of UV irradiation with 12h recovery. Then the chromatin fraction was isolated, and the chromatin bound proteins were ran on Western Blot.

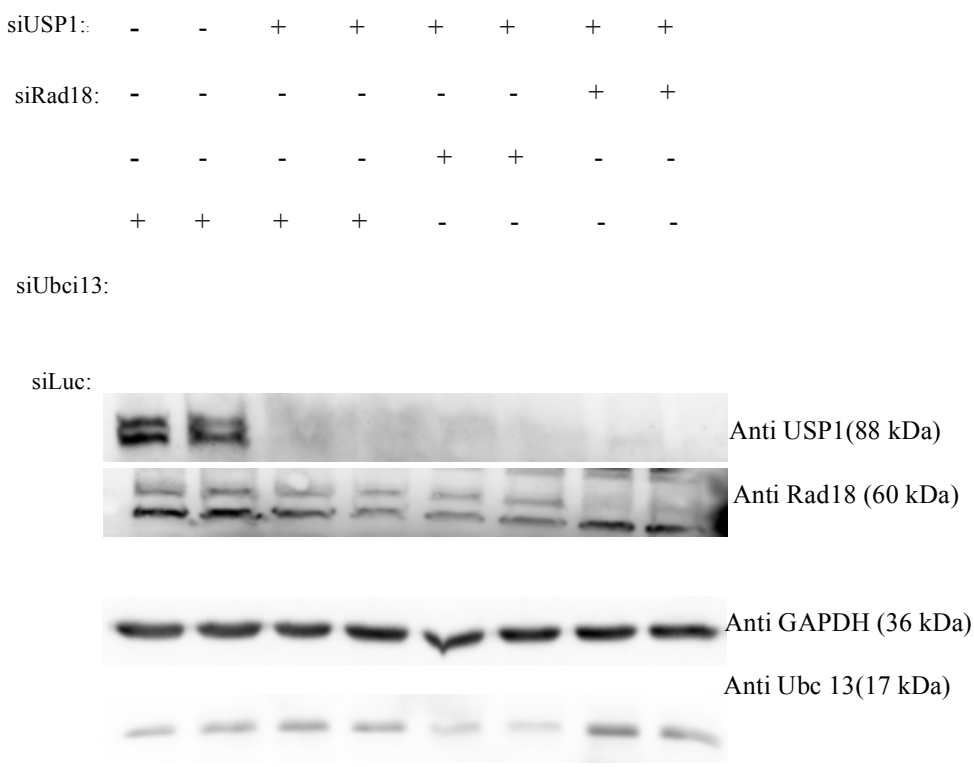

Figure 2.24. **Western Blot showing downregulation efficiency of particular proteins.**

Since we could not confidently follow endogenous polyubiquitination of PCNA (mostly diUbPCNA), we decided to try to express either wild type or K63 mutant FLAG tagged ubiquitin in HEK293T cells, treat them with high doses of UV as in previous experiments, and perform chromatin enrichment, followed with immunoprecipitation using anti-FLAG beads. We reasoned that this way we could enrich for ubiqitinated species, among them mono, di, tri etc. Ub PCNA molecules. So we transfected the cells with either empty vector, FLAG tagged WT ubiquitin, or FLAG tagged K63 mutant ubiquitin. Then we treated them with 40 J/m2 of UV irradiation following 12h recovery and then performed above mentioned procedure. Even in the cells expressing K63 mutant we could still see the and above monoubiquitinated PCNA band (Figure 2.25), further suggesting that this band does not entail K63-dependent PCNA polyubiqutination and may instead represent a different type of post-translational modification of PCNA.

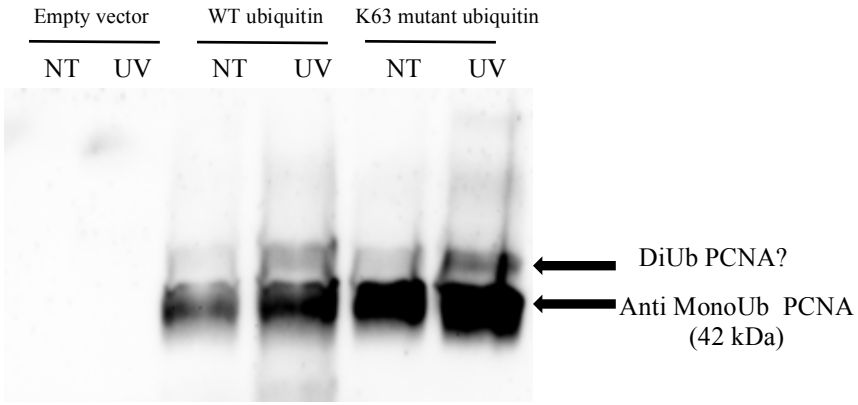

Figure 2.25. **Western Blot showing monoubiquitinated PCNA that was immunoprecipitated from the cells expressing either wild type or K63 mutant version of ubiquitin.** Cells were transfected, then left untreated or treaded with UV, chromatin enrichment was performed and then

To consolidate these results, we also decided to use the ubiquitin replacement system, already described in chapter 2.5.4. This tetracycline inducible system allows for shut down of expression of endogenous ubiquitin, and expression of HA tagged WT or HA tagged K63 mutant. In the absence of Tet, endogenous ubiquitin is expressed, while in its presence either the WT or the K63R-ubiquitin mutant replace endogenous ubiquitin. We optionally treated the cells with high doses of MMC (15 μM; 24h), to possibly boost PCNA ubiquitination), and performed chromatin enrichment prior to protein analysis by Western Blot with the Ub-PCNA antibody (Fig. 2.26)

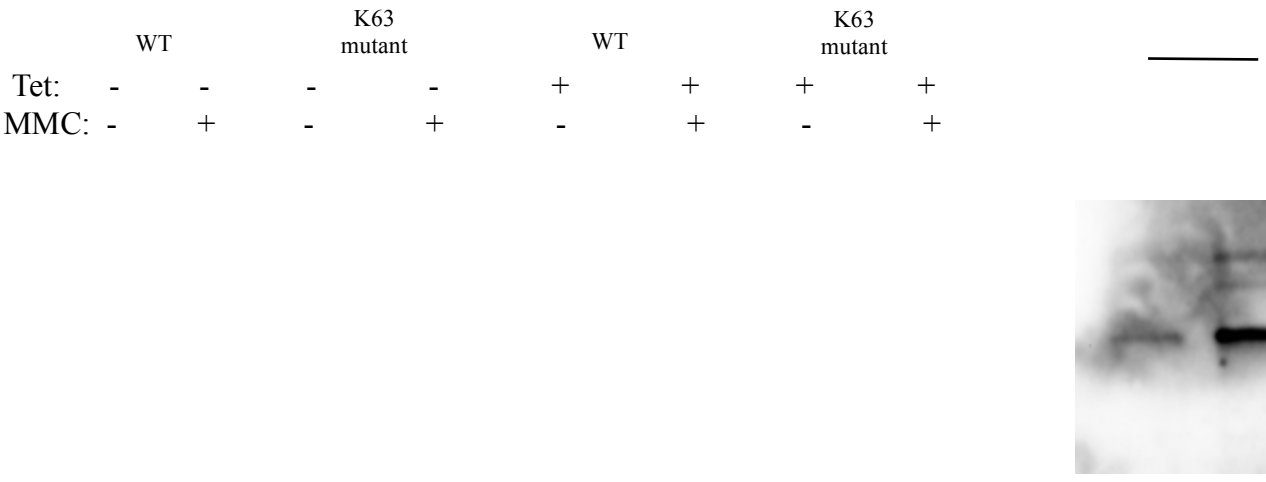

Figure 2.26. **Western Blot showing monoubiquitinated PCNA isolated from cells that were expressing either WT or K63 mutant ubiquitin.** After treatment with 15 μM of MMC for 24h, chromatin was enriched and then ran on Western Blot.

Also in this case, we detected retarded bands above mono-ubiquitinated PCNA, but we failed to observe any difference in the intensity of those bands when endogenous ubiquitin is replaced by the K63R mutant. Thus, these bands seem unrelated from K63-linked polyubiquitin chains and we need to conclude that we have not yet identified controlled experimental conditions to reveal endogenous levels of polyubiquitinated PCNA. Additional experiments, based on different methods of enrichment, are currently ongoing in the lab and may possibly lead to successful detection of polyubiquitinated PCNA.

2.10 Contribution to collaborative projects with the lab of Prof. Alessandro Vindigni (Department of Biochemistry and Molecular Biology, Edward A. Doisy Research Center, Saint Louis University School of Medicine, St. Louis, USA).

2.10.1 RecQ1 involvement in reversed replication fork restart.

A previous study from our lab had showed that inhibition of PARP1 activity led to dramatic drop of reversed replication fork frequency upon low doses of camptothecin (Ray Chaudhuri A, et al., 2012). I participated in 2012 into a first collaborative project with the Vindigni lab, investigating the role of RecQ1 helicase in the process of reversed replication forksrestart. The work was published in 2013 in Nature Structural and Molecular Biology, and the manuscript is here included in the next few pages. In this study it was shown that RecQ1 interacts with PARylated PARP1, and that this interaction is strongly inhibiting RecQ1 fork restoration activity (biochemical data). To investigate replication fork progression in TopI inhibited cells after treatment with PARP1 inhibitor Olaparib, we performed DNA fibers assay. The experiment confirmed that PARP1 inhibition rescues replication fork speed upon TopI inhibition, but showed that this is suppressed by depleted of RecQ1. My contribution to the project was to extend this set of experiments and to investigate the potential role of two other members of the RecQ helicase family, i.e. Bloom protein (BLM) and Werner syndrome protein (WRN), in the process of replication fork restart.

Unlike RecQ1 downregulation, downregulation of BLM and WRN did not affect the rescue of replication fork speed induced by PARP1 inhibition upon TopI poisoning (Figure 3e and d), proving the specific role of RECQ1 in this context.

Human RECQ1 promotes restart of replication forks reversed by DNA topoisomerase I inhibition

Matteo Berti[1,11], Arnab Ray Chaudhuri[2,11], Saravanabhavan Thangavel[1], Shivasankari Gomathinayagam[1], Sasa Kenig[3], Marko Vujanovic[2], Federico Odreman[4], Timo Glatter[5,10], Simona Graziano[1], Ramiro Mendoza-Maldonado[4], Francesca Marino[3], Bojana Lucic[4], Valentina Biasin[4], Matthias Gstaiger[5,6], Ruedi Aebersold[5–7], Julia M Sidorova[8], Raymond J Monnat Jr[8,9], Massimo Lopes[2] & Alessandro Vindigni[1]

Topoisomerase I (TOP1) inhibitors are an important class of anticancer drugs. The cytotoxicity of TOP1 inhibitors can be modulated by replication fork reversal through a process that requires poly(ADP-ribose) polymerase (PARP) activity. Whether regressed forks can efficiently restart and what factors are required to restart fork progression after fork reversal are still unknown. We have combined biochemical and EM approaches with single-molecule DNA fiber analysis to identify a key role for human RECQ1 helicase in replication fork restart after TOP1 inhibition that is not shared by other human RecQ proteins. We show that the poly(ADP-ribosyl)ation activity of PARP1 stabilizes forks in the regressed state by limiting their restart by RECQ1. These studies provide new mechanistic insights into the roles of RECQ1 and PARP in DNA replication and offer molecular perspectives to potentiate chemotherapeutic regimens based on TOP1 inhibition.

TOP1 inhibitors are an important class of anticancer drugs that exert their function by perturbing DNA replication[1,2]. The mechanisms of tumor response to TOP1 inhibitors and combinations of TOP1 inhibitors with other drugs for more effective tumor treatment are areas of active investigation[3,4]. One widely accepted mechanism for the cytotoxicity of TOP1 inhibitors has been their ability to create single-strand breaks (SSBs), which are converted to toxic DNA double-strand breaks (DSBs) upon colliding with the replication fork during replication[5]. This notion was recently challenged by the discovery that TOP1 inhibitors also impair TOP1 relaxation activity, inducing an accumulation of positive supercoils ahead of the replication fork that may hamper fork progression and the conversion of SSBs to DSBs[1,6]. Recent studies extended this observation by showing that replication forks rapidly slow and undergo fork reversal upon treatment with clinically relevant doses of camptothecin (CPT), the prototype TOP1 inhibitor[7,8]. This prevents DSB formation and requires the activity of PARP1, a well-known chromatin-associated enzyme that modifies various nuclear proteins by poly(ADP-ribosyl)ation (PARylation), to accumulate regressed forks[7]. However, the exact role of PARP1 in promoting fork reversal remains unexplained. In addition, other factors are likely to be involved in this process, and the protein(s) required to restore and restart reversed replication forks after the lesion is repaired have not been identified.

RecQ helicases have long been proposed to assist replication forks in dealing with replication stress and have attracted considerable interest in recent years owing to their connection to heritable human diseases associated with cancer predisposition[9,10]. RecQ helicase enzymatic activities (such as DNA unwinding, branch migration and strand annealing) may have multiple roles during replication by virtue of their ability to interconvert numerous replication and recombination intermediates[11–13]. Moreover, previous studies have pointed to a potential role of RecQ helicases in fork reversal and restart by showing that two of the five human RecQ helicases, BLM and WRN, promote both regression and re-establishment of model replication forks *in vitro*[14–16]. However, distinct roles or molecular functions for the five human RecQ helicases in replication stress and cancer remain to be defined[10,17].

For the present study, we combined biochemical, single-molecule DNA fiber and EM approaches to investigate the function of the human RECQ1 helicase (also known as RECQL or RECQL1) during the replication stress response. Of the five human RecQ proteins, RECQ1 was the first to be discovered, owing to its potent ATPase activity, and it is the most abundant in cells[18,19]. However, little is known about its cellular functions to date. Here, we show that RECQ1 has an essential role—one not shared by other human RecQ helicases—in restoring active replication forks that have regressed as a result of TOP1 inhibition. Moreover, we provide a rationale for the

[1]Department of Biochemistry and Molecular Biology, Saint Louis University School of Medicine, St. Louis, Missouri, USA. [2]Institute of Molecular Cancer Research, University of Zurich, Zurich, Switzerland. [3]Structural Biology Laboratory, Sincrotrone Trieste, Trieste, Italy. [4]International Centre for Genetic Engineering and Biotechnology, Trieste, Italy. [5]Institute for Molecular Systems Biology, Swiss Federal Institute of Technology (ETH) Zurich, Zurich, Switzerland. [6]Competence Center for Systems Physiology and Metabolic Diseases, ETH Zurich, Zurich, Switzerland. [7]Faculty of Science, University of Zurich, Zurich, Switzerland. [8]Department of Pathology, University of Washington, Seattle, Washington, USA. [9]Department of Genome Sciences, University of Washington, Seattle, Washington, USA. [10]Present address: Proteomics Core Facility, Biozentrum, University of Basel, Basel, Switzerland. [11]These authors contributed equally to this work. Correspondence should be addressed to A.V. (avindign@slu.edu) or M.L. (lopes@imcr.uzh.ch).

Received 18 June 2012; accepted 26 December 2012; published online 10 February 2013; doi:10.1038/nsmb.2501

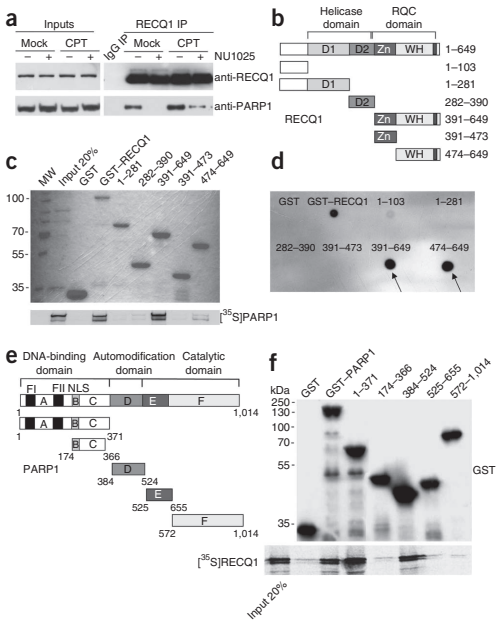

Figure 1 Analysis of the RECQ1-PARP1 interaction. (**a**) Immunoprecipitation from U-2 OS cells using the anti-RECQ1 antibody with (+) or without (–) NU1025 (50 μM) and with CPT (100 nM for 2 h) or without DNA damage (mock). Rabbit IgG IP served as a negative control. Immunoblots were developed with anti-RECQ1 and anti-PARP1 antibodies. (**b**) Schematic representation of the domain structure of RECQ1 and the GST-tagged RECQ1 fragments. D1 and D2, RecA-like domains. (**c**) Pulldown assays with GST-tagged RECQ1 fragments. Top, Coomassie-stained gel of GST-RECQ1 fragments. Bottom, autoradiography of *in vitro* GST pulldown assay using ^{35}S-labeled PARP1. MW, molecular weight (kDa). (**d**) Analysis of PAR binding to GST-RECQ1 fragments (2 pmol) dot-blotted onto a nitrocellulose membrane. The arrows indicate the two RECQ1 fragments that interact with ^{32}P-labeled PAR. (**e**) Schematic representation of the domain structure of PARP1 and the GST-tagged PARP1 fragments: A, DNA binding domain; B, nuclear localization signal; D, BRCT automodification domain; E, contains a WGR motif; F, catalytic domain; FI and FII, zinc-finger motifs; NLS, nuclear localization sequence. A third zinc-finger motif has been recently identified in domain C[36,37] in addition to FI and FII. (**f**) Pulldown assays with GST-tagged PARP1 (GST-PARP) fragments. Bound proteins were detected by autoradiography (bottom). Purified GST or GST-PARP1 proteins were detected with an anti-GST antibody (top). Input, 20% of the amount used in binding reactions.

requirement of the PARylation activity of PARP1 in replication fork reversal. Our observations give new insight into a pivotal mechanism responsible for replication stress response and replication fork restart after chemotherapeutic drug damage. These findings have important clinical implications, as RECQ1 inactivation might affect the efficacy of combinatorial therapies that employ PARP inhibitors and DNA-damaging agents and are already in promising clinical trials.

RESULTS

RECQ1 interacts with PARP1 and PAR

To better define the role of human RECQ1 helicase in DNA replication and repair, we first identified proteins associated with RECQ1 using a new, integrated proteomic approach[20]. We used human embryonic kidney (HEK293) cells to generate a stable, inducible cell line expressing a doubly tagged version of RECQ1 (consisting of a streptavidin-binding peptide and a hemagglutinin epitope tag), then isolated protein complexes containing RECQ1 by affinity purification (**Supplementary Fig. 1a–d**); we characterized the resulting complexes by MS[20]. Among the most abundant co-purified proteins were PARP1, Ku70 and Ku80 (key components of the DNA nonhomologous end–joining pathway) and several nucleosomal components (**Supplementary Fig. 1e**). Given recent reports indicating a role for PARP1 in replication stress response[7,21], we decided to focus our work on defining the role of RECQ1 interactions with PARP1.

We confirmed the RECQ1-PARP1 interaction by co-immunoprecipitation (co-IP) using nuclear extracts from human osteosarcoma (U-2 OS) cells and an antibody to RECQ1 (anti-RECQ1) that recognizes the C terminus of RECQ1 (residues 633–648). We obtained similar results using an anti-RECQ1 antibody that recognizes the N terminus of the protein (data not shown). We also performed reciprocal co-IPs using an anti-PARP1 antibody (**Fig. 1a** and **Supplementary Fig. 1f**). All co-IPs were performed in the presence of ethidium bromide or Benzonase to ensure that DNA did not mediate the interactions. We obtained similar results with other cell lines (**Supplementary Fig. 1f** and data not shown), indicating that the association between RECQ1 and PARP1 is not cell-type specific. These observations are in agreement with a previous report showing that RECQ1 and PARP1 interact at viral replication origins and with a recent study reporting an interaction between RECQ1 and PARP1 in human cells[22,23].

The RECQ1–PARP1 interaction is regulated by PARP1 PARylation activity: we observed increased association of the two proteins upon DNA damage and sharply reduced association upon inhibition of PARP1 activity with the PARP inhibitor NU1025 (**Fig. 1a** and **Supplementary Fig. 1g**). Using recombinant, purified PARP1 and RECQ1, we found that these two proteins interact directly, and the interaction was considerably stronger when we used a PARylated form of PARP1, indicating that the PAR modification of PARP1 is important for the interaction with RECQ1 (**Supplementary Fig. 2a**,**b**). Indeed, we observed that RECQ1 interacted with PAR, and binding to PAR was resistant to extensive washing with 1 M salt, although we could not identify any canonical PAR binding motifs in RECQ1 (ref. 24) (**Supplementary Fig. 2c**). We verified that NU1025 did not affect the interaction between recombinant RECQ1 and PARP1 *in vitro*, indicating that the reduced RECQ1-PARP1 interaction we observed by co-IP in the presence of this inhibitor is due to the inhibition of PARP1 PARylation activity rather than to a potential effect of NU1025 on PARP conformation (**Supplementary Fig. 2b**).

We next mapped the domains of RECQ1 that interact with PARP1 and PAR using a series of glutathione *S*-transferase (GST)-tagged RECQ1 fragments (**Fig. 1b–d**). Both PARP1 and PAR interacted with the C-terminal region of RECQ1 (residues 391–649; fragment names below indicate residue numbers), which contains the zinc-binding (Zn) and winged helix (WH) domains that form the 'RecQ–C-terminal' (RQC) domain, but not with fragment 391–473, which contains the Zn domain alone (**Fig. 1c**). The WH domain alone (fragment 474–649) also bound PARP1, although more weakly than fragment 391–649. These results suggest that the region containing residues 391–473 might be important for the stability and/or conformation of the WH domain. Our data also suggest that the region containing residues 391–649 is PARylated by PARP1 *in vitro* (**Supplementary Fig. 2d** and **Supplementary Note**); however, RECQ1 does not seem to be PARylated *in vivo*[22].

To determine which region(s) of PARP1 are involved in RECQ1 interaction, we overexpressed truncated versions of PARP1 fused to

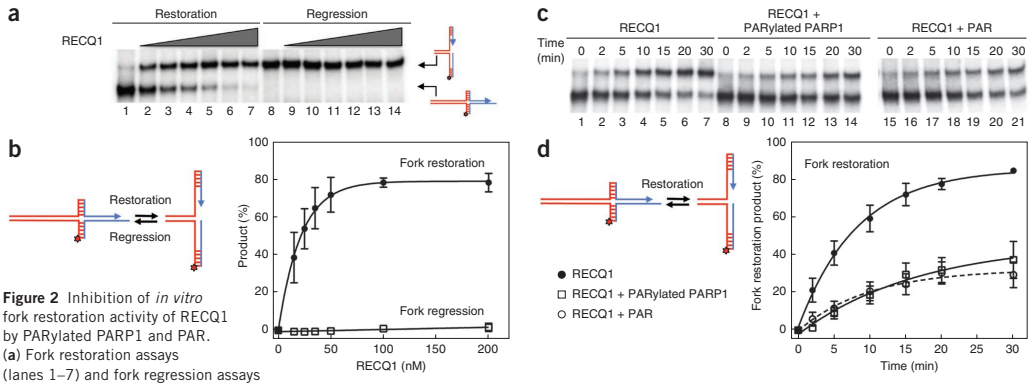

Figure 2 Inhibition of *in vitro* fork restoration activity of RECQ1 by PARylated PARP1 and PAR. (**a**) Fork restoration assays (lanes 1–7) and fork regression assays (lanes 8–14) performed using increasing RECQ1 concentrations (0, 15, 25, 35, 50, 100 and 200 nM) and a fixed concentration of chicken-foot substrate (2 nM, for restoration assay) or replication fork structure (2 nM, for regression assay). Right, schematic of the reaction products. (**b**) Left, schematic of restoration and regression reactions. Lined regions indicate heterologous sequences included in the vertical arms to prevent complete strand separation. In addition, we inserted two mismatches and a single isocytosine modification to prevent spontaneous fork regression and restoration (**Supplementary Fig. 3**). Stars indicate [γ-^{32}P]ATP-labeled 5 ends. Right, percentage of fork restoration and regression products plotted as a function of protein concentration. (**c**) Kinetic experiments using RECQ1 (40 nM) and the chicken-foot substrate (2 nM), visualized by gel electrophoresis. Lanes 1–7, RECQ1 alone; lanes 8–14, RECQ1 in the presence of PARylated PARP1 (40 nM); lanes 15–21, RECQ1 in the presence of PAR (100 nM). (**d**) Left, schematic of restoration reaction. Right, percentage of fork restoration for RECQ1 alone and RECQ1 in the presence of PARylated PARP1 or PAR. Data in **a**–**d** represent the mean of three independent experiments. Error bars, s.e.m.

GST in HeLa cells (**Fig. 1e**,**f**). Only fragments 1–371 and 384–524 could efficiently pull down RECQ1 in immunoprecipitation experiments, and fragment 174–366 did not pull down RECQ1. These results indicate that the interaction with RECQ1 involves the first 173 N-terminal residues of PARP1 (containing the DNA binding domain) and residues 384–524 (containing the BRCT domain, which is also the automodification domain). These two PARP1 domains are also involved in homodimerization and the binding of several partners, including WRN helicase[25,26].

RECQ1 catalyzes restoration of synthetic replication forks

On the basis of the recent discovery that PARP1 has an important role in reversal of replication forks after CPT treatment[7], we investigated whether RECQ1 is required for the cellular response to TOP1 inhibition. First, we confirmed previous observations that RECQ1 depletion leads to increased CPT sensitivity[27]. Flow-cytometric analysis showed that RECQ1-depleted cells are only mildly sensitive to most replication inhibitors and DNA-damaging agents, apart from CPT and etoposide (**Supplementary Fig. 3a** and **Supplementary Note**). These two drugs inhibit DNA replication by suppressing the relaxation activity of the type IB and type IIA topoisomerases, respectively[2]. Next, to confirm that RECQ1 binds to replication forks *in vivo* and that the interaction increases upon CPT treatment, we labeled newly replicated DNA with 5-chlorodeoxyuridine (CldU), and confirmed RECQ1 co-IP with CldU in the presence and absence of CPT (**Supplementary Fig. 3b** and **Supplementary Note**).

We then tested whether RECQ1 mediates replication fork regression and/or restoration on synthetic DNA substrates and whether PARP1 affects RECQ1 activity. To measure these RECQ1 activities *in vitro*, we used a set of four oligonucleotides that can anneal into two alternative substrates that mimic model replication fork and 'chicken-foot' structures[14,28] (**Supplementary Fig. 3c** and **Supplementary Table 1**). We found that RECQ1 promotes model replication fork restoration very efficiently and in a concentration-dependent fashion: 50 nM RECQ1 converted >75% of the chicken-foot structure into the model replication fork after 20 min (**Fig. 2a**,**b**). In contrast, RECQ1 failed to catalyze the opposite reaction (fork regression): we detected <2% of chicken-foot structure, even at the highest RECQ1 concentration. We obtained identical results using a variant of the same substrate lacking the 6-nucleotide (nt) single-stranded DNA (ssDNA) gap on the leading-strand template, thus ruling out the possibility that the presence of the ssDNA gap prevented RECQ1-mediated fork regression (**Supplementary Figs. 3d** and **4a**). Next, we confirmed that the ATPase activity of RECQ1 is essential to promote branch migration of the chicken-foot structure and restoration of the active replication fork. We observed that the poorly hydrolyzable ATP analog ATPγS and the nonhydrolyzable analog AMP-PNP strongly inhibited the reaction, and two previously characterized ATPase-deficient RECQ1 mutants, K119R and E220Q, lacked fork restoration (**Supplementary Fig. 4b**). Additional experiments using Holliday junction substrates with heterology regions of 1 and 4 bases confirmed that RECQ1 has a strong branch migration activity and that its helicase activity may be important to bypass regions of heterology. However, we observed a 50% reduction in the formation of the branch migration product when the heterology region was increased from 1 to 4 bases (**Supplementary Fig. 5a**,**b**).

On the basis of our results showing that RECQ1 interacts with PARylated PARP1 and previous observations that the PARylation activity of PARP has a key role in mediating the accumulation of regressed forks after DNA damage[7], we examined the effect of PARylated PARP1 on RECQ1 fork restoration activity. We found that PARylated PARP1 strongly inhibited the fork restoration rates of RECQ1: 40 nM RECQ1 converted approximately 80% of the chicken-foot structure into a replication fork structure within 20 min. Addition of an equimolar concentration of PARylated PARP1 reduced the fraction of restored fork structures to <30% (**Fig. 2c**,**d**). Experiments performed at increasing concentrations of PARylated PARP1 showed that a two-fold excess of PARylated PARP1 did not inhibit the reaction further, indicating that equimolar concentrations are sufficient for maximal inhibition (**Supplementary Fig. 4c**). We observed a similar

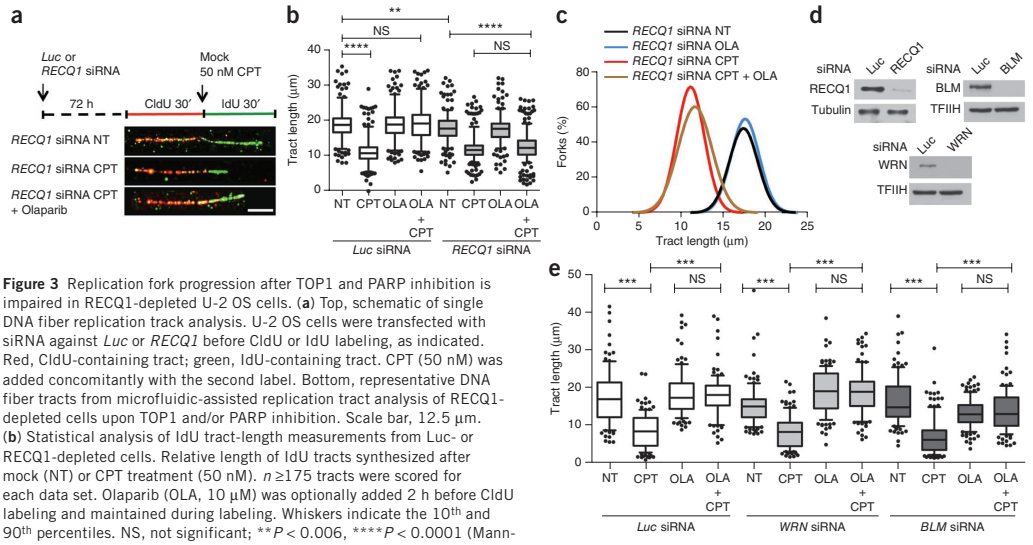

Figure 3 Replication fork progression after TOP1 and PARP inhibition is impaired in RECQ1-depleted U-2 OS cells. (**a**) Top, schematic of single DNA fiber replication track analysis. U-2 OS cells were transfected with siRNA against *Luc* or *RECQ1* before CldU or IdU labeling, as indicated. Red, CldU-containing tract; green, IdU-containing tract. CPT (50 nM) was added concomitantly with the second label. Bottom, representative DNA fiber tracts from microfluidic-assisted replication tract analysis of RECQ1-depleted cells upon TOP1 and/or PARP inhibition. Scale bar, 12.5 µm. (**b**) Statistical analysis of IdU tract-length measurements from Luc- or RECQ1-depleted cells. Relative length of IdU tracts synthesized after mock (NT) or CPT treatment (50 nM). $n \geq 175$ tracts were scored for each data set. Olaparib (OLA, 10 µM) was optionally added 2 h before CldU labeling and maintained during labeling. Whiskers indicate the 10th and 90th percentiles. NS, not significant; $^{**}P < 0.006$, $^{****}P < 0.0001$ (Mann-Whitney test). (**c**) Smoothed histogram of IdU tract-length distribution after TOP1 and/or PARP inhibition in RECQ1-depleted (*RECQ1* siRNA) cells. (**d**) RECQ1, BLM and WRN expression after siRNA knockdown, detected by western blotting. Tubulin and transcription factor II H (TFIIH) were detected as loading controls. (**e**) Statistical analysis of IdU tract-length measurements from Luc-, WRN- and BLM-depleted cells, as in **b**. $^{***}P < 0.0001$.

inhibition of RECQ1 activity in the presence of PARylated PARP1 using the Holliday junction (**Supplementary Fig. 5c**,**d**). To confirm that PARylated PARP1 is also able to inhibit the DNA unwinding activity of RECQ1, we used a fork duplex substrate with a duplex region of 20 bp (**Supplementary Fig. 5e**,**f**). In agreement with previous findings[29], electrophoretic mobility shift assays using increasing concentrations of PARylated PARP1 confirmed that PARylated PARP1 binds DNA with low affinity, indicating that the inhibitory effect of PARylated PARP1 on RECQ1 activity is not due to a competition for DNA binding (**Supplementary Fig. 6**). Additional fork restoration assays performed with PAR instead of PARylated PARP1 supported this conclusion, confirming that the interaction of RECQ1 with PAR is responsible for the inhibition of the fork restoration activity (**Fig. 2**). Collectively, our biochemical data show that RECQ1 has strong fork restoration activity that could be responsible for restarting reversed forks associated with CPT treatment. PARylated PARP1 inhibits this RECQ1 activity through a process that does not involve competition for DNA binding.

To investigate whether other human RecQ helicases share this activity, we performed additional experiments with an exonuclease-deficient WRN mutant (WRN-E84A) that allows the branch migration reaction to be monitored without possible complications arising from substrate digestion. WRN-E84A promoted fork restoration and regression with similar efficiency, with a slight bias toward fork restoration (**Supplementary Fig. 7**). Furthermore, the presence of PARylated PARP1 did not inhibit the fork restoration activity of WRN-E84A, in agreement with previous studies in which a different set of substrates was used[26]. These results, along with previous observations for BLM[14], show that although other helicases are able to promote fork restoration and regression, RECQ1 has a marked preference to promote fork restoration over fork regression, and its activity is uniquely regulated by PARylated PARP1.

RECQ1 and PARP control CPT-induced replication fork slowing

Next, we used genome-wide single-molecule DNA replication assays to test whether RECQ1 depletion affects the rate of replication fork progression upon TOP1 inhibition in a cellular context. We pulse-labeled U-2 OS cells with the thymidine analog CIdU for 30 min then treated cells with 50 nM CPT, concomitantly labeling them with a second thymidine analog (IdU) for an additional 30 min (**Fig. 3**). We then analyzed the IdU tract-length distributions after CPT treatment with or without PARP inhibition. Using this approach, we initially confirmed previous findings that replication forks rapidly slow upon treatment with low CPT doses (50 nM), and that this effect requires the action of PARP1 (refs. 7,8). This is consistent with the notion that PARP inactivation does not perturb normal fork progression but prevents fork slowing after TOP1 inhibition. We then measured rates of fork progression in RECQ1-depleted cells treated with CPT and the PARP inhibitor olaparib. Our results showed that PARP inhibition does not rescue CPT-induced fork slowing in RECQ1-deficient cells. These results identify an essential role for RECQ1 in the control of fork progression upon TOP1 inhibition. RECQ1 downregulation using a lentiviral system and a different RNA interference (RNAi) targeting sequence showed similar results, supporting the notion that the observed effect was specifically associated with RECQ1 loss (**Fig. 4** and data not shown). Additional DNA fiber experiments showed that—in contrast to the results obtained with RECQ1-depleted cells—PARP inhibition was still able to rescue CPT-induced fork slowing in BLM- and WRN-depleted cells. These results strongly support the notion that the identified role of RECQ1 in the control of fork progression upon TOP1 inhibition reflects a specific function and not a more general role of the RecQ helicase family (**Fig. 3e**). Genetic knockdown–rescue experiments confirmed that complementation in RECQ1-depleted U-2 OS cells with short hairpin RNA (shRNA)-resistant wild-type RECQ1 abrogated the effect of RECQ1

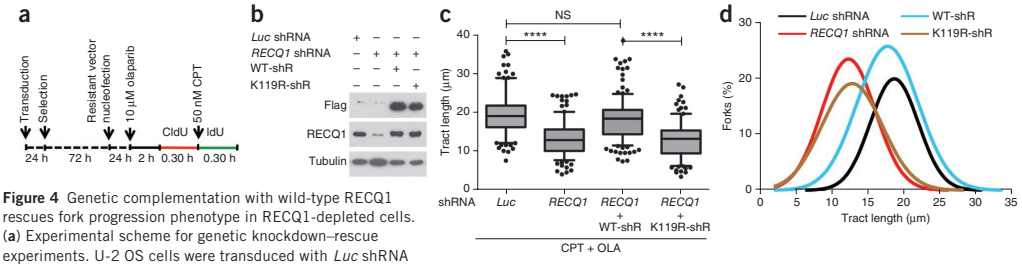

Figure 4 Genetic complementation with wild-type RECQ1 rescues fork progression phenotype in RECQ1-depleted cells. (**a**) Experimental scheme for genetic knockdown–rescue experiments. U-2 OS cells were transduced with *Luc* shRNA or *RECQ1* shRNA. RECQ1-depleted cells were nucleofected to express RNAi-resistant wild-type (WT-shR) or K119R (K119R-shR) RECQ1 before CldU labeling. (**b**) Western blot analysis of RECQ1-depleted cells expressing Flag-tagged WT-shR or K119R-shR. Tubulin was detected as a loading control. (**c**) Statistical analysis of IdU tract-length measurements from **a**. Relative length of IdU tracts synthesized after CPT treatment (50 nM). $n \geq 175$ tracts were scored for each data set. Olaparib (10 μM) was added 2 h before CldU labeling and maintained during labeling. Whiskers indicate the 10th and 90th percentiles. NS, not significant; $^{****}P < 0.0001$ (Mann-Whitney test). (**d**) Smoothed histogram of IdU tract length after TOP1 and PARP inhibition in RECQ1-depleted cells alone and genetically complemented with WT-shR or K119R-shR.

depletion on replication fork progression upon TOP1 inhibition (**Fig. 4**). Moreover, expression of the ATPase-deficient RECQ1 mutant K119R in RECQ1-depleted cells confirmed that the ATPase activity of RECQ1 is essential for its role in replication fork progression upon TOP1 inhibition (**Fig. 4**). Notably, we observed a minor but statistically significant ($P < 0.006$) difference between the mean length of the replication tracts measured in RECQ1-depleted cells relative to luciferase-depleted cells in the absence of CPT treatment (**Fig. 3b**). This is in line with our previous studies, in which we observed that the replication tracts were slightly shorter in RECQ1-depleted cells than in luciferase-depleted control cells in the absence of DNA damage[19]. These data might reflect an additional role for RECQ1 in replication fork progression in unperturbed cells.

Previous work has showed that CPT-induced fork slowing is uncoupled from DSB formation in human cells[7]. To determine whether RECQ1 depletion also influenced DSB accumulation after CPT treatment, we used a recently optimized pulsed-field gel electrophoresis (PFGE) protocol[7,30]. Our PFGE analysis confirmed that PARP inhibition in U-2 OS cells leads to the induction of high levels of DSBs after CPT treatment (100 nM) (**Fig. 5a**,**b**). These results are consistent with the notion that PARP-inhibited or PARP-depleted cells do not slow or accumulate reversed forks after CPT treatment, leading to DSB formation even at low CPT doses[7]. RECQ1 depletion, however, had the opposite effect: PARP1 inhibition did not prevent fork slowing after CPT or lead to increased DSB formation in RECQ1-depleted cells (**Fig. 5a**,**b**). As an alternative method of monitoring DSB formation, we looked at phosphorylated histone H2AX (γH2AX) and p53-binding protein 1 (53BP1) foci colocalization under the same conditions used for the PFGE experiments. In agreement with previous findings, we found that only a minor fraction of γH2AX foci colocalized with 53BP1 upon 100 nM CPT treatment and that PARP inhibition led to a considerably higher degree of γH2AX and 53BP1 colocalization[7] (**Fig. 5c**,**d**). However, RECQ1 depletion reduced the fraction of colocalizing foci in the presence of olaparib, supporting

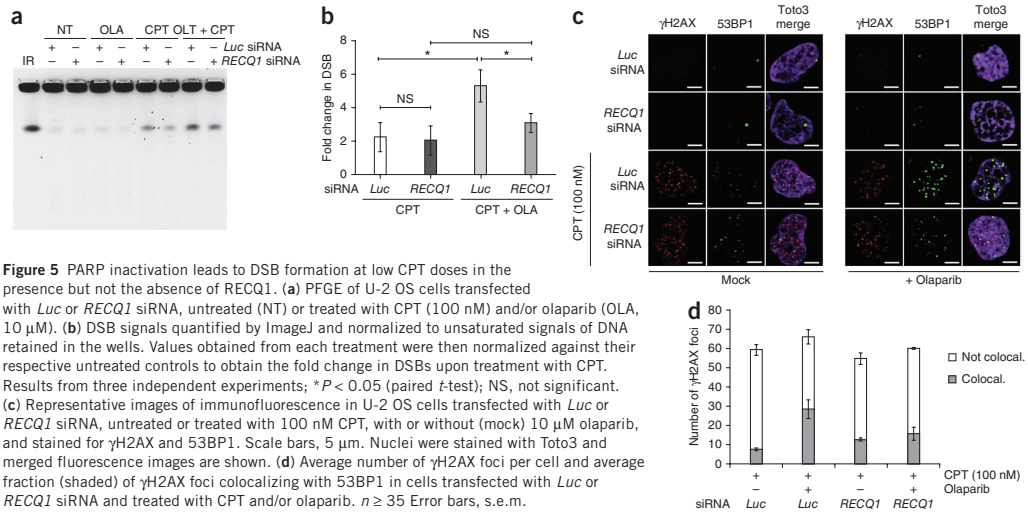

Figure 5 PARP inactivation leads to DSB formation at low CPT doses in the presence but not the absence of RECQ1. (**a**) PFGE of U-2 OS cells transfected with *Luc* or *RECQ1* siRNA, untreated (NT) or treated with CPT (100 nM) and/or olaparib (OLA, 10 μM). (**b**) DSB signals quantified by ImageJ and normalized to unsaturated signals of DNA retained in the wells. Values obtained from each treatment were then normalized against their respective untreated controls to obtain the fold change in DSBs upon treatment with CPT. Results from three independent experiments; $^{*}P < 0.05$ (paired *t*-test); NS, not significant. (**c**) Representative images of immunofluorescence in U-2 OS cells transfected with *Luc* or *RECQ1* siRNA, untreated or treated with 100 nM CPT, with or without (mock) 10 μM olaparib, and stained for γH2AX and 53BP1. Scale bars, 5 μm. Nuclei were stained with Toto3 and merged fluorescence images are shown. (**d**) Average number of γH2AX foci per cell and average fraction (shaded) of γH2AX foci colocalizing with 53BP1 in cells transfected with *Luc* or *RECQ1* siRNA and treated with CPT and/or olaparib. $n \geq 35$ Error bars, s.e.m.

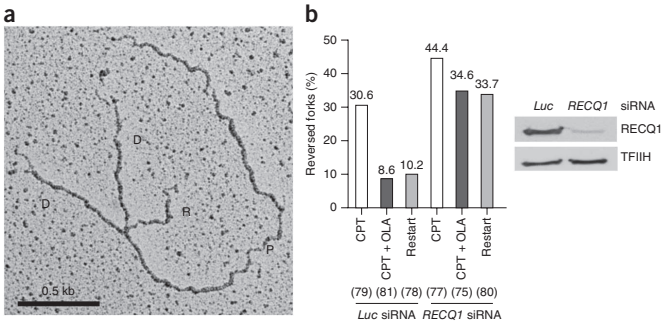

Figure 6 Reversed forks accumulate and are unable to restart in RECQ1-depleted cells after CPT treatment. (**a**) Representative electron micrograph of a reversed fork observed on genomic DNA from U-2 OS cells transfected with *RECQ1* siRNA and treated with CPT (25 nM) and olaparib (10 μM). D, daughter strand; P, parental strand; R, reversed arm. (**b**) Frequency of fork reversal in U-2 OS cells transfected with *Luc* siRNA or *RECQ1* siRNA and treated with CPT and/or olaparib. Restart experiments measuring the frequency of fork reversal were performed 3 h after CPT removal. Numbers above bars indicate proportion of reversed forks as a percentage of total number of molecules (bottom, parentheses). Right, RECQ1 expression after siRNA knockdown detected by western blotting. TFIIH, loading control.

the notion that RECQ1 depletion prevents DSB formation after PARP inhibition. Collectively, these data indicate that RECQ1 regulates the rate of replication fork progression and that RECQ1 depletion makes PARP activity dispensable in the prevention of DSB accumulation after TOP1 inhibition.

RECQ1 is essential for fork restart upon TOP1 inhibition

The observation that RECQ1 loss makes PARP activity dispensable in the prevention of fork slowing and DSB formation in CPT-treated cells suggests that regressed forks accumulate in RECQ1-depleted cells. This is in agreement with our biochemical results pointing to a role for RECQ1 in replication fork restart. To provide more direct evidence for this idea, we used EM to visualize the fine architecture of *in vivo* replication intermediates[31,32]. A previous EM analysis of replication intermediates showed that replication forks undergo rapid fork reversal upon TOP1 inhibition[7]. Furthermore, effective fork reversal required PARP1 activity, possibly by promoting the accumulation or stabilization of regressed replication forks and thus preventing fork collision with a CPT-induced lesion to generate a DSB[7]. To test the hypothesis that the accumulation of reversed forks is increased in RECQ1-depleted, CPT-treated cells, we used EM to compare RECQ1-depleted, CPT-treated U-2 OS cells in which PARP was inhibited to those in which it was not inhibited (**Fig. 6**). Consistent with previous findings, we observed a high frequency of fork reversal (approximately 30% of molecules analyzed) in control U-2 OS cells transfected with a small interfering RNA (siRNA) against *Luc* (encoding luciferase) and treated with 25 nM CPT. The same experiments performed in the presence of olaparib confirmed that PARP inhibition in control cells markedly decreased the fraction of reversed forks, from 30% to <10%. RECQ1 depletion by siRNA upon CPT treatment resulted in a higher frequency of fork reversal events (~44%) than that observed in control cells. Notably, PARP inactivation in RECQ1-depleted cells did not result in marked reduction in the fraction of regressed forks, suggesting that regressed forks do not restart upon RECQ1 inactivation, even in the absence of PARP activity. To test this hypothesis directly, we performed recovery experiments in which we measured reversed fork frequency after CPT removal. Whereas control cells showed a marked decrease in the frequency of fork reversal (from 30% to 10%) after drug removal, RECQ1-depleted cells maintained a high frequency of reversed forks (~33%) 3 h after CPT withdrawal. These data strongly suggest that RECQ1 is essential in restarting reversed forks and indicate that the requirement of PARP for CPT-induced fork reversal reflects a unique role for PARP in limiting RECQ1-mediated fork reactivation.

DISCUSSION

Replication fork regression is rapidly emerging as a pivotal response mechanism to the induction of replication stress. This notion is supported by the recent discovery that TOP1 inhibition by CPT induces replication fork slowing and reversal, preventing DSB formation at clinically relevant doses of CPT[7,8]. PARP1 is a crucial cellular mediator required for the accumulation or stabilization of regressed forks upon TOP1 poisoning. PARP1 itself is a target for anticancer therapies, particularly breast and ovarian cancers involving mutation of the genes *BRCA1* and *BRCA2*. PARP inactivation prevents the accumulation of regressed forks without affecting the checkpoint response[7]. However, the mechanism by which PARP activity promotes fork reversal is still unknown, and the requirements for the restart of reversed forks have not been defined. Our work provides new insight into these mechanisms by showing that regressed forks

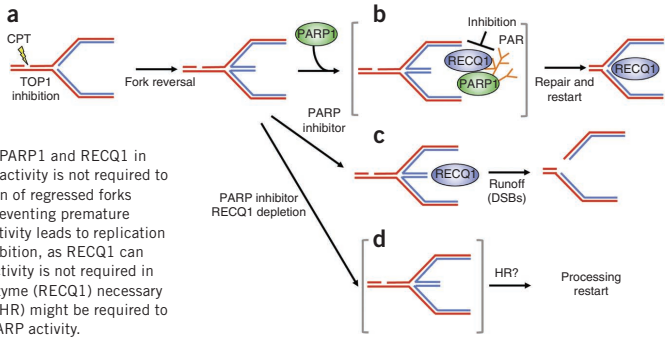

Figure 7 Schematic model of the combined roles of PARP1 and RECQ1 in response to TOP1 inhibition. (**a**,**b**) PARP PARylation activity is not required to form reversed forks, but it promotes the accumulation of regressed forks by inhibiting RECQ1 fork restoration activity, thus preventing premature restart of regressed forks. (**c**) Inhibition of PARP1 activity leads to replication runoff and increased DSB formation upon TOP1 inhibition, as RECQ1 can cause untimely restart of reversed forks. (**d**) PARP activity is not required in RECQ1-depleted cells because the cells lack the enzyme (RECQ1) necessary to promote fork restart. Homologous recombination (HR) might be required to promote fork restart in the absence of RECQ1 and PARP activity.

can restart *in vivo* and identifying a key role for human RECQ1 in promoting, through ATPase and branch migration activities, efficient replication fork restart after TOP1 inhibition (**Fig. 7**). Our results also show that this function of RECQ1 is not shared by other helicases, such as BLM and WRN. Furthermore, our results provide new insight into the molecular role of PARP in fork reversal by showing that the PARylation activity of PARP is important in regulating RECQ1 activity on replication forks after CPT treatment. A notable aspect of these data is that PARP activity is dispensable in the formation of reversed forks (**Fig. 7a**) but required to 'accumulate' them—that is, to maintain or protect them from counteracting activity (by RECQ1) that would otherwise cause an untimely restart of reversed forks, leading to DSB formation (**Fig. 7b**,**c**). Indeed, we show that in RECQ1-depleted cells, PARP activity is dispensable in the accumulation of reversed forks or the avoidance of CPT-induced DSBs (**Fig. 7d**). We propose that PARP 'signals' the presence of lesions on the template and inhibits RECQ1 locally, thereby restraining the restart of reversed forks until repair of the TOP1 cleavage complex is complete (**Fig. 7b**). An important next step will be to identify factors that modulate RECQ1-catalyzed fork restart by PARP activity.

These data provide a new mechanistic insight that could help to predict the efficiency of anticancer therapies that include both PARP and TOP1 inhibitors. These combinations are now in clinical trials. Our results also suggest that RECQ1 might represent a new therapeutic target to be used in conjunction with TOP1 inhibitors. In principle, induction of fork reversal (by TOP1 poisons) and inhibition of reversed fork reactivation (by RECQ1 depletion) should synergize, which would explain the observed CPT sensitivity of RECQ1-depleted cells.

RecQ helicases are DNA unwinding enzymes essential for the maintenance of genome stability in many organisms. Why human cells should express five RecQ homologs, and microorganisms such as *Escherichia coli*, *Saccharomyces cerevisiae* and *Schizosaccharomyces pombe* only one or two, remains unexplained. Our previous studies provided new insight by identifying important and distinct roles for RECQ1 and RECQ4 during DNA replication[19]. These data, combined with previous observations that RECQ1 depletion leads to increased DNA damage and affects cellular proliferation[27,33,34], suggest that RECQ1 might have a distinct role in the stabilization and repair of replication forks. Our discovery that RECQ1 is required for replication fork restoration after TOP1 poisoning provides what is, to our knowledge, the first indication of a specific cellular function for this RecQ helicase. U-2 OS cells lacking BLM or WRN do not show similar defects in replication fork restoration upon TOP1 poisoning, suggesting that RECQ1 is the RecQ helicase specifically responsible for promoting replication fork restart upon CPT-induced fork reversal. Moreover, RECQ1 shows a striking preference for fork restoration over regression, and its activity, unlike that of WRN, is specifically regulated by PARylation of PARP1 (ref. 26) (**Supplementary Fig. 7**). However, we cannot yet rule out the possibility that other human RecQ helicases are involved in different steps of the same process.

It will be important for future studies to determine whether reversed forks are detected in response to genotoxic stress other than TOP1 inhibition and whether RECQ1 or other helicases are implicated in replication fork reversal or restart, depending on the type of DNA damage. WRN- and BLM-deficient cells show increased sensitivity to select genotoxic agents[35], whereas RECQ1-deficient cells are markedly sensitive to CPT and etoposide, supporting the notion that these three RecQ helicases have distinct roles in replication stress response. The fact that RECQ1-depleted cells show increased sensitivity to etoposide opens the possibility that a similar mechanism of fork reversal and restart might take place upon treatment with topoisomerase II poisons. EM analysis of replication intermediates after treatment with different classes of chemotherapeutic drugs will provide early clues about combinations of drugs and RecQ helicases to pursue in future studies.

The discovery that RECQ1 is essential for fork restart upon TOP1 poisoning suggests that RECQ1 may itself be a new therapeutic target and that it could modulate the efficacy of combinatorial cancer therapies using PARP and TOP1 inhibitors that are already in clinical trials. A key experimental goal will be to determine the fate of regressed replication forks that accumulate in the absence of RECQ1. One possibility is that active replication forks are restored by the homologous-recombination machinery in the absence of the fork restart activity of RECQ1 (**Fig. 7d**). Thus, RECQ1 depletion or inhibition might result in synthetic lethality in a background deficient for homologous recombination, providing a new way to target and increase the efficacy of cancer therapies when homologous-recombination repair is inefficient or inhibited.

METHODS

Methods and any associated references are available in the online version of the paper.

Note: Supplementary information is available in the online version of the paper.

ACKNOWLEDGMENTS

We are grateful to A. Mazin for sharing information regarding the substrate preparation. We thank P. Janscak (University of Zurich) and D. Orren (University of Kentucky College of Medicine) for providing aliquots of purified WRN and WRN-E84A proteins, respectively. We thank G. de Murcia (École Supérieure de Biotechnologie de Strasbourg) for providing the constructs for the production of the PARP1 fragment. We thank Y. Ayala for critical discussions and G. Triolo for help in recombinant protein production. We thank the Nano Research Facility of the School of Engineering and Applied Science at Washington University in St. Louis, which is part of the National Nanotechnology Infrastructure Network supported by the US National Science Foundation under grant no. ECS-0335765, for microfabrication and the use of clean-room facility. We also thank the Center for Microscopy and Image Analysis of the University of Zurich for technical assistance with EM. This work was supported by startup funding from the Doisy Department of Biochemistry and Molecular Biology at the Saint Louis University School of Medicine and the Saint Louis University Cancer Center and grants from the President's Research Fund of Saint Louis University and the Associazione Italiana per la Ricerca sul Cancro (AIRC10510) to A.V.; US National Institutes of Health grant CA77852 to R.J.M. Jr.; Swiss National Science Foundation grants PP0033-114922 and PP00P3-135292 to M.L.; and a contribution from Fonds zur Förderung des Akademischen Nachwuchses (FAN) of the Zürcher Universitätsverein (ZUNIV) to M.L. and A.R.C.

AUTHOR CONTRIBUTIONS

M.B. conducted the immunoprecipitation, GST-pulldown, far-western and dot-blot experiments and the *in vitro* fork regression and restoration studies with the synthetic DNA substrates. A.R.C. conducted PFGE and EM analysis. S.T. conducted the single-molecule DNA replication assays. S. Gomathinayagam expressed the recombinant proteins and contributed to the *in vitro* fork regression and restoration assays. S.K. performed the immunofluorescence experiments and contributed to the cell-survival assays. M.V. conducted the single-molecule DNA replication assays with the BLM- and WRN-depleted cells. F.O. performed the protein complex purification experiments. T.G. contributed to the design of the proteomic experiments and performed MS analysis. S. Graziano performed the cell-survival assays. R.M.-M. contributed to the production of the GST-tagged fragments used in the GST-pulldown assays. F.M. contributed to the far-western analysis. B.L. produced the RECQ1 mutants and contributed to the optimization of protocols for RECQ1 expression. V.B. induced expression of the recombinant PARP1 protein. M.G. contributed to the design and supervision of the proteomic experiments. R.A. supervised the proteomic experiments. J.M.S. and R.J.M. Jr. contributed to the establishment of the single-molecule DNA replication assays in A.V.'s lab. R.J.M. Jr. assisted A.V. in finalizing the manuscript. M.L. planned, designed and supervised the PFGE and EM experiments and assisted A.V. in finalizing the manuscript. A.V. planned and supervised the project and wrote the manuscript.

COMPETING FINANCIAL INTERESTS
The authors declare no competing financial interests.

Published online at http://www.nature.com/doifinder/10.1038/nsmb.2501.
Reprints and permissions information is available online at http://www.nature.com/reprints/index.html.

1. Koster, D.A., Palle, K., Bot, E.S., Bjornsti, M.A. & Dekker, N.H. Antitumour drugs impede DNA uncoiling by topoisomerase I. *Nature* **448**, 213–217 (2007).
2. Pommier, Y., Leo, E., Zhang, H. & Marchand, C. DNA topoisomerases and their poisoning by anticancer and antibacterial drugs. *Chem. Biol.* **17**, 421–433 (2010).
3. Pommier, Y. Topoisomerase I inhibitors: camptothecins and beyond. *Nat. Rev. Cancer* **6**, 789–802 (2006).
4. Rodriguez-Galindo, C. *et al.* Clinical use of topoisomerase I inhibitors in anticancer treatment. *Med. Pediatr. Oncol.* **35**, 385–402 (2000).
5. Pommier, Y. *et al.* Repair of and checkpoint response to topoisomerase I–mediated DNA damage. *Mutat. Res.* **532**, 173–203 (2003).
6. Koster, D.A., Crut, A., Shuman, S., Bjornsti, M.A. & Dekker, N.H. Cellular strategies for regulating DNA supercoiling: a single-molecule perspective. *Cell* **142**, 519–530 (2010).
7. Ray Chaudhuri, A. *et al.* Topoisomerase I poisoning results in PARP-mediated replication fork reversal. *Nat. Struct. Mol. Biol.* **19**, 417–423 (2012).
8. Sugimura, K., Takebayashi, S., Taguchi, H., Takeda, S. & Okumura, K. PARP-1 ensures regulation of replication fork progression by homologous recombination on damaged DNA. *J. Cell Biol.* **183**, 1203–1212 (2008).
9. Bernstein, K.A., Gangloff, S. & Rothstein, R. The RecQ DNA helicases in DNA repair. *Annu. Rev. Genet.* **44**, 393–417 (2010).
10. Chu, W.K. & Hickson, I.D. RecQ helicases: multifunctional genome caretakers. *Nat. Rev. Cancer* **9**, 644–654 (2009).
11. Bachrati, C.Z. & Hickson, I.D. RecQ helicases: guardian angels of the DNA replication fork. *Chromosoma* **117**, 219–233 (2008).
12. Bohr, V.A. Rising from the RecQ-age: the role of human RecQ helicases in genome maintenance. *Trends Biochem. Sci.* **33**, 609–620 (2008).
13. Vindigni, A., Marino, F. & Gileadi, O. Probing the structural basis of RecQ helicase function. *Biophys. Chem.* **149**, 67–77 (2010).
14. Bugreev, D.V., Rossi, M.J. & Mazin, A.V. Cooperation of RAD51 and RAD54 in regression of a model replication fork. *Nucleic Acids Res.* **39**, 2153–2164 (2011).
15. Machwe, A., Karale, R., Xu, X., Liu, Y. & Orren, D.K. The Werner and Bloom syndrome proteins help resolve replication blockage by converting (regressed) Holliday junctions to functional replication forks. *Biochemistry* **50**, 6774–6788 (2011).
16. Machwe, A., Lozada, E., Wold, M.S., Li, G.M. & Orren, D.K. Molecular cooperation between the Werner syndrome protein and replication protein A in relation to replication fork blockage. *J. Biol. Chem.* **286**, 3497–3508 (2011).
17. Hickson, I.D. RecQ helicases: caretakers of the genome. *Nat. Rev. Cancer* **3**, 169–178 (2003).
18. Seki, M. *et al.* Purification of two DNA-dependent adenosinetriphosphatases having DNA helicase activity from HeLa cells and comparison of the properties of the two enzymes. *J. Biochem.* **115**, 523–531 (1994).
19. Thangavel, S. *et al.* Human RECQ1 and RECQ4 helicases play distinct roles in DNA replication initiation. *Mol. Cell Biol.* **30**, 1382–1396 (2010).
20. Glatter, T., Wepf, A., Aebersold, R. & Gstaiger, M. An integrated workflow for charting the human interaction proteome: insights into the PP2A system. *Mol. Syst. Biol.* **5**, 237 (2009).
21. Ying, S., Hamdy, F.C. & Helleday, T. Mre11-dependent degradation of stalled DNA replication forks is prevented by BRCA2 and PARP1. *Cancer Res.* **72**, 2814–2821 (2012).
22. Sharma, S., Phatak, P., Stortchevoi, A., Jasin, M. & Larocque, J.R. RECQ1 plays a distinct role in cellular response to oxidative DNA damage. *DNA Repair (Amst.)* **11**, 537–549 (2012).
23. Wang, Y., Li, H., Tang, Q., Maul, G.G. & Yuan, Y. Kaposi's sarcoma-associated herpesvirus ori-Lyt-dependent DNA replication: involvement of host cellular factors. *J. Virol.* **82**, 2867–2882 (2008).
24. Kleine, H. & Luscher, B. Learning how to read ADP-ribosylation. *Cell* **139**, 17–19 (2009).
25. Schreiber, V. *et al.* Poly(ADP-ribose) polymerase-2 (PARP-2) is required for efficient base excision DNA repair in association with PARP-1 and XRCC1. *J. Biol. Chem.* **277**, 23028–23036 (2002).
26. von Kobbe, C. *et al.* Poly(ADP-ribose) polymerase 1 regulates both the exonuclease and helicase activities of the Werner syndrome protein. *Nucleic Acids Res.* **32**, 4003–4014 (2004).
27. Sharma, S. & Brosh, R.M. Jr. Human RECQ1 is a DNA damage responsive protein required for genotoxic stress resistance and suppression of sister chromatid exchanges. *PLoS ONE* **2**, e1297 (2007).
28. Bugreev, D.V., Mazina, O.M. & Mazin, A.V. Rad54 protein promotes branch migration of Holliday junctions. *Nature* **442**, 590–593 (2006).
29. Ferro, A.M. & Olivera, B.M. Poly(ADP-ribosylation) *in vitro*. Reaction parameters and enzyme mechanism. *J. Biol. Chem.* **257**, 7808–7813 (1982).
30. Hanada, K. *et al.* The structure-specific endonuclease Mus81 contributes to replication restart by generating double-strand DNA breaks. *Nat. Struct. Mol. Biol.* **14**, 1096–1104 (2007).
31. Lopes, M. Electron microscopy methods for studying *in vivo* DNA replication intermediates. *Methods Mol. Biol.* **521**, 605–631 (2009).
32. Neelsen, K.J., Ray Chaudhuri, A., Follonier, C., Herrador, R. & Lopes, M. Visualization and interpretation of eukaryotic DNA replication intermediates by electron microscopy *in vivo*. *Methods Mol. Biol.* (in the press).
33. Mendoza-Maldonado, R. *et al.* The human RECQ1 helicase is highly expressed in glioblastoma and plays an important role in tumor cell proliferation. *Mol. Cancer* **10**, 83 (2011).
34. Sharma, S. *et al.* RECQL, a member of the RecQ family of DNA helicases, suppresses chromosomal instability. *Mol. Cell Biol.* **27**, 1784–1794 (2007).
35. Mao, F.J., Sidorova, J.M., Lauper, J.M., Emond, M.J. & Monnat, R.J. The human WRN and BLM RecQ helicases differentially regulate cell proliferation and survival after chemotherapeutic DNA damage. *Cancer Res.* **70**, 6548–6555 (2010).
36. Langelier, M.F., Servent, K.M., Rogers, E.E. & Pascal, J.M. A third zinc-binding domain of human poly(ADP-ribose) polymerase-1 coordinates DNA-dependent enzyme activation. *J. Biol. Chem.* **283**, 4105–4114 (2008).
37. Tao, Z., Gao, P., Hoffman, D.W. & Liu, H.W. Domain C of human poly(ADP-ribose) polymerase-1 is important for enzyme activity and contains a novel zinc-ribbon motif. *Biochemistry* **47**, 5804–5813 (2008).

ONLINE METHODS

Materials. The antibodies used were rabbit polyclonal antibody to PARP1 (anti-PARP1) Enzo, ALX-210-302-R100) (1:2,000), mouse monoclonal anti-PARP1 (Santa Cruz, sc-8007) (1:1,000), mouse monoclonal anti-PAR (Enzo, ALX-804-220-R100, clone 10H) (1:2,000), rabbit polyclonal anti-PAR (Trevigen, 4336-BPC-100) (1:2,000), mouse monoclonal anti-Ku70 and anti-Ku86 (Santa Cruz, sc-5309 and sc-5280) (1:2,000), mouse monoclonal anti-tubulin (Sigma, T5168) (1:5,000), mouse monoclonal anti-WRN (BD laboratories, 611169) (1:1,000), rabbit polyclonal anti-BLM (Abcam, ab476) (1:1,000), rabbit polyclonal anti-TFIIH (Santa Cruz, sc293) (1:2,000), rabbit polyclonal anti-RECQ1 raised against residues 1–110 (Santa Cruz, sc-25547) (1:2,000) and a custom-made rabbit anti-RECQ1 polyclonal antibody to a synthetic peptide of a unique sequence in the last 16 residues at the C terminus of RECQ1 (Sigma) (1:2,000)[33]. Camptothecin and etoposide were from Sigma. The PARP1 inhibitors olaparib and NU1025 were from Selleck Chemicals and Sigma, respectively.

Protein complex purification. To isolate protein complexes containing a RECQ1 bait protein, we prepared a HEK293 cell line expressing a double-tagged version of the human RECQ1 helicase by Flp recombinase-mediated integration. This system allows the generation of stable mammalian cell lines exhibiting tetracycline-inducible expression of a gene of interest from a single genomic location[20]. The protein complexes containing RECQ1 were isolated and analyzed by MS as previously described[20] (**Supplementary Fig. 1**).

Immunoprecipitation. HEK293T or human osteosarcoma U-2 OS cells were treated as indicated, washed two times with ice-cold PBS and resuspended in cytoplasmic extraction buffer (10 mM Tris-HCl (pH 7.9), 0.34 M sucrose, 3 mM CaCl2, 2 mM magnesium acetate, 0.1 mM EDTA, 1 mM DTT, 20 mM NaF, 10 mM β-glycerophosphate, 0.2 mM Na_3VO_4, 0.5% Nonidet P-40 and protease inhibitors (Roche)) for 10 min at 4 °C. Intact nuclei were pelleted by low-speed centrifugation, washed with cytoplasmic lysis buffer (without Nonidet P-40) and lysed in nuclear lysis buffer (20 mM HEPES (pH 7.9), 150 mM KCl, 1.5 mM $MgCl_2$, 20 mM NaF, 10 mM β-glycerophosphate, 0.2 mM Na_3VO_4 10% glycerol, 0.5% Nonidet P-40 and protease inhibitors) by homogenization, and DNA and RNA in the suspension were digested with 50 U per microliter Benzonase (Sigma) at 4 °C for 1 h. The nuclear-soluble extract was clarified from insoluble material by centrifugation at 20,000 × *g* for 20 min, pre-cleared with a 50-µl slurry of protein A beads (Santa Cruz) at 4 °C for 1 h and incubated overnight with anti-RECQ1 (Sigma), anti-PARP1 (Enzo) or a control IgG rabbit polyclonal antibody at 4 °C. Immunocomplexes were captured by adding 50 µl of a protein A bead slurry for 2 h at 4 °C. After extensive washing, proteins were eluted from beads with 2× Laemmli sample buffer at 95 °C for 5 min, separated by SDS-PAGE and detected by immunoblotting with the appropriate antibodies.

GST pulldown experiments with *in vitro*–translated PARP1. Pulldown assays with GST-RECQ1 fragments were performed as previously described[38]. Briefly, [^{35}S]Met-labeled, *in vitro*–translated PARP1 was incubated with GST-fused RECQ1 fragments bound to 10 µl of glutathione-Sepharose beads (Amersham) in binding buffer TNEN (20 mM Tris-HCl (pH 7.5), 150 mM NaCl, 1.0 mM EDTA (pH 8.0), 0.5% NP-40, 1 mM DTT and 1 mM PMSF) supplemented with 0.1 mg/ml ethidium bromide for 2 hr at 4 °C. The beads were subsequently washed two times in ethidium bromide–supplemented TNEN buffer and three times with TNEN buffer. Bound proteins were eluted with SDS sample buffer, resolved by gel electrophoresis and visualized by autoradiography. For the pull-downs with the GST-PARP1 fragments, [^{35}S]Met-labeled, *in vitro*-translated RECQ1 was incubated with immobilized GST or GST–PARP1 domains. The GST-PARP fragments were expressed in HeLa cells as previously described[25,26]. Cells were lysed 48 h later in 50 mM Tris-HCl (pH 8), 250 mM NaCl, 0.5% NP-40, 0.5 mM PMSF and protease inhibitors. Lysates were cleared by centrifugation and incubated for 2 h with glutathione-Sepharose beads. Beads were washed three times with lysis buffer and two times with lysis buffer supplemented with 1 M NaCl and resuspended in GST binding buffer for pulldown experiments with the purified GST-PARP1 fragments.

PAR binding assay. The PAR binding assays were performed using 1 M NaCl for the washing step as previously described[39].

Purification of recombinant proteins and *in vitro* PARylation of PARP1. Recombinant RECQ1 and PARP1 were purified from insect cells as previously described[40,41]. For *in vitro* poly(ADP-ribosyl)ation of PARP1, recombinant PARP-1 was incubated in 20 µl of activity buffer (50 mM Tris (pH 7.5), 4 mM $MgCl_2$, 50 mM NaCl, 200 µM DTT, 0.1 µg/µl BSA, 4 ng/µl DNaseI-activated calf thymus DNA and 400 µM NAD^+) for 10 min at 37 °C.

***In vitro* fork regression and restart assays.** The oligonucleotide sequences and the procedure used for the preparation of [γ-^{32}P]ATP-labeled substrate are shown in **Supplementary Table 1** and **Supplementary Figure 3**, respectively. Reactions were performed using the indicated protein concentrations and 2 nM DNA substrate in branch migration buffer (35 mM Tris-HCl (pH 7.5), 20 mM KCl, 5 mM $MgCl_2$, 0.1 mg/ml BSA, 2 mM DTT, 15 mM phosphocreatine, 30 U/ml creatine phosphokinase and 5% glycerol) at 37 °C. The reaction was started by the addition of 2 mM ATP. Concentration-dependence experiments were stopped after 20 min. For the poly(ADP-ribosyl)ation experiments, the indicated concentrations of PARP1 and 200 µM NAD or 100 nM purified PAR were added to the reaction mixture without ATP and pre-incubated together with RECQ1 and the substrate at 37 °C for 10 min. DNA substrates were deproteinized by adding 3× stop reaction (1.2% SDS, 30% glycerol supplemented with proteinase K (3mg/ml)) at room temperature for 10 min before being resolved on a native 8% polyacrylamide gel run in Tris-borate-EDTA (TBE) buffer at 4 °C.

Genetic knockdown–rescue assays. siRNA-mediated transient depletion of RECQ1 was achieved using an siRNA SMART pool against human *RECQ1* (NM_032941, Dharmacon) in U-2 OS cells and a previously described protocol in which we established the specificity of the siRNA pool[19,33]. siRNA-mediated depletion of WRN and BLM was achieved using the following siRNAs from Microsynth: *WRN* siRNA (5′-UAGAGGGAAACUUGGCAAAdTdT-3′) and *BLM* siRNA (5′-CCGAAUCUCAAUGUACAUAGA dTdT-3′). shRNA-mediated downregulation was achieved by cloning the sequence targeting *RECQ1* (5′-GAGCTTATGTTACCAGTTA-3′) into the pLKO.1 lentiviral shRNA expression vector. Virus was generated by transient cotransfection of pLKO.1 and the packaging plasmids psPAX2 and pM2D.G into 293T cells. Viral supernatants were filtered through a 0.45 µM filter and transduced on U-2 OS cells for 24 h, followed by selection with puromycin (8 µg/ml) for 3 d. Control transductions were performed using the pLKO.1 vector expressing a shRNA targeting the gene encoding Luciferase (5′-ACGCTGAGTACTTCGAAATGT-3′). The level of depletion was verified by western blotting. For the complementation assays, we cloned a *RECQ1* RNAi–resistant open reading frame into a pIRES vector under the control of the CMV promoter. Specifically, the nucleotides targeted by the RNAi (5′-GAGCTTATGTTACCAGTTA-3′) were partially substituted without changing the amino acid sequence (5′-GTCACTATGCTATCAATTA-3′) by site-directed mutagenesis. Lentiviral depletion of endogenous RECQ1 was achieved using the protocol described above, and the resulting RECQ1-depleted cells were then nucleofected with a shRNA-resistant RECQ1 expression vector. Expression of the RNAi-resistant, Flag-tagged RECQ1 and K119R mutant was verified in control and RECQ1-depleted cells by western analysis 48 h after transfection.

Microfluidic-assisted DNA fiber stretching and replication fork progression analysis. Asynchronous U-2 OS cells were transiently transfected for 72 h with siRNA SMART pools (or specific shRNA) against RECQ1 or Luciferase as reported earlier[19,33]. RECQ1- or Luciferase-depleted U-2 OS cells were labeled for 30 min each with 50 µM CldU followed by 50 µM IdU. Cells were collected by trypsinization, and high–molecular weight DNA from cells embedded in agarose plugs was isolated and stretched using a microfluidic platform as described earlier[42]. For immunostaining, stretched DNA fibers were denatured with 2.5 N HCl for 45 min, neutralized in 0.1 M sodium borate (pH 8.0) and PBS, and blocked with PBS, 5% BSA and 0.5% Tween-20 for 30 min. Rat anti-CldU/BrdU (Abcam, ab6326) (1:6), goat anti-rat Alexa 594 (Invitrogen, A11007) (1:1,000), mouse anti-IdU/BrdU (BD Biosciences, 347580) (1:6) and goat anti-mouse Alexa 488 (Invitrogen, A11001) (1:1,000) antibodies were used to reveal CldU- and IdU-labeled tracts, respectively. A Leica SP5X confocal microscope was used to visualize the labeled tracts, and tract lengths were measured using ImageJ (http://rsbweb.nih.gov/ij/). Statistical analysis of the tract length was performed using GraphPad Prism (http://www.graphpad.com/scientific-software/prism/).

Double-strand break detection by pulsed-field gel electrophoresis. DSB detection by PFGE was performed as previously described with minor modifications[7,30].

Immunofluorescence analyses. U-2 OS cells were grown on coverslips, fixed in 3.7% PFA, permeabilized in 0.5% Triton X-100 and blocked in 3% BSA. Coverslips were then stained with rabbit polyclonal anti-53BP1 (Novus Biologicals, NB100-304) (1:500) and mouse monoclonal anti-γH2AX (Millipore, 05-636) (1:300), and detected by appropriate Alexa 488– and Alexa 594–conjugated secondary antibodies (1:700). Toto3 iodide (Life Technologies, T3604) was used as a nuclear counter-stain. Cells were imaged using a Zeiss LSM 510 Meta confocal microscope. Images were acquired using the LSM 5 software. Foci were counted with ImageJ 'Analyze particles' function and 'JACoP' plugin was used to calculate colocalization. The average number of foci was obtained from three independent experiments analyzing at least 35 cells per sample.

Electron microscopy analysis of genomic DNA in mammalian cells. EM analysis of replication intermediates has been described in detail[31,32], including a description of the important parameters to consider specifically for the identification and the scoring of reversed forks[32].

38. Lucic, B. *et al.* A prominent β-hairpin structure in the winged-helix domain of RECQ1 is required for DNA unwinding and oligomer formation. *Nucleic Acids Res.* **39**, 1703–1717 (2011).
39. Ahel, D. *et al.* Poly(ADP-ribose)-dependent regulation of DNA repair by the chromatin remodeling enzyme ALC1. *Science* **325**, 1240–1243 (2009).
40. Cui, S. *et al.* Analysis of the unwinding activity of the dimeric RECQ1 helicase in the presence of human replication protein A. *Nucleic Acids Res.* **32**, 2158–2170 (2004).
41. Muzzolini, L. *et al.* Different quaternary structures of human RECQ1 are associated with its dual enzymatic activity. *PLoS Biol.* **5**, e20 (2007).
42. Sidorova, J.M., Li, N., Schwartz, D.C., Folch, A. & Monnat, R.J. Jr. Microfluidic-assisted analysis of replicating DNA molecules. *Nat. Protoc.* **4**, 849–861 (2009).

doi:10.1038/nsmb.2501

2.10.2 DNA2 /WRN contribution to reversed replication fork restart, by regressed arm processing.

A second collaborative effort was done with the same group of Dr. Vindigni in 2014, resulting in the publication in 2015 of an article in the Journal of Cell Biology, included here in the next few pages. In this study it was revealed that the nuclease activity of the DNA2 protein, and the ATP-ase dependent helicase activity of WRN, play a role in a second pathway of replication fork restart upon prolonged nucleotide depletion, which is uncovered in the absence of RECQ1. The conserted action of DNA and WRN in these specific experimental conditions leads to controlled reversed forks restart by resection of the regressed arm. I significantly contributed to perform several electron microscopy experiments and to analyze the resulting data, finally leading to the results published in Figure 6.

THE JOURNAL OF CELL BIOLOGY

JCB: Article

DNA2 drives processing and restart of reversed replication forks in human cells

Saravanabhavan Thangavel,[1]* Matteo Berti,[1]* Maryna Levikova,[2] Cosimo Pinto,[2] Shivasankari Gomathinayagam,[1] Marko Vujanovic,[2] Ralph Zellweger,[2] Hayley Moore,[3] Eu Han Lee,[4] Eric A. Hendrickson,[4] Petr Cejka,[2] Sheila Stewart,[3] Massimo Lopes,[2] and Alessandro Vindigni[1]

[1]Department of Biochemistry and Molecular Biology, Saint Louis University School of Medicine, St. Louis, MO 63104
[2]Institute of Molecular Cancer Research, University of Zurich, CH-8057 Zurich, Switzerland
[3]Department of Cell Biology and Physiology, Washington University School of Medicine, St. Louis, MO 63110
[4]Department of Biochemistry, Molecular Biology, and Biophysics, University of Minnesota, Minneapolis, MN 55455

Accurate processing of stalled or damaged DNA replication forks is paramount to genomic integrity and recent work points to replication fork reversal and restart as a central mechanism to ensuring high-fidelity DNA replication. Here, we identify a novel DNA2- and WRN-dependent mechanism of reversed replication fork processing and restart after prolonged genotoxic stress. The human DNA2 nuclease and WRN ATPase activities functionally interact to degrade reversed replication forks with a 5′-to-3′ polarity and promote replication restart, thus preventing aberrant processing of unresolved replication intermediates. Unexpectedly, EXO1, MRE11, and CtIP are not involved in the same mechanism of reversed fork processing, whereas human RECQ1 limits DNA2 activity by preventing extensive nascent strand degradation. RAD51 depletion antagonizes this mechanism, presumably by preventing reversed fork formation. These studies define a new mechanism for maintaining genome integrity tightly controlled by specific nucleolytic activities and central homologous recombination factors.

Introduction

The accurate replication of our genome is an essential requirement for the high-fidelity transmission of genetic information to daughter cells. DNA replication forks are constantly challenged and arrested by DNA lesions, induced by endogenous and exogenous agents, and by a diverse range of intrinsic replication fork obstacles, such as transcribing RNA polymerases, unusual DNA structures or tightly bound protein–DNA complexes (Carr and Lambert, 2013). An emerging model of how stalled or damaged forks are processed is that replication forks can reverse to aid repair of the damage (Atkinson and McGlynn, 2009; Ray Chaudhuri et al., 2012; Berti et al., 2013). This model implies significant remodeling of replication fork structures into four-way junctions and the molecular determinants required for reversed fork processing and restart are just beginning to be elucidated. The first evidence that supports the physiological relevance of this DNA transaction during replication stress in human cells arose from studies with DNA topoisomerase I (TOP1) inhibitors (Ray Chaudhuri et al., 2012). Additional studies established that the human RECQ1 helicase promotes the restart of replication forks that have reversed upon TOP1 inhibition by virtue of its ATPase and branch migration activities (Berti et al., 2013). These observations were recently extended to show that the RECQ1 mechanism of reversed fork restart is a more general response to a wide variety of replication challenges (Zellweger et al., 2015). Nonetheless, new lines of evidence point to alternative mechanisms and factors that might mediate either formation or processing of reversed replication forks (Bétous et al., 2012; Gari et al., 2008). These putative mechanisms likely include nucleases that are capable of processing stalled replication intermediates upon genotoxic stress (Cotta-Ramusino et al., 2005; Schlacher et al., 2011; Hu et al., 2012; Ying et al., 2012).

Here, we investigate the contribution of the human DNA2 nuclease/helicase in reversed fork processing. DNA2 is a highly conserved nuclease/helicase initially identified in *Saccharomyces cerevisiae* screening for mutants deficient in DNA replication (Kuo et al., 1983; Budd and Campbell, 1995). Yeast Dna2 plays

*S. Thangavel and M. Berti contributed equally to this paper.

Correspondence to Alessandro Vindigni: avindign@slu.edu

Abbreviations used in this paper: CPT, camptothecin; DSB, double-strand DNA break; EXO1, human exonuclease I; HDR, Homology directed repair; HR, homologous recombination; HU, hydroxyurea; MMC, mitomycin C; MRN, MRE11-RAD50-NBS1; TOP1, DNA topoisomerase I.

The Rockefeller University Press $30.00
J. Cell Biol. Vol. 208 No. 5 545–562
www.jcb.org/cgi/doi/10.1083/jcb.201406100

an essential role in Okazaki fragment maturation during lagging strand DNA replication (Budd and Campbell, 1997; Bae et al., 2001; Ayyagari et al., 2003). However, increasing evidence suggests that DNA2 has important—albeit yet undefined—roles in DNA replication stress response and DNA repair, which go beyond its postulated role in Okazaki fragment processing (Duxin et al., 2012; Karanja et al., 2012; Peng et al., 2012). The notion that DNA2 is important for DNA replication is strengthened by the observation that DNA2 forms a complex with various replication core components, including the replisome protein And-1 (Wawrousek et al., 2010; Duxin et al., 2012). Moreover, human DNA2 seems to play a partially redundant role with human exonuclease I (EXO1) in replication-coupled repair (Karanja et al., 2012), whereas a recent study in *S. pombe* suggested that the nuclease activity of DNA2 is required to prevent stalled forks from reversing upon HU treatment (Hu et al., 2012).

DNA2 also has an independent function in dsDNA break repair. Two distinct pathways act redundantly to mediate processive DSB resection downstream from the MRE11-RAD50-NBS1 (MRN) and CtIP factors in eukaryotic cells: one requires DNA2 and the other EXO1 (Gravel et al., 2008; Mimitou and Symington, 2008; Zhu et al., 2008; Nicolette et al., 2010). Specifically, DNA2 and EXO1 resect the 5′ ends of double-strand DNA breaks (DSBs) to generate 3′ single-stranded overhangs, which are essential to initiate homologous recombination. In yeast, DNA2-dependent dsDNA-end resection reaction requires the Sgs1 helicase to unwind the DNA from the break (Zhu et al., 2008; Cejka et al., 2010; Niu et al., 2010). This mechanism appears to be largely conserved in mammalian cells where DNA2 cooperates with the human BLM helicase to resect dsDNA ends in vitro (Nimonkar et al., 2011). However, mammalian cells possess five human RecQ homologues (RECQ1, RECQ4, RECQ5, BLM, and WRN) and WRN can also assist DNA2-dependent end resection, suggesting that BLM might not be the sole RecQ homologue required for this process (Liao et al., 2008; Sturzenegger et al., 2014). The ability of DNA2 and EXO1 to process dsDNA ends might also be relevant in the context of DNA replication to prevent the accumulation of replication-associated DSBs by promoting homologous recombination (HR) repair (Peng et al., 2012). Alternatively, these nucleases might be involved in the recovery of replication fork blockage by processing specific stalled replication fork structures.

This work uncovers a new DNA2- and WRN-dependent mechanism that mammalian cells use to process replication forks that have reversed as a result of replication inhibition. Importantly, it also shows that this mechanism is tightly regulated by human RECQ1 and the HR factor RAD51. Our observations shed light on a novel pathway for the suppression of chromosomal instability in mammalian cells and provide important new insight into the mechanisms of replication stress response associated with chemotherapeutic drug damage.

Results

DNA2 is required for stalled fork processing and restart

To begin elucidating the role of human DNA2 during replication stress, we monitored replication perturbation by genome-wide single-molecule DNA fiber replication assays. We pulse-labeled human osteosarcoma (U-2 OS) cells with the thymidine analogue CldU for 20 min, followed by a 60-min exposure to a selected genotoxic agent during the CldU labeling period, and by labeling with the second thymidine analogue, IdU, for an additional 40 min after removal of the genotoxic drug. We found that DNA2 plays an important role in restarting replication forks after treatment with the ribonucleotide reductase inhibitor hydroxyurea (HU), the topoisomerase I inhibitor camptothecin (CPT), and the interstrand cross-linking agent mitomycin C (MMC) (Fig. 1 A). In addition, DNA2 depletion increased the percentage of origin firing, but not of fork termination events (Fig. S1 A). Genetic knockdown–rescue experiments confirmed that complementation in DNA2-depleted U-2 OS cells with siRNA-resistant WT DNA2 abrogated the effect of DNA2 depletion on replication fork restart upon HU treatment. Moreover, expression of the nuclease-deficient DNA2 mutant D294A in DNA2-depleted cells revealed that the nuclease activity of DNA2 was essential for its role in replication fork restart (Fig. 1 B and Fig. S1 B).

We next measured whether DNA2 uses its nuclease activity to process stalled replication intermediates by monitoring the integrity of the newly synthesized DNA after HU treatment. To this purpose, we changed the DNA labeling scheme. We first pulsed U-2 OS cells with IdU for 45 min, and then varied the exposure time to HU from 0 to 8 h. The mean length of the IdU tracts progressively decreased during HU treatment from 18.2 µm (0 h) to 12.0 µm (8 h; Fig. 1 C). However, shRNA-mediated DNA2 depletion largely prevented IdU tract shortening, confirming that DNA2 is responsible for the observed nascent strand degradation (Fig. 1 D). Double-labeling experiments confirmed that the observed nascent tract shortening is indeed caused by the DNA2-dependent processing of ongoing replication forks and that this degradation is important to mediate efficient replication fork restart upon prolonged HU treatment (Fig. 1 E). Clonogenic analysis of U-2 OS cells treated with the same HU concentration used for the DNA fiber experiments showed a significantly reduced cell survival upon DNA2 depletion, indicating that the DNA2-dependent processing of stalled replication intermediates is critical for recovery from replication fork blockage (Fig. 2 A). The results obtained with the shRNA DNA2-depleted U-2 OS cells were validated using a new conditional knockout human colorectal carcinoma cell line (HCT116) where addition of tamoxifen to the culture medium led to DNA2-null cells. Analysis of the mean tract lengths confirmed that DNA2 knockout in HCT116 cells abrogates the prominent degradation observed upon HU treatment (Fig. 2 B). Collectively, these results indicate that human DNA2 degrades nascent strands at stalled replication forks to facilitate fork restart and promote viability after genotoxic stress induction.

RECQ1 regulates the fork processing activity of DNA2

On the basis of the recent discovery that RECQ1 is required to restart replication forks that have reversed upon genotoxic stress induction (Berti et al., 2013), we investigated whether RECQ1 regulates the fork processing activity of DNA2. Nascent IdU

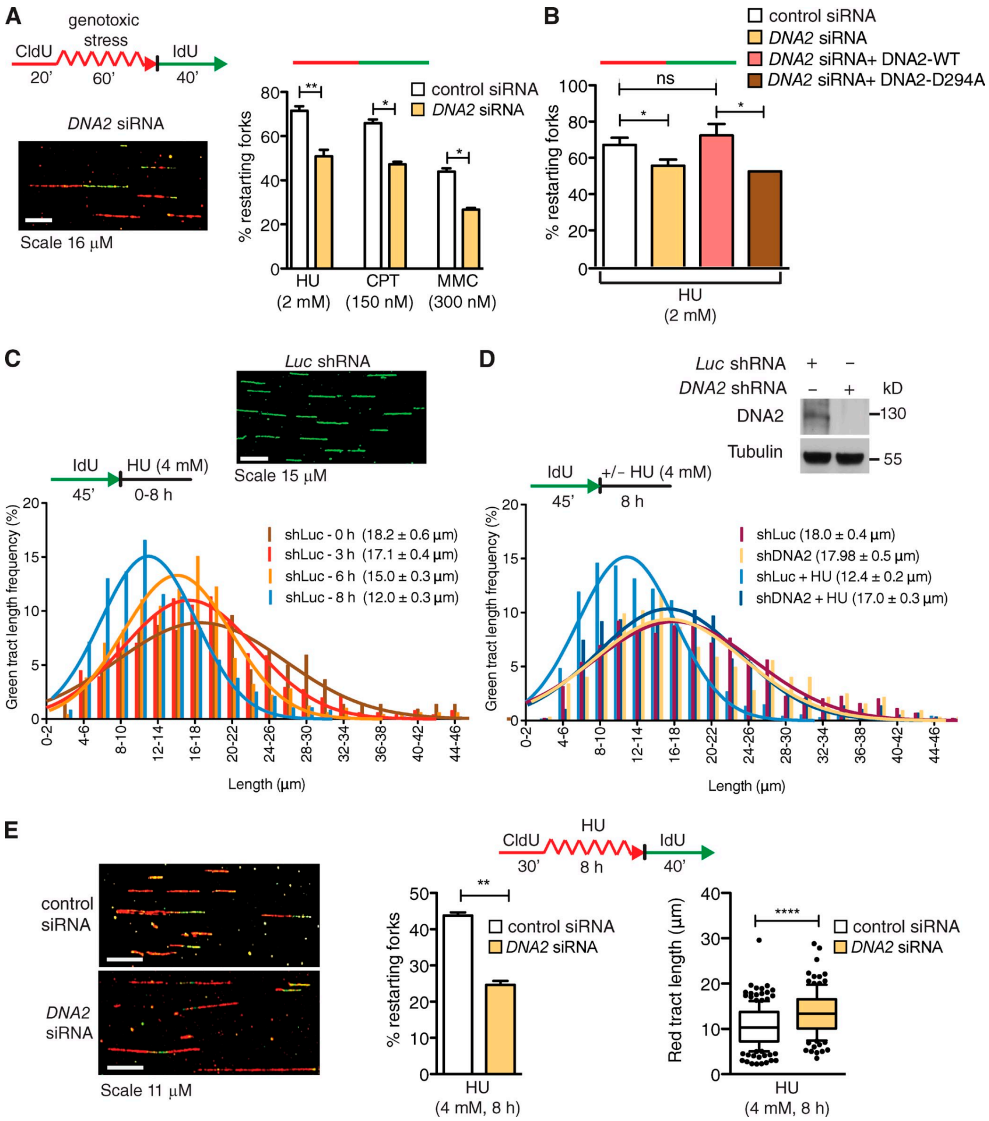

Figure 1. **DNA2 is required for replication fork restart and stalled fork processing upon genotoxic stress.** (A) Schematic of DNA fiber tract analysis. U-2 OS cells were transfected with control siRNA or *DNA2* siRNA before CldU or IdU labeling. Red tracts, CldU; curved red tracts, CldU with genotoxic agents (HU or CPT or MMC); green tracts, IdU. (bottom) Representative DNA fiber image. (right) quantification of red-green contiguous tracts (restarting forks). Mean shown, $n = 3$. Error bars, standard error. ns, not significant; *, $P < 0.05$; **, $P < 0.01$ (paired *t* test). (B) Quantification of restarting forks in DNA2-depleted cells expressing DNA-WT or DNA2-D294A. ns, not significant; *, $P < 0.05$ (paired Student's *t* test). (C, top) Representative DNA fiber image. (bottom) Representative IdU tract length distributions in Luc-depleted cells during different exposure time to HU (out of 3 repeats; $n \geq 300$ tracts scored for each dataset). Mean tract lengths are indicated in parentheses. (D) Top, DNA2 expression after shRNA knockdown. Bottom, representative IdU tracts in DNA2-depleted U-2 OS cells in the presence or absence of HU (out of 2 repeats; $n \geq 700$ scored for each dataset). (E, left) Representative DNA fiber images. (middle) Quantification of red-green contiguous tracts (restarting forks) after 8 h of HU. Mean shown, $n = 3$. Error bars, standard error. **, $P < 0.01$ (paired Student's *t* test). (right) Statistical analysis of CldU tracts detected within contiguous red-green tracts. Whiskers the 10th and 90th percentiles. ****, $P < 0.0001$ (Mann-Whitney test).

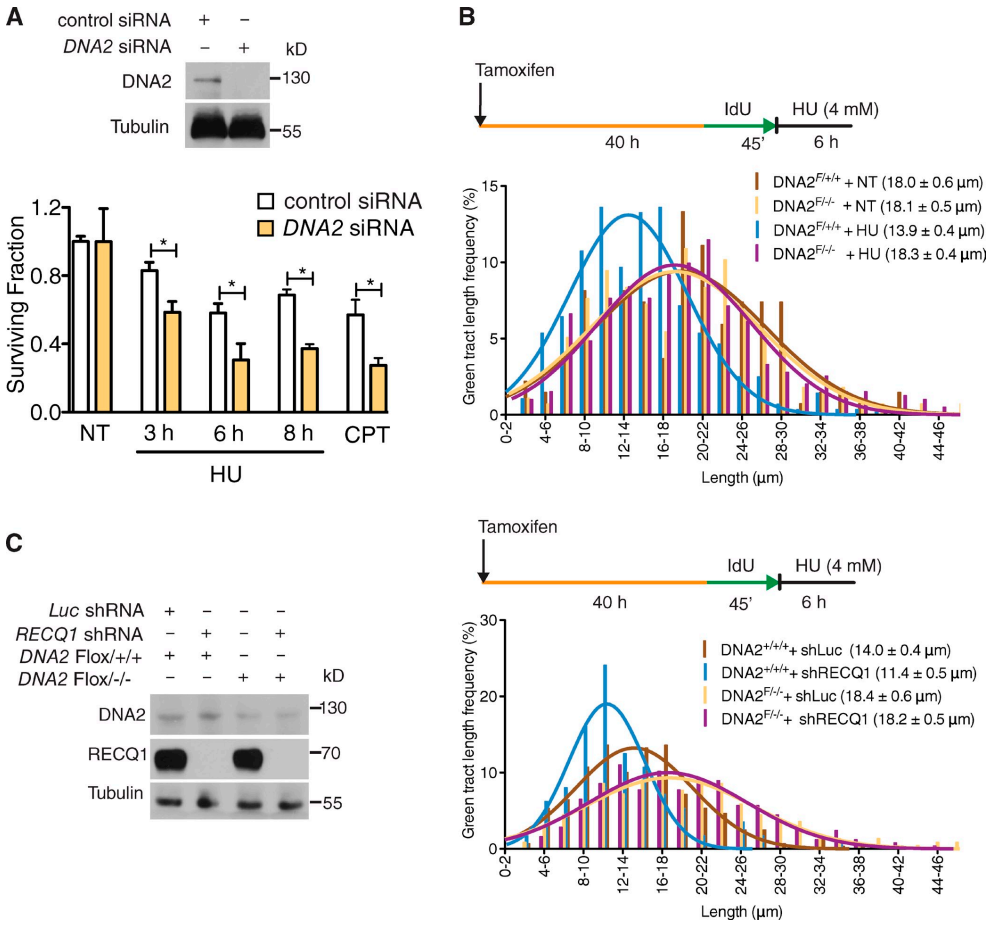

Figure 2. **DNA2 processes stalled replication forks.** (A, top) DNA2 expression after siRNA knockdown. (bottom) Colony-forming assays in control and DNA2-depleted U-2 OS cells treated with 4 mM HU for the indicated time. (B) Representative IdU tracts in DNA2 conditional knockout HCT116 cells (out of two repeats). Tamoxifen was added to generate conditional knockout cells (see Materials and methods). (C, left) Expression of DNA2 and RECQ1 in tamoxifen-treated HCT116 cells. Right, representative IdU tracts in DNA2 conditional knockout HCT116 cells depleted for Luc or RECQ1 (out of three repeats). $n \geq 300$ tracts scored for each dataset shown in B and C.

tracts were substantially shorter in RECQ1-depleted cells compared with control when replication forks were stalled with HU (after 8 h of HU treatment, the mean tract lengths were 7.9 and 12.0 µm, respectively; $P < 0.0001$; Fig. 3, A and B). In agreement with results from luciferase-depleted cells, DNA2 was also responsible for the nascent strand degradation phenotype observed in RECQ1-deficient U-2 OS cells (Fig. 3 C). Analogous results were obtained using the conditional DNA2 knockout HCT116 cell line (Fig. 2 C). In addition, we confirmed that the DNA2-dependent nascent strand degradation observed in the absence of RECQ1 is not limited to a specific replication inhibitor by replacing HU with CPT or MMC (Fig. 3, D and E).

Genetic knockdown–rescue experiments confirmed that complementation in RECQ1-depleted U-2 OS cells with shRNA-resistant WT RECQ1 abrogates the effect of RECQ1 depletion on replication fork processing upon HU treatment (Fig. 3 F). Interestingly, expression of the ATPase-deficient RECQ1 mutant K119R in RECQ1-depleted cells also abrogated the effect of RECQ1 depletion indicating that the ATPase activity of RECQ1 was not required for its role in protecting stalled forks from DNA2-dependent degradation (Fig. 3 F). These results point to an additional role of RECQ1 in protecting replication forks from extensive DNA2-dependent degradation, which is independent of RECQ1 ATPase activity.

DNA2 function in stalled fork processing is distinct from EXO1, Mre11, and CtIP

Next, we tested whether other nucleases share a function similar to DNA2 in stalled fork processing. To address this point, we depleted Mre11, EXO1, and CtIP in U-2 OS cells with siRNA-mediated technologies. We found that none of these nucleases share the same phenotype of DNA2 in RECQ1-proficient cells (Fig. 4 A). Furthermore, depletion of these nucleases had only a marginal effect on the rescue of the prominent nascent strand degradation phenotype observed in the absence of RECQ1, indicating that DNA2 has a unique function in reversed fork processing that is not shared by these human nucleases (Fig. 4, B–D). MUS81 is another structure-specific nuclease that plays a critical role in replication fork rescue by converting stalled replication forks into DNA DSBs that can be processed by Homology Directed Repair (HDR) (Hanada et al., 2007; Franchitto et al., 2008). This raised the possibility that the DNA2-dependent degradation originated from the processing of MUS81-dependent DSBs. However, MUS81 depletion did not prevent nascent strand degradation, indicating that DNA2 is not processing stalled replication intermediates that are cleaved by MUS81 (Fig. 4 E).

DNA2 and WRN act together to process stalled replication forks

DNA2-dependent dsDNA-end resection needs the support of a RecQ helicase to unwind the DNA from the break (Cejka et al., 2010; Niu et al., 2010; Nimonkar et al., 2011). To determine the identity of the helicase that acts in conjunction with DNA2 in stalled fork processing, we measured the extent of nascent strand degradation in BLM-, WRN-, and RECQ4-depleted U-2 OS cells. Our DNA fiber analysis showed that WRN depletion mimicked the effect of DNA2-depletion, completely abrogating the prominent nascent strand degradation phenotype observed in RECQ1-depleted U-2 OS cells (Fig. 5 A). The same results were confirmed using WRN and DNA2 codepleted cells, suggesting that DNA2 and WRN are epistatic in nucleolytic processing of stalled forks (Fig. S1 C). The partial nascent strand degradation observed in RECQ1-proficient U-2 OS cells was also abrogated by WRN depletion (Fig. S1 D). Conversely, BLM depletion had only a marginal effect on the nascent strand degradation phenotype observed in RECQ1-depleted cells, whereas RECQ4 depletion had no effect (Fig. S2, A and B). Thus, the WRN helicase plays a prominent role in assisting DNA2-dependent degradation of stalled replication forks.

We next compared the percentage of restarting replication forks in DNA2-depleted, WRN-depleted, and DNA2/WRN-codepleted cells. WRN depletion leads to a decrease in restarting forks (69 to 50%; $P = 0.0068$). These results are almost identical to those obtained with the DNA2-depleted or DNA2/WRN-codepleted cells, implying that WRN and DNA2 are epistatic also in the restart process (Fig. 5 B). The notion that DNA2 and WRN functionally interact to process stalled replication intermediates is further supported by our observation that the two proteins form a complex both in the presence and absence of replication stress (Fig. 5 C). Of note, RECQ1 is not part of the WRN:DNA2 complex. Collectively, these results suggest that DNA2 cooperates with WRN to promote nascent strand processing and fork restart after HU treatment.

The nuclease activity of DNA2 and the ATPase activity of WRN are essential to process stalled replication forks

DNA2 is characterized by an N-terminal nuclease domain and by a C-terminal helicase domain, but the function of its helicase activity is still debated (Masuda-Sasa et al., 2006). To assess the roles of these two activities in stalled fork processing, we performed genetic knockdown-rescue experiments where we depleted DNA2 and then attempted to rescue fork processing by expressing a Flag-tagged siRNA resistant WT DNA2 control, nuclease-deficient DNA2-D294A, or ATPase-deficient DNA2-K671E. All the experiments were performed in RECQ1-depleted cells, where the effect of DNA2 is more apparent. DNA fiber analysis showed that complementation with nuclease-deficient DNA2 prevents fork processing, whereas complementation with WT or ATPase-deficient DNA2 leads to the same fork processing phenotype observed in DNA2-proficient cells (Fig. 5 D and Fig. S2 C). Therefore, the nuclease, but not the ATPase activity of DNA2, is necessary for fork processing.

Next, we used a Werner Syndrome (WS) fibroblast cell line (AG11395) expressing missense mutant forms of WRN, which inactivate either the exonuclease (WRN-E84A) or the ATPase (K577M) activity of WRN (Pirzio et al., 2008). The ATPase, but not the nuclease activity of WRN, was important for fork processing (Fig. 5 E and Fig. S2 D). These findings were validated by genetic knockdown-rescue experiments where we complemented WRN-depleted U-2 OS cells either with an shRNA resistant WT WRN control or the ATPase-deficient WRN-K577M mutant and found that complementation with the ATPase-deficient mutant prevented fork processing (Fig. S2, E and F). Collectively, these results show that human DNA2 needs the support of the ATPase activity of WRN to promote degradation of the nascent DNA strands.

DNA2 processes reversed replication forks

To gain insight into the actual replication structures processed by DNA2, we inspected the fine architecture of the replication intermediates using a combination of in vivo psoralen cross-linking and EM (Neelsen et al., 2014). Our analysis showed a substantial fraction of reversed replication forks (~24% of molecules analyzed) in control U-2 OS cells treated with 4 mM HU. RECQ1-depletion, and to an even greater extent DNA2-depletion, resulted in a higher frequency of fork reversal events (~30 and 40%, respectively) compared with HU-treated cells. Co-depletion of RECQ1 and DNA2 further increased the frequency of reversed forks (~50%), suggesting that RECQ1 and DNA2 are involved into two distinct mechanisms of reversed fork processing. Interestingly, RECQ1 and/or DNA2 depletion also led to a significant amount of fork reversal events in unperturbed U-2 OS cells (Fig. 6, A and B). WRN-depletion phenocopied DNA2-depletion in terms of reversed fork accumulation, both the presence and in the absence of HU. Moreover, DNA2/

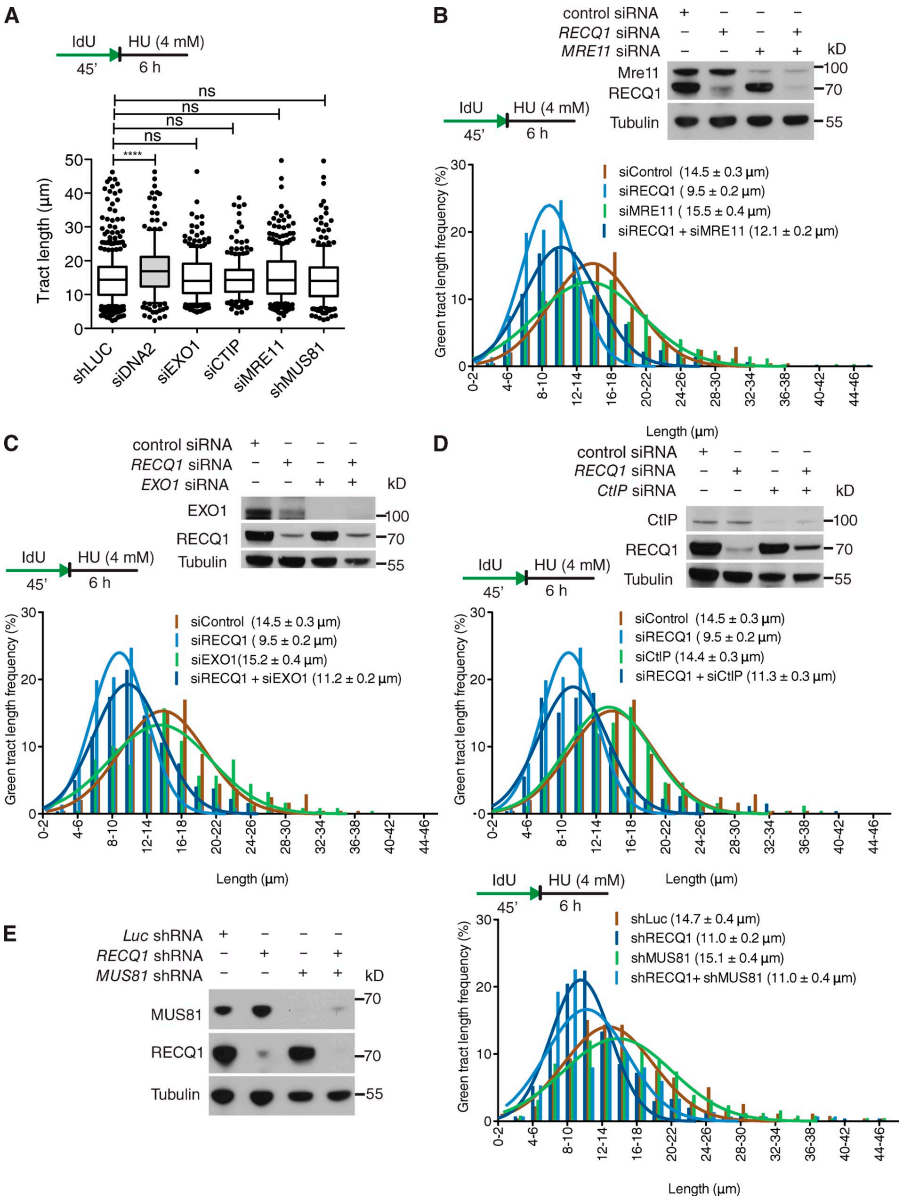

Figure 4. **EXO1, MRE11, CtIP, and MUS81 depletion does not affect stalled fork processing.** (A) Statistical analysis of IdU tracts from U-2 OS cells depleted for the indicated proteins in the presence of 4 mM HU. (B) Representative IdU tracts in control, RECQ1-, MRE11-, or RECQ1/MRE11-codepleted U-2 OS cells (out of 2 repeats). (top) Expression of RECQ1 and MRE11 after siRNA knockdown. (C) Representative IdU tracts in control, RECQ1-, EXO1-, or RECQ1/EXO1-codepleted U-2 OS cells (out of 2 repeats). (top) Expression of RECQ1 and EXO1 after siRNA knockdown. (D) Representative IdU tracts in control, RECQ1-, CtIP-, or RECQ1/CtIP-codepleted U-2 OS cells (out of 2 repeats). (top) Expression of RECQ1 and CtIP after siRNA knockdown. (E) Representative IdU tracts in Luc-, RECQ1-, MUS81-, or RECQ1/MUS81-codepleted U-2 OS cells in the presence of HU (out of 2 repeats). (left) Expression of RECQ1 and MUS81 after shRNA knockdown. $n \geq 300$ tracts scored for each dataset shown in A–E.

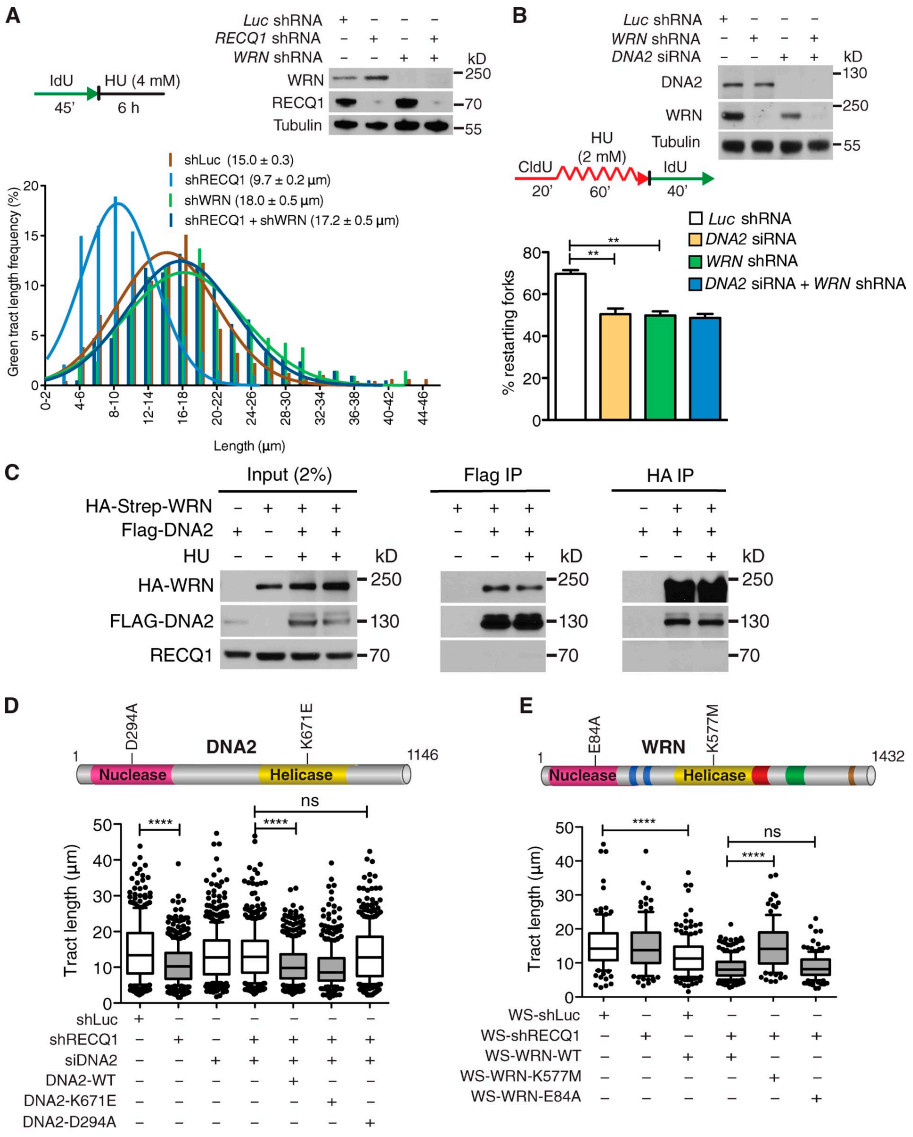

Figure 5. **DNA2 and WRN are epistatic in stalled fork processing and replication restart.** (A) Representative IdU tracts in RECQ1-, WRN-, or RECQ1/WRN-codepleted U-2 OS cells (out of 2 repeats; $n \geq 300$ tracts scored for each dataset). (top) RECQ1 and WRN expression after shRNA knockdown. (B) Quantification of restarting forks in DNA2-, WRN-, or DNA2/WRN-codepleted cells. Mean shown, $n = 3$. Error bars, standard error. *, $P < 0.05$; **, $P < 0.01$ (paired t test). (top) Expression of WRN and DNA2 after shRNA knockdown. (C) Co-IP experiments in HEK293T cells transfected with empty vectors, Flag-DNA2, or Strep-HA-WRN. Cells were treated with 4 mM HU (3 h) where indicated. Whole-cell extracts were analyzed before (input) and after IP. (D) Statistical analysis of IdU tracts from RECQ1/DNA2-codepleted U-2 OS cells complemented with WT, ATPase-deficient (K671E), or nuclease-deficient (D294A) DNA2, when indicated. (E) Statistical analysis of IdU tracts from RECQ1-depleted WS cells complemented with WT, ATPase-deficient (K577M), or nuclease-deficient (E84A) WRN. Whiskers in D and E indicate the 10th and 90th percentiles. ns, not significant; ****, $P < 0.0001$ (Mann-Whitney test). $n \geq 300$ tracts scored for each dataset shown in D and E.

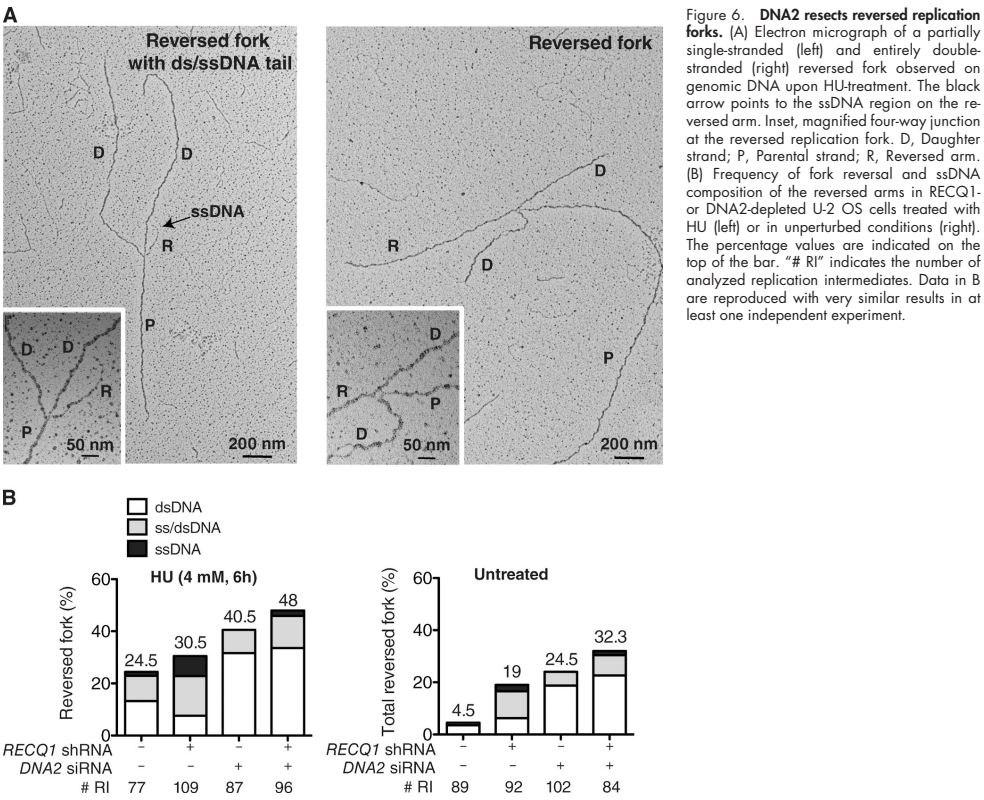

Figure 6. **DNA2 resects reversed replication forks.** (A) Electron micrograph of a partially single-stranded (left) and entirely double-stranded (right) reversed fork observed on genomic DNA upon HU-treatment. The black arrow points to the ssDNA region on the reversed arm. Inset, magnified four-way junction at the reversed replication fork. D, Daughter strand; P, Parental strand; R, Reversed arm. (B) Frequency of fork reversal and ssDNA composition of the reversed arms in RECQ1- or DNA2-depleted U-2 OS cells treated with HU (left) or in unperturbed conditions (right). The percentage values are indicated on the top of the bar. "# RI" indicates the number of analyzed replication intermediates. Data in B are reproduced with very similar results in at least one independent experiment.

WRN-codepletion did not cause a further increase in reversed fork frequency, thus supporting our conclusion that DNA2 and WRN work together in reversed fork processing (Fig. S3 A).

Next, we evaluated the single-strand composition of the regressed arms. To measure ssDNA, we carefully inspected the frequency and length of ssDNA regions on the regressed arms by detecting local difference in filament thickness. DNA2 depletion led to a higher frequency of reversed forks with a dsDNA arm—and a corresponding decrease of partially or entirely single-stranded reversed forks—in both RECQ1-proficient and deficient cells (Fig. 6). Thus, DNA2-mediated resection is directed to completely or partially digest one strand of the reversed arm leading to reversed forks that are either entirely single stranded or have a protruding ssDNA tail. However, prolonged stalling by HU was associated with accumulation of postreplicative ssDNA gaps on replicated duplexes, which was maximal in RECQ1-depleted cells and suppressed by DNA2 depletion (Fig. S3, B and C). Consequently, ssDNA gaps may reflect additional activity of the same nucleolytic apparatus along the postreplicated duplexes or restart of partially resected reversed forks.

As an alternative readout for DNA2-dependent resection, we examined the phosphorylation status of RPA and the checkpoint kinase Chk1 (Zeman and Cimprich, 2014). DNA2 depletion caused a reduction in RPA and Chk1 phosphorylation in both RECQ1-proficient and RECQ1-deficient U-2 OS cells, suggesting that the DNA2-dependent resection of nascent strands might also contribute to checkpoint activation (Fig. S3 D).

RAD51 promotes DNA2-dependent degradation of reversed replication forks

The central recombinase factor RAD51 is directly implicated in reversed fork formation upon genotoxic stress (Zellweger et al., 2015). Thus, we investigated whether RAD51 depletion may affect the reversed fork processing activity of DNA2. We found that RAD51 knockdown largely prevents DNA2 nucleolytic processing both in RECQ1 proficient and RECQ1-deficient cells (Fig. 7 A). Genetic knockdown–rescue experiments confirmed that expression of exogenous RAD51 in RAD51-depleted U-2 OS cells restored the fork processing phenotype (Fig. 7 B). These results indicate that DNA2-dependent nucleolytic

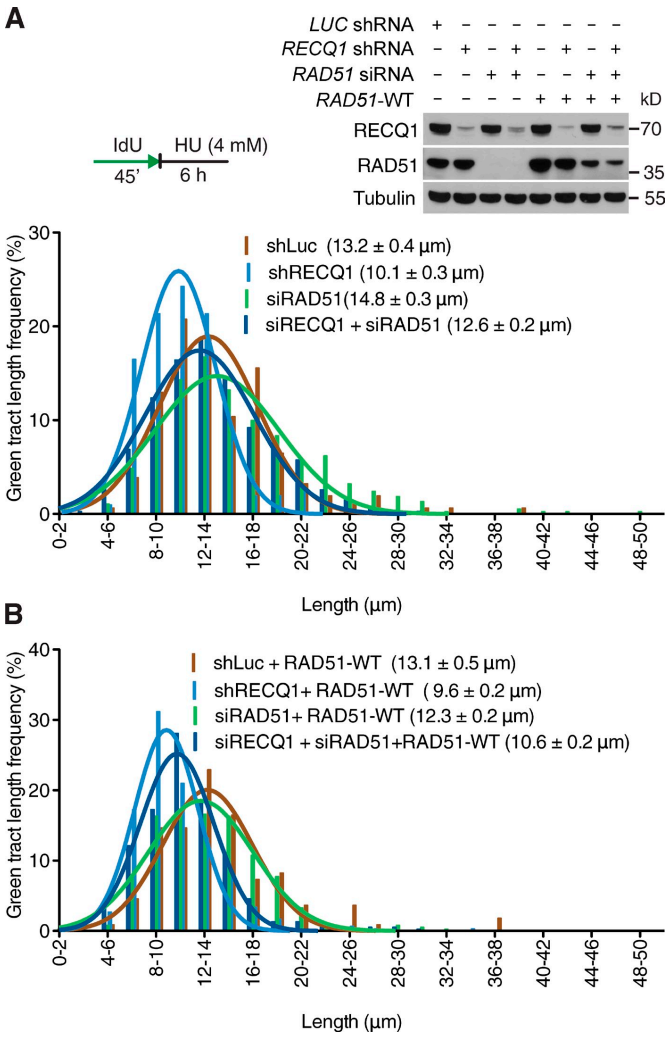

Figure 7. **RAD51 promotes DNA2-depedent degradation of reversed replication forks.** (A) Representative IdU tracts in RECQ1-, RAD51-, or RECQ1/RAD51-codepleted U-2 OS cells (out of 2 repeats). Above, RECQ1 and RAD51 expression after siRNA knockdown RAD51-WT are U-2 OS cells stably expressing siRNA resistant exogenous RAD51. (B) Representative IdU tracts in U-2 OS cells expressing exogenous RAD51 (out of 2 repeats). $n \geq 300$ tracts scored for each dataset shown in A and B.

processing is specifically targeted to reversed fork structures because it is not detected in a genetic background that prevents reversed fork formation—i.e., RAD51 knockdown.

DNA2 preferentially degrades reversed fork structures with a 5′-to-3′ polarity

The notion that DNA2 end resection has a preferential polarity in vivo is consistent with biochemical studies showing that even though DNA2 has the intrinsic capacity to degrade both 5′- and 3′-terminated ssDNA, RPA enforces a primarily 5′-to-3′ end-resection bias (Cejka et al., 2010; Niu et al., 2010; Nimonkar et al., 2011). Thus, we set up new biochemical assays to test whether human DNA2 prefers four-way junction substrates—i.e., reversed replication forks—versus linear DNA duplexes and whether it degrades these substrates with a 5′-to-3′ polarity in the presence of RPA (Fig. 8, A and B). The sequences of the four arms of the four-way junction substrates are mutually heterologous to prevent four-way junction branch migration. DNA2-degraded four-way junction substrates more efficiently than linear dsDNA duplexes, with 20 nM DNA2 required to degrade ∼60% of the four-way junction substrates versus only ∼30% of the linear duplex (Fig. 8 C). Importantly, supplementing the reaction with RPA greatly stimulated the degradation activity of human DNA2 (Fig. 8 D and Fig. S4 A). Additional

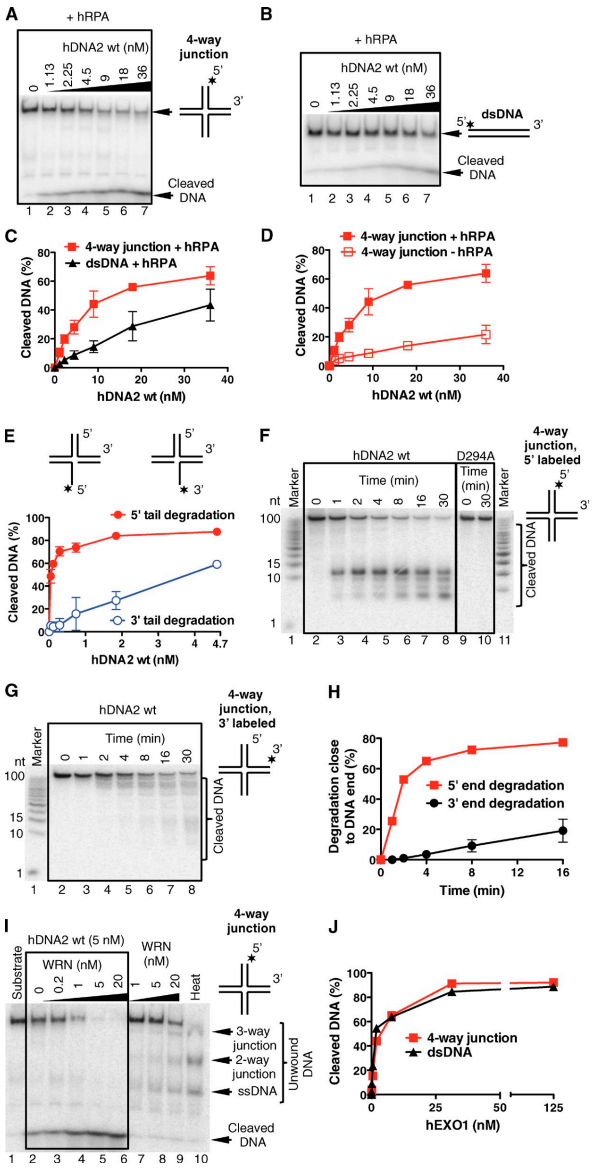

Figure 8. **Human DNA2 preferentially degrades branched DNA in a 5′-3′ direction in reactions stimulated by WRN.** (A) Degradation of a four-way junction by human DNA2 (hDNA2) in the presence of hRPA (native 6% polyacrylamide gel) (B) Experiment as in A, but with dsDNA. (C) Quantitation of data from A and B. Averages shown ± SEM; *n* = 2. (D) DNA degradation is stimulated by hRPA. The data points from +hRPA condition are the same as in C. Averages shown ± SEM; *n* = 2. (E) Quantitation of degradation of a 3′ or 5′ ssDNA-tailed three-way junction by hDNA2. The reactions were performed in 3 mM magnesium acetate and 22.3 nM hRPA. Averages shown ± SEM; *n* = 2. (F) Kinetics of degradation of a four-way junction by hDNA2 (9 nM) in the presence of hRPA (denaturing 20% polyacrylamide gel). The substrate was labeled at the 5′ end (*). D294A, nuclease-dead variant of hDNA2. (G) Experiment as in F, but using a four-way junction labeled at the 3′ end. (H) Quantitation of DNA cleavage near (less than 15 nt) a 5′ or 3′ DNA end from experiments of F and G. Averages shown ± SEM; *n* = 2. (I) WRN and hDNA2 degrade four-way junction DNA in a synergistic manner. Reactions with indicated hDNA2 and/or WRN concentrations and 65 nM hRPA were analyzed on a 6% native polyacrylamide gel. Heat, partially heated DNA substrate indicating the positions of DNA unwinding intermediates. (J) Quantitation of four-way junction and dsDNA degradation by human EXO1 (hEXO1). Averages shown ± SEM; *n* = 2.

experiments using either 5′-end or 3′-end ^{32}P-labeled four-way junctions confirmed that human DNA2 had a strong 5′-to-3′ bias in end resection in the presence of RPA (Fig. 8, E–H; and Fig. S4, B and C). Catalytically dead DNA2 D294A had no capacity to degrade DNA, showing that the nuclease activity is inherent to WT DNA2 (Fig. 8 F). The same results were recapitulated using purified yeast DNA2 (Fig. S5, A–F). Interestingly, addition of the ATPase-deficient RECQ1 mutant (RECQ1-K119R) to the reaction mix significantly inhibited the four-way junction degradation activity of human DNA2 (Fig. S4, D and E). These results suggest that the binding of RECQ1 to stalled replication forks limits the fork processing

activity of DNA2, as inferred by our cellular studies. However, we cannot rule out the possibility that the inhibitory effect observed in the biochemical assays is simply associated with competition for substrate recognition between the two proteins. In agreement with our in vivo data, we show that WRN promoted the degradative capacity of DNA2 on nicked, gapped, or four-way junction substrates (Fig. 8 I and Fig. S4, F and G); similar behavior was observed when yeast Dna2 was coupled with the Sgs1 helicase (Fig. S5, G and H). DNA was degraded by WRN and DNA2 in a remarkably synergistic manner: 5 nM concentration of either WRN or DNA2 alone led only to a minor DNA unwinding/degradation (Fig. 8 I, lanes 2 and 8). When combined, both enzymes completely degraded the four-way junction DNA (Fig. 8 I, lane 5). In contrast, no such synergy was observed when human DNA2 was combined with the noncognate yeast meiotic Mer3 helicase (Fig. S4 H), suggesting that the species-specific interaction between DNA2 and WRN results in a vigorous DNA degradation. Similarly, WT RECQ1 did not promote DNA degradation by DNA2 (Fig. S4 I).

On the basis of our results that DNA2 does not share the same function of EXO1 in reversed fork processing, we decided to compare the end-resection activities of human DNA2 and human EXO1 using the four-way junction substrates. EXO1—unlike DNA2—degraded both four-way junction substrates and linear duplexes with equal efficiency (Fig. 8 J and Fig. S4, J and K). The use of yeast variants of Dna2 and Exo1 yielded analogous results (Fig. S5, I–K). Collectively, these studies further implicate DNA2, and its nuclease activity, in reversed replication fork degradation—that is specifically stimulated by WRN—and point to an important difference in substrate preference between DNA2 and EXO1. Moreover, the polarity of reversed fork degradation by DNA2 measured in the presence of RPA displays the same bias anticipated from the EM analysis of the replication intermediates.

Discussion

The present work uncovers a new mechanism for reversed fork processing and restart that requires the coordinated activities of the human DNA2 nuclease and WRN helicase (Fig. 9). The DNA2-dependent end resection leads to partially single-stranded reversed forks and is required for efficient replication fork restart under conditions of persistent replication blockage. WRN interacts with DNA2 and its ATPase activity is needed for DNA2-dependent degradation, presumably to transiently open the dsDNA arm of the reversed replication forks.

To date, we have identified two mechanisms of reversed replication fork resolution, one dependent on RECQ1 ATPase and branch migration activity (Berti et al., 2013) and the other on DNA2 nuclease and WRN ATPase activity. Moreover, the DNA2/WRN mechanism is tightly regulated by an ATPase-independent function of RECQ1 that might limit DNA2 activity by binding to reversed forks. Of note, our EM experiments show that reversed replication forks accumulate in RECQ1- and DNA2-depleted cells also in unperturbed conditions suggesting that fork reversal is remarkably frequent when DNA replication faces intrinsic replication fork obstacles, and that RECQ1 and DNA2 have a conserved role in restarting reversed forks in unperturbed S-phase.

DNA2 function during DNA replication is vital for maintenance of genome stability (this study; Duxin et al., 2012; Karanja et al., 2012). These findings indicate that the controlled DNA2-dependent degradation of reversed replication forks is a physiologically relevant mechanism to provide resistance to prolonged genotoxic treatments. This mechanism is distinct from the pathological MRE11-dependent degradation of stalled replication intermediates detected in the absence of crucial Fanconi Anemia (FA)/HR factors (Schlacher et al., 2011, 2012; Hashimoto et al., 2012; Ying et al., 2012).

We find that depletion of the central recombinase factor RAD51 prevents nascent strand degradation. This finding, coupled with the recent observation that RAD51 is directly implicated in reversed fork formation (Zellweger et al., 2015), reinforce our conclusion that the DNA2-dependent pathway starts from the reversed arm of stalled replication forks and acts downstream of the RAD51-mediated replication fork reversal. Given that RAD51 is required for reversed fork formation (Zellweger et al., 2015), we speculate that the MRE11-dependent pathway is only uncovered in the absence of fork reversal—i.e., via a perturbation in RAD51 function—and likely attacks unprotected and nonreversed forks upon prolonged stalling. A crucial challenge for future studies will be to investigate why we do not observe a contribution of the MRE11 pathway in nascent strand degradation upon RAD51 depletion. It is tempting to speculate that RAD51 depletion might interfere with MRE11-dependent fork processing, in addition to preventing fork reversal. Conversely, perturbation of RAD51 function—e.g., via BRCA2 depletion (Schlacher et al., 2011)—might be sufficient to prevent fork reversal—hence DNA2-dependent degradation—but still allow residual RAD51 loading to promote MRE11-dependent degradation.

Our DNA fiber analysis suggests that DNA2 degrades stalled replication intermediates beyond the maximum length of the reversed arms measured by EM (up to several kilobases). A possible interpretation of these results is that after the initial DNA2/WRN-mediated regressed arm degradation is complete, other nucleolytic activities or DNA2 itself may codegrade both sides of the replication fork, thus leading to extensive degradation events detectable by DNA fibers. In this scenario, our EM images likely represent snapshots of the "slow steps" of this reaction—i.e., the DNA2/WRN-mediated degradation of the regressed arms—resulting in the drastic increase in reversed fork frequency observed in the absence of DNA2. Once the regressed arm has been resolved, the nucleolytic degradation might quickly proceed to degrade nascent strands behind the junction—as suggested by the DNA2-dependent increase in ssDNA gaps behind the observed forks—finally leading to reannealing of the parental strands and backtracking of the fork (Fig. S3 E). A new reversal event may occur when this extensive degradation leads to asymmetric ssDNA accumulation at the fork (Zellweger et al., 2015), resetting the backtracked fork to the slow step of the process. However, fork backtracking is only one possible model to explain the extensive degradation detected by DNA fibers and further work would be required to uncover additional nucleolytic activities that might be involved in this process.

Biochemical studies suggested that *Schizosaccharomyces pombe* Dna2 cleaves the leading and lagging reversed strands of

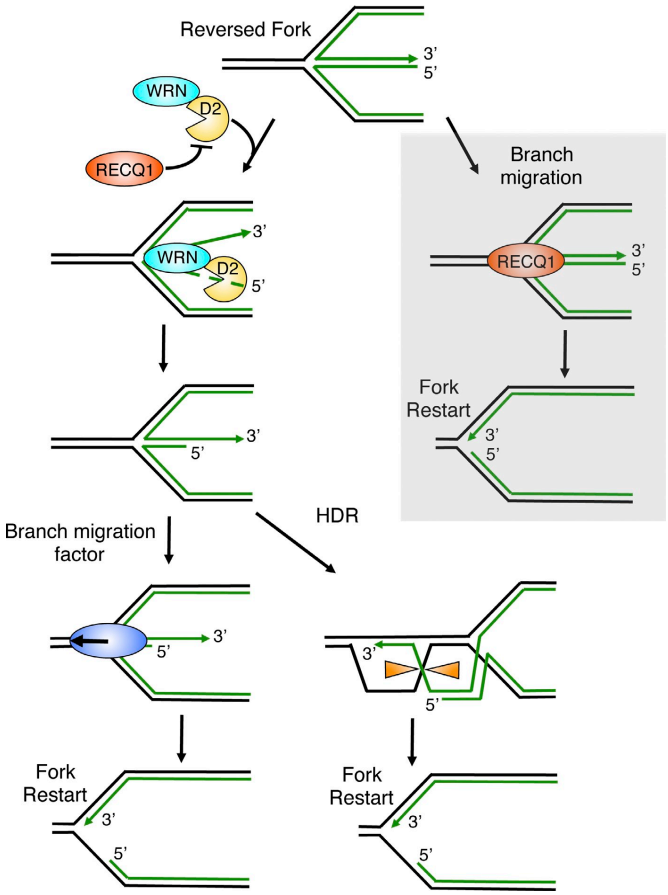

Figure 9. **Schematic model for the combined roles of DNA2 and WRN in reversed fork processing.** DNA2 and WRN functionally interact to process reversed forks. DNA2 degrades reversed forks with a 5′-to-3′ polarity. WRN ATPase activity assists DNA2 degradation possibly by promoting the opening of the reversed arm of the fork. RECQ1 limits DNA2 activity by an ATPase-independent function. Branch migration factors specifically recognize the partially resected reversed forks to promote fork restart. Alternatively, the newly formed 3′ overhang of the reversed fork invades the duplex ahead of the fork, resulting in Holliday junction structures that can be resolved by specific resolvases or dissolvases to promote fork restart. Gray box, RECQ1 can independently restart reversed forks by virtue of its ATPase and branch migration activity.

a model replication fork with similar efficiency in the absence of replication protein A (Hu et al., 2012). However, it is likely that only the 5′-to-3′ directionality is important in vivo, because RPA is known to stimulate the 5′-to-3′ and inhibit the 3′-to-5′ nuclease activity of yeast DNA2 (Cejka et al., 2010; Niu et al., 2010). In agreement with this conclusion, our biochemical data show that DNA2-dependent end resection proceeds with a 5′ to 3′ polarity in the presence of RPA. Moreover, our EM experiments clearly show that DNA2 depletion affects the frequency of reversed forks that are either entirely or partially single-stranded supporting the notion that DNA2-dependent degradation of reversed forks occurs with a preferential polarity in vivo.

The resection activity of human DNA2 was postulated to activate the ATR/Chk1 checkpoint under conditions of replication stress (Karanja et al., 2012). Indeed, we find that DNA2 depletion prevents ATR checkpoint activation after HU treatment. Moreover, the increased origin firing observed upon DNA2 depletion is consistent with observations that the deregulation of checkpoint activity leads to a large increase in the number of newly initiated origins (Couch et al., 2013). However, the extent of ATR activation does not necessarily reflect the amount of ssDNA detected at replication forks, whether at the junction, at ssDNA gaps, or at regressed arms (Zellweger et al., 2015). In light of these findings, we rather suggest that DNA2-dependent ATR activation may reflect DNA2 recruitment to the stalled forks per se, or subtle changes of fork architecture that are associated with its recruitment but possibly escape our EM analysis. This interpretation is supported by the recent discovery that yeast Dna2 has a direct role in Mec1 activation (the ortholog of human ATR), independent from its nuclease or helicase activity (Kumar and Burgers, 2013). Of note, the increased origin firing frequency observed upon DNA2 depletion is not associated to a parallel increase in the frequency of termination events (Fig. S1 A) possibly because the defects in replication fork restart associated

with DNA2 depletion limit the number of termination events even under conditions of increased origin firing.

WRN plays an important—albeit mechanistically ill-defined—role in the recovery from replication blockage, and mutations in the *WRN* gene are linked to the cancer predisposition disorder Werner Syndrome (Sidorova et al., 2008; Murfuni et al., 2012). Our studies infer that the high genomic instability of WRN-deficient cells may result from aberrant processing of reversed replication intermediates. In particular, given the consolidated role of WRN at difficult-to-replicate regions—e.g., telomeres and fragile sites (Crabbe et al., 2004; Murfuni et al., 2012)—we speculate that WRN, in conjunction with DNA2, is required to process reversed forks arising spontaneously at these genomic loci. Biochemical studies pointed to a putative role of WRN in fork reversal and/or restart by showing that WRN efficiently promotes both the formation and restoration of oligonucleotide-based reversed fork substrates (Machwe et al., 2011). We show that WRN ATPase activity is needed for the DNA2-dependent degradation of reversed replication forks. Our interpretation for the role of WRN ATPase activity is that it facilitates DNA2-dependent degradation of the reversed forks by transiently opening the dsDNA arm of the reversed fork. This mechanism is reminiscent to the DNA2-dependent mechanism of DSB resection where the yeast Sgs1 helicase is required to transiently open the DNA duplex to generate a 5′ ssDNA tail that is in turn degraded by DNA2 (Zhu et al., 2008; Cejka et al., 2010; Niu et al., 2010). We suggest that WRN is the functional homologue of Sgs1 in mammalian cells, at least in the context of DNA2-dependent reversed replication fork processing. However, BLM was also shown to interact and cooperate with DNA2 to resect dsDNA ends in vitro opening the possibility that other human RecQ helicases might substitute for WRN, depending on the nature of the DNA lesion being processed or the particular cellular context (Nimonkar et al., 2011; Sturzenegger et al., 2014). This mechanism seems to be well-conserved throughout evolution because it is highly reminiscent of the stalled fork processing pathway described in *E. coli* where the RecJ nuclease cooperates with bacterial RecQ to process blocked replication intermediates (Courcelle et al., 2003). In addition, the prokaryotic RecBCD helicase-nuclease plays an important role in resecting replication forks after reversal (Seigneur et al., 1998) and DNA2 is of the same family of nucleases as RecB. Whether the DNA2/WRN-mediated resection activity can degrade additional stalled replication intermediates other than reversed forks is worth future investigation.

EXO1, MRE11, and CtIP play central roles in DNA repair and are also implicated in the recovery from replication fork blockage (Cotta-Ramusino et al., 2005; Schlacher et al., 2011; Yeo et al., 2014). None of these nucleases, however, participates in the DNA2-dependent processing of reversed replication forks pointing to a specific role of DNA2 that, unlike its function in DSB resection, is not shared by other nucleases. A possible interpretation of these results is that the reversed forks are characterized by a particular structure of the terminal end that does not require the trimming activity of other nucleases to promote DNA2-dependent resection. However, some of these nucleases might still be able to access stalled forks under specific genetic backgrounds. For example, MRE11 degrades stalled replication intermediates only in a BRCA2-deficent background, as already discussed (Schlacher et al., 2011). Moreover, the cleavage of unresolved replicative intermediates by the structure-specific MUS81 endonuclease is a late response to replicative stress, which becomes activated only when other attempts to overcome stalled replication have been exhausted (Hanada et al., 2007; Franchitto et al., 2008). Thus, MUS81 might still resolve reversed replication forks as a back-up system to unlink sister chromatids and facilitate mitotic segregation in the absence of DNA2 or WRN.

Collectively, these studies highlight a new important mechanism for the recovery from replication blockage. This mechanism relies on the DNA2-dependent processing of reversed forks—leading to ssDNA stretches on the regressed arms—which appear to promote efficient fork restart. A possible explanation for the need of partially single-stranded DNA structures to promote fork restart is that they represent a key intermediate to activate an HDR-like mechanism of reversed fork restart, as recently proposed in *S. pombe* (Carr and Lambert, 2013). In particular, the newly formed 3′ overhang of the reversed fork might invade the duplex ahead of the fork resulting in Holliday junction structures that can be resolved by specific resolvases or dissolved by the combined action of the BLM helicase (Sgs1 in yeast) and the type I topoisomerase TOP3 (Fig. 9). Alternatively, resumption of DNA replication might be obtained by reverse branch migration, where the partially resected reversed fork structures might be specifically recognized by a motor protein—e.g., SMARCAL1 (Béous et al., 2013) or a human RecQ helicase—to promote the branch migration-assisted reestablishment of a functional replication fork.

Materials and methods

Cell lines, culture conditions, and reagents

U-2 OS, HEK 293, and Werner Syndrome fibroblast (AG11395) cells were grown in DMEM supplemented with 10% FBS at 37°C in 5% CO_2. HCT116 cells were grown in McCoy's 5A medium supplemented with 10% FBS. CldU, IdU, BrdU, hydroxyurea, mitomycin C, camptothecin, tamoxifen, puromycin, and hygromycin were obtained from Sigma-Aldrich.

DNA2 conditional knockout HCT116 cells

To examine the response of cells to the complete absence of DNA2, we used a DNA2 conditional knockout cell line where exon 2 of the DNA2 gene is deleted (Karanja et al., 2014). The colorectal carcinoma HCT116 cell line carries 3 copies of DNA2 due to a duplication on chromosome 10. Two chromosomal copies were disrupted using rAAV-mediated gene targeting technology and exon 2 of the third allele was replaced with a conditional exon where the exon was flanked by loxP sites (DNA2flox/−/−). To create a conditional cell line these cells were stably transduced with a tamoxifen (4-OHT)-inducible Cre recombinase. Thus, the cell line is viable and can be propagated. The addition of tamoxifen to the culture media leads to excision of the endogenous DNA2 and the generation of a true DNA2-null cell. Complete loss of DNA2 occurs after 72 h of tamoxifen treatment. However, the DNA fiber experiments were performed after 40 h of tamoxifen treatment to have enough S-phase cells for DNA labeling.

Antibodies

Anti-DNA2 rabbit polyclonal (ab96488; 1:1,000), anti-MUS81 mouse monoclonal (ab14387; 1:1,000), and anti-CldU/BrdU rat monoclonal (ab6326; 1:6) antibodies (all from Abcam); anti-CtIP rabbit polyclonal (A300-488A; 1:1,000), anti-EXO1 rabbit polyclonal (A302-639A; 1:1,000), anti-pRPA32 (S4/S8) rabbit polyclonal (A300-245A; 1:1,000), and anti-pRPA32 (S33) rabbit polyclonal (300-246A; 1:2,000; all from

Bethyl); anti-WRN rabbit polyclonal (NB100-471; 1:1,000); and anti-MRE11 rabbit polyclonal (NB100-142; 1:2,000; Novus); anti-RAD51 (H-92) rabbit polyclonal (sc-8349; 1:1,000) and anti-RECQ1 rabbit polyclonal (sc-25547; 1:2,000) from Santa Cruz; anti-rat Alexa (594-A11007; 1:1,000); and anti–mouse Alexa Flour (488-A11001; 1:1,000; Invitrogen); anti-rabbit (31460; 1:10,000; Thermo Fisher Scientific); anti-tubulin mouse monoclonal (T5168; 1:5,000; Sigma-Aldrich); anti-IdU/BrdU mouse monoclonal (347580; 1:6) from BD; anti-Chk1 mouse monoclonal (sc-8408; 1:1,000; Santa Cruz Biotechnology, Inc.); anti-p-Chk1 (S345) rabbit monoclonal (2348; 1:1,000; Cell Signaling Technology); anti-RPA32 mouse monoclonal (NA19L; 1:1,000) from EMD Millipore; anti-RECQ1 rabbit polyclonal, raised against residues 634–649 of human RECQ1, is custom made (Mendoza-Maldonado et al., 2011); anti-BLM rabbit polyclonal, raised against residues 1–449 of human BLM (Wu and Hickson, 2003), was a gift from I. Hickson (University of Copenhagen, Copenhagen, Denmark); and anti-RECQ4 rabbit polyclonal, raised against residues 60–111 of human RECQ4 (Yin et al., 2004), was a gift from W. Wang (National Institute on Aging, Baltimore, MD).

Recombinant proteins

Yeast Dna2 was expressed in yeast WDH668 strain from pGAL:DNA2 vector (Budd et al., 2000) and purified as previously described (Levikova et al., 2013). In brief, the cells were lysed and Dna2 was purified by affinity chromatography on Ni-NTA agarose (QIAGEN) and anti-Flag M2 affinity gel (Sigma-Aldrich). Yeast RPA was expressed in yeast BJ5464 strain containing three plasmids coding for Rfa1, Rfa2, and Rfa3 and purified as previously described (Kantake et al., 2003). In brief, the cells were lysed and yeast RPA was purified by affinity on ssDNA cellulose column (USB corporation) and by ion exchange chromatography using HiTrap Q column (GE Healthcare). Human DNA2 was expressed in Sf9 cells from a pFastBac:hDNA2 vector (polyhedrin promoter) provided by J. Campbell (Masuda-Sasa et al., 2006). The soluble extracts were obtained by salt extraction as previously described for Sgs1 (Cejka and Kowalczykowski, 2010). The subsequent purification of hDNA2 was performed as previously described for yeast Dna2 (Levikova et al., 2013) by affinity chromatography using Ni-NTA agarose (QIAGEN) and Anti-Flag M2 affinity gel (Sigma-Aldrich). Human RPA was expressed from p11d-tRPA vector (Henricksen et al., 1994) in BL21 *E. coli* cells and purified as described (Henricksen et al., 1994). In brief, hRPA was first bound to HiTrap Blue column (GE healthcare) and then to HiTrap Q column. The sequence coding for yeast Mer3 helicase was amplified from yeast genomic DNA (SK1 strain) using primers Mer3FO (5′-GCGCGCGGGCCCATGAAAACAAAGTTTGATCGCCTCGGTACAGGAAAAAGAAGTAGACCCTCTCCAAATAATATTGACTTTAACGACCAG-3′) and Mer3RE (5′-CGCGCGCTCGAGTTCAAACTCTATATCGGAAC-3′). The PCR product was digested with ApaI and XhoI restriction endonucleases (both from New England Biolabs) and cloned into corresponding sites in pFB-MBP-Sgs1-his after the polyhedrin promoter, creating pFB-MBP-Mer3-his vector. Mer3 was then expressed in Sf9 cells and purified using affinity chromatography as previously described for Sgs1 (Cejka and Kowalczykowski, 2010). In brief, MBP-tagged Mer3 was first bound to amylose resin (New England Biolabs), eluted and digested with PreScission protease to cleave the MBP tag. Mer3 was further purified by affinity on Ni-NTA agarose (QIAGEN) exploiting the 10x His-tag at its C-terminus. Sequence information is available on request.

Genetic knock-down-rescue experiments

RECQ1, DNA2, and RAD51 genetic knockdown-rescue experiments were performed using the procedure described (Berti et al., 2013; Yata et al., 2012). In brief, RECQ1 is depleted using the pLKO.1-puro-shRECQ1 (5′-GAGCTTATGTTACCAGTTA-3′) construct and rescue experiments are performed using the shRNA resistant pIRES-RECQ1-WT or K119R (ATPase dead) constructs as described (Berti et al., 2013). DNA2 is depleted using an siRNA targeting the 3′UTR of DNA2 (5′-CAGUAUCUCCUCUAGCUAG-3′). At least one isoform of DNA2 is not targeted by this sequence. DNA2 rescue experiments are performed using the pBabe-hygro-3xFLAG-DNA2 WT, D294A (Nuclease dead), or K671E (helicase dead) constructs. RAD51 is depleted using siRNAs targeting the 3′UTR (5′-GACUGCCAGGAUAAAGCUU-3′ and 5′-GUGCUGCAGCCUAAUGAGA-3′) in U-2 OS stable cell lines expressing WT RAD51 as described (Yata et al., 2012). WRN depletions were achieved using pRS-puro-shWRN (5′-AGGCAGGTGTAGGAATTGAAGGAGATCAG-3′; sequence ID: TI333414) and exogenous expression is done with the shRNA resistant Flag-pCMVTag2B-WRN WT or K577M (helicase dead) constructs. Constructs for WRN depletion and overexpression of WT WRN and ATPase-deficient WRN (WRN-K577M) were kind gifts from Dr. Pietro Pichierri (Insituto Superiore di Sanità, Rome, Italy). All transfections were done with Lipofectamine 2000 (Life technologies Catalog no: 11668027). An shRNA targeting luciferase (5′-ACGCTGAGTACTTCGAAATGT-3′) was used for control shRNA experiments. The silencer select negative control (Life technologies, Catalog no. 4390843) or an siRNA targeting luciferase (5′-CGUACGCGGAAUACUUCGA-3′) were used for control siRNA experiments, as indicated. Lentiviral mediated shRNA depletions were achieved using the following sequences cloned into the pLKO.1 lentiviral shRNA expression vector: BLM (5′-CGAAGGAAGTTGTATGCACTA-3′), WRN (5′-GCTGGCAATTACCAGAACAAT-3′), and MUS81 (5′-CACGCGCTTCGTATTTCAGAA-3′). The procedure for lentiviral generation and transduction has been described (Berti et al., 2013). Transduced U-2 OS cells were selected with 6 µg/ml puromycin. siRNA-mediated depletions were achieved using the following siRNAs from Invitrogen: DNA2 (5′-AUAGCCAGUAGUAUUCGAU-3′), CtIP (5′-CGAAUCUUAGAUGCACAAA-3′), EXO1 (Invitrogen-HSS113557), and RAD51 (Invitrogen-1299001). In brief, siRNAs were transfected using Lipofectamine RNAiMAX (Life Technologies) following the manufacturer's protocol. MRE11 (5′-GAAAGGCUCUAUCGAAUGU-3′) and RECQ4 (SMART pool) siRNAs were from Dharmacon and were transfected as previously described (Thangavel et al., 2010).

Microfluidic-assisted DNA fiber stretching

For DNA replication fork restart analysis, asynchronous cells were pulse-labeled with 50 µM CldU for 20–30 min. 2 mM HU, 300 nM MMC, or 150 nM CPT was added to the CldU containing media and incubated for the indicated times. Cells were washed three times with medium and released with 50 µM IdU for 40 min. For nascent strand degradation analysis, asynchronous cells were pulse-labeled with 50 µM IdU for 45 min, washed three times with medium, incubated with 4 mM HU, 100 nM CPT, 200 nM MMC, or medium for times indicated. The pulse-labeled cells were trypsin collected and lysed in agarose plugs to prevent any mechanical breakage of replication tracts. Microfluidic platform for stretching the high-molecular weight DNA, coverslips, immunostaining and image acquisition of replication tracts were performed as described (Sidorova et al., 2009; Berti et al., 2013). In brief, polydimethylsiloxane (PDMS) stamps with microchannels were Oxygen plasma treated and reversibly sealed to the silanized coverslips. High-molecular weight DNA was loaded and stretched by capillary force into the microchannels. PDMS stamps were peeled-off and coverslips were left drying overnight. For immunostaining, DNA-stretched coverslips were denatured (2.5N HCL for 45 min), neutralized (0.1 M sodium borate and 3 washes with PBS), blocked (5% BSA and 0.5% Tween 20 in PBS for 30 min), incubated with primary antibodies (Anti-IdU/BrdU or both anti-IdU/BrdU and anti-CldU/BrdU for 30 min), washed (1% BSA and 0.1% Tween 20 in PBS, 3 times 5 min each) and incubated with secondary antibodies (anti–mouse Alexa Fluor 488-conjugated, or both anti–mouse Alexa Fluor 488–conjugated and anti–rat Alexa Fluor 594–conjugated for 1 h). Washed slides were mounted in prolong gold anti-fade reagent (Life Technologies) and images were sequentially acquired (for double-label) with LAS AF software using TCS SP5 confocal microscope (Leica). A 63×/1.4 oil immersion objective was used. Images were captured at room temperature. $n \geq 300$ fiber tracts scored for each dataset. The DNA tract lengths were measured using ImageJ and the pixel length values were converted into micrometers using the scale bars created by the microscope. Statistical analysis was done using GraphPad Prism.

Clonogenic survival assay

Colony-forming assays were performed as previously described (Franken et al., 2006). In brief, 1,000 cells were plated per well and treated on the next day with 4 mM HU for 3, 6, and 8 h or 100 nM CPT for 6 h. Colonies were fixed, stained, and quantified 10 d after release from genotoxic stress. The plating efficiency and survival fraction were calculated as previously described (Franken et al., 2006). In brief, colonies were counted using an inverted stereomicroscope and the plating efficiency was calculated using the following formula: Plating Efficiency (PE) = (no. of colonies formed/no. of cells seeded) × 100%. From the plating efficiency, the surviving fraction (SF) was calculated as: SF = (no. of colonies formed after treatment/no. of cells seeded) × PE. The experiments were performed in triplicate and the statistical analysis was performed using GraphPad Prism.

Western blotting

Cells were washed with PBS and lysed either in standard RIPA buffer (PBS, 1% NP-40, 0.5% sodium deoxycholate, 0.1% SDS, 10 µg/ml aprotinin, 10 µg/ml PMSF, 1 mM Na_3VO_4, and 1 mM NaF) or MCL buffer (50 mM Tris, pH 8.0, 5 mM EDTA, 0.5% NP-40, 100 mM NaCl, 2 mM DTT, and freshly added protease and phosphatase inhibitors from Roche (1 tablet/10 ml of buffer). Cell lysates were resolved by SDS-PAGE and transferred to

PVDF membrane (GE Healthcare). Incubation with antibodies was performed overnight at 4°C. Proteins were visualized using ECL (Thermo Fisher Scientific) according to the manufacturer's instructions.

Co-immunoprecipitation experiments

HEK293T cells were transfected with empty vectors, FLAG-DNA2, and Strep-HA-WRN by calcium phosphate. 48 h after transfection, cells were treated with 4 mM HU for 3 h, lysed in benzonase lysis buffer (50 mM Tris-HCl, pH 7.5, 75 mM KCl, 2 mM $MgCl_2$, 20 mM NaF, 10 mM β-glycerophosphate, 0.2 mM Na_3VO_4, and 0.2% Triton X-100) supplemented with protease inhibitors (EDTA-free tablet; Sigma-Aldrich) by passing 10 times through a 26-G syringe needle and incubated 1 h at 4°C with 2 U/µl Benzonase (Sigma-Aldrich) to digest genomic DNA. KCl and EDTA concentrations were adjusted to 120 and 3 mM, respectively, and lysates were centrifuged at 14,000 rpm for 30 min. Immunoprecipitations of clarified lysates were performed with FLAG M2 or HA affinity agarose resin (Sigma-Aldrich) overnight at 4°C. Beads were washed 5 times with wash buffer (50 mM Tris-HCl, pH 7.5, 150 mM KCl, 3 mM EDTA, 2 mM $MgCl_2$, 20 mM NaF, 10 mM β-glycerophosphate, 0.2 mM Na_3VO_4, and 0.2% Triton X-100) and bound proteins were eluted by boiling in SDS-PAGE sample buffer.

EM analysis of genomic DNA in mammalian cells

EM analysis of replication intermediates has been described in detail (Ray Chaudhuri et al., 2012; Neelsen et al., 2014), including a description of the important parameters to consider specifically for the identification and the scoring of reversed forks (Neelsen et al., 2014). In brief, 5–10 × 10^6 U-2 OS cells were harvested and genomic DNA was cross-linked by two rounds of incubation in 10 µg/ml 4,5′,8-trimethylpsoralen (Sigma-Aldrich) and 3 min of irradiation with 366 nm UV light on a precooled metal block. Cells were lysed and genomic DNA was isolated from the nuclei by proteinase K (Roche) digestion and phenol-chloroform extraction. DNA was purified by isopropanol precipitation, digested with PvuII HF in the proper buffer for 3–5 h at 37°C, and replication intermediates were enriched on a benzoylated naphthoylated DEAE–cellulose (Sigma-Aldrich) column. EM samples were prepared by spreading the DNA on carbon-coated grids in the presence of benzyl-dimethyl-alkylammonium chloride and visualized by platinum rotary shadowing. Images were acquired on a transmission electron microscope (JOEL 1200 EX) with side-mounted camera (AMTXR41 supported by AMT software v601) and analyzed with ImageJ (National Institutes of Health).

Preparation of oligonucleotide-based DNA substrates

DNA oligonucleotides were purchased from Microsynth and ^{32}P-labeled either at the 5′ terminus with [γ-^{32}P] ATP and T_4 polynucleotide kinase (New England Biolabs), or at the 3′ end with [α-^{32}P] cordycepin-5′-triphosphate and terminal transferase (New England Biolabs) according to manufacturer's instructions. Unincorporated nucleotides were removed using MicroSpin G25 columns (GE Healthcare). The substrates were prepared by heating the respective oligonucleotides at 95°C and gradually cooling to room temperature. The following oligonucleotides were used for the preparation of the four-way junction (X12-3 TOP L, HJ 1, HJ 2, and HJ 3), three-way junction with 3′ tail (X12-3 TOP L, HJ 1, HJ 2Sb, and HJ 3), three-way junction with 5′ ssDNA tail (X12-3 TOP L, HJ 1S, HJ 2, and HJ 3), nicked four-way junction (X12-3 TOP L, HJ 1, HJ 2Sa, HJ 2Sb, and HJ 3), replication fork (X12-3 TOP L, HJ 1S, HJ 2Sb, and HJ 3), and dsDNA (X12-3 TOP L and Bottom LC), respectively. The sequences of the oligonucleotides were: X12-3 TOP L (93 nt), 5′-GACGTCATAGACGATTACATTGCTAGGACATGCTGTCTAGAGACTATC-GCGACTTACGTTCCATCGCTAGGTTATTTTTTTTTTTTTTTTTT-3′ X12-3 HJ 1 (93 nt), 5′-AAAAAAAAAAAAAAAAAAAATAACCTAGCGATGGAACGTA-AGTCGCGATGGGCTTAACTAGGATGCTACTGGCCCCGAATCAACCGT-ACTTGGG-3′ X12-3 HJ 1S (48 nt), 5′-AAAAAAAAAAAAAAAAAAAT-AACCTAGCGATGGAACGTAAGTCGCGAT-3′ X12-3 HJ 2 (93 nt), 5′-CCCAAGTACGGTTGATTCGGGGCCAGTAGCATCCTAGTTAAGCCCA-TTACGATTCGTTACCCATTCACTGTCAGAAGGCACCAGATAGATCTC-3′ X12-3 HJ 2Sa (45 nt), 5′-CCCAAGTACGGTTGATTCGGGGCCAGTAGCA-TCCTAGTTAAGCCC-3′ X12-3 HJ 2Sb (48 nt), 5′-ATTACGATTCGTTACCC-ATTCACTGTCAGAAGGCACCAGATAGATCTC-3′ X12-3 HJ 3 (93 nt), 5′-GAGATCTATCTGGTGCCTTCTGACAGTGAATGGGTAACGAATCGT-AATAGTCTCTAGACAGCATGTCCTAGCAATGTAATCGTCTATGACGTC-3′ X12-3 BOTTOM LC, 5′-AAAAAAAAAAAAAAAAAAAATAACCTAGCGAT-GGAACGTAAGTCGCGATAGTCTCTAGACAGCATGTCCTAGCAATGTA-ATCGTCTATGACGTC-3′.

Nuclease assays

The experiments were performed in a 15-µl volume in 25 mM Tris-acetate (pH 7.5), 2 mM magnesium acetate, 1 mM ATP, 1 mM dithiothreitol, 0.1 mg/ml BSA (New England Biolabs), 1 mM phosphoenolpyruvate, 80 U/ml pyruvate kinase, 1 nM DNA substrate (molecules), and recombinant proteins, as indicated. The reactions were assembled on ice and incubated for 30 min at 30°C for yeast proteins and at 37°C for human proteins. Unless indicated otherwise, RPA was present in the reactions at saturating concentrations corresponding to a threefold excess over DNA, assuming all DNA was single-stranded and a DNA-binding site size of 25 nt for hRPA and of 20 nt for yRPA. The reactions were terminated by adding 5 µl Stop buffer (150 mM EDTA, 2% SDS, 30% glycerol, and 0.01% bromophenol blue), incubated for 30 min at room temperature and separated on polyacrylamide gels in TBE buffer under native conditions. Alternatively, for denaturing conditions, the reaction were terminated by adding 15 µl Formamide stop buffer (95% (vol/vol) formamide, 20 mM EDTA, 0.01% bromophenol blue), denatured by heating at 95°C for 5 min and separated on 20% denaturing polyacrylamide gels in TBE buffer. Gels were fixed, dried, exposed to a storage phosphor screen, and analyzed on Typhoon phosphor imager (GE Healthcare).

Online supplemental material

Fig. S1 shows quantification of stalled forks, new origins, and termination events in DNA2-depleted cells upon genotoxic stress induction, as well as the statistical analysis of IdU tracts from RECQ1-, DNA2-, WRN-, RECQ1/DNA2-, RECQ1/WRN-, WRN/DNA2-, and RECQ1/WRN/DNA2-depleted U-2 OS cells. Fig. S2 shows the IdU tract length distribution in BLM- and RECQ4-depleted cells, respectively, as well as statistical analysis of IdU tracts from RECQ1/WRN-codepleted cells complemented with WT WRN or with ATPase-deficient WRN. Fig. S3 shows additional EM analysis, as well as the Western blot analysis of ATR-checkpoint activation in RECQ1- and/or DNA2-depleted U-2 OS cells. Fig. S4 shows additional biochemical analysis of substrate specificity of human DNA2 and human EXO1. TFig. S5 shows biochemical assays of substrate specificity of yeast Dna2 and yeast Exo1. Online supplemental material is available at http://www.jcb.org/cgi/content/full/jcb.201406100/DC1.

We are grateful to Pietro Pichierri (Istituto Superiore di Sanità, Rome) for providing the WS cells and WRN constructs, Damian Dalcher for his help with the EM analysis, Stephanie Felscher (University of Zurich) for kindly providing human EXO1 protein, Marc Wold (University of Iowa) for human RPA expression construct, Lepakshi Ranjha (University of Zurich) for Mer3 protein, Fumiko Esashi (University of Oxford) for the Rad51 siRNAs and the U-2 OS cells stably expressing exogenous RAD51, and Judith Campbell (California Institute of Technology) for human and yeast DNA2/Dna2 expression constructs. We thank the Research Microscopy Core Facility of Saint Louis University for technical support.

This work was supported by National Institutes of Health grant R01GM108648 to A. Vindigni, by startup funding from the Doisy Department of Biochemistry and Molecular Biology and from the Saint Louis University Cancer Center to A. Vindigni, by grants from the President's Research Fund of Saint Louis University and by the GLIOMA-Interreg (Slovenian-Italian Cooperation 2007-2013) project to A. Vindigni, by the Swiss National Science Foundation grants 31003A_146924 to M. Levikova and PP00P3 133636 to P. Cejka, by National Institutes of Health grant GM0088351 and CA15446 to E.A. Hendrickson, and by a research contract from Horizon Discovery, Ltd to E.A. Hendrickson. M. Berti was supported by an EMBO short-term fellowship to perform EM experiments in M. Levikova laboratory.

The authors declare no competing financial interests.

Submitted: 24 June 2014
Accepted: 14 January 2015

References

Atkinson, J., and P. McGlynn. 2009. Replication fork reversal and the maintenance of genome stability. *Nucleic Acids Res.* 37:3475–3492. http://dx.doi.org/10.1093/nar/gkp244

Ayyagari, R., X.V. Gomes, D.A. Gordenin, and P.M. Burgers. 2003. Okazaki fragment maturation in yeast. I. Distribution of functions between FEN1 AND DNA2. *J. Biol. Chem.* 278:1618–1625. http://dx.doi.org/10.1074/jbc.M209801200

Bae, S.H., K.H. Bae, J.A. Kim, and Y.S. Seo. 2001. RPA governs endonuclease switching during processing of Okazaki fragments in eukaryotes. *Nature.* 412:456–461. http://dx.doi.org/10.1038/35086609

Berti, M., A. Ray Chaudhuri, S. Thangavel, S. Gomathinayagam, S. Kenig, M. Vujanovic, F. Odreman, T. Glatter, S. Graziano, R. Mendoza-Maldonado, et al. 2013. Human RECQ1 promotes restart of replication forks reversed by DNA topoisomerase I inhibition. *Nat. Struct. Mol. Biol.* 20:347–354. http://dx.doi.org/10.1038/nsmb.2501

Bétous, R., A.C. Mason, R.P. Rambo, C.E. Bansbach, A. Badu-Nkansah, B.M. Sirbu, B.F. Eichman, and D. Cortez. 2012. SMARCAL1 catalyzes fork regression and Holliday junction migration to maintain genome stability during DNA replication. *Genes Dev.* 26:151–162. http://dx.doi.org/10.1101/gad.178459.111

Bétous, R., F.B. Couch, A.C. Mason, B.F. Eichman, M. Manosas, and D. Cortez. 2013. Substrate-selective repair and restart of replication forks by DNA translocases. *Cell Reports*. 3:1958–1969. http://dx.doi.org/10.1016/j.celrep.2013.05.002

Budd, M.E., and J.L. Campbell. 1995. A yeast gene required for DNA replication encodes a protein with homology to DNA helicases. *Proc. Natl. Acad. Sci. USA*. 92:7642–7646. http://dx.doi.org/10.1073/pnas.92.17.7642

Budd, M.E., and J.L. Campbell. 1997. A yeast replicative helicase, Dna2 helicase, interacts with yeast FEN-1 nuclease in carrying out its essential function. *Mol. Cell. Biol.* 17:2136–2142.

Budd, M.E., W. Choe, and J.L. Campbell. 2000. The nuclease activity of the yeast DNA2 protein, which is related to the RecB-like nucleases, is essential in vivo. *J. Biol. Chem.* 275:16518–16529. http://dx.doi.org/10.1074/jbc.M909511199

Carr, A.M., and S. Lambert. 2013. Replication stress-induced genome instability: the dark side of replication maintenance by homologous recombination. *J. Mol. Biol.* 425:4733–4744. http://dx.doi.org/10.1016/j.jmb.2013.04.023

Cejka, P., and S.C. Kowalczykowski. 2010. The full-length *Saccharomyces cerevisiae* Sgs1 protein is a vigorous DNA helicase that preferentially unwinds holliday junctions. *J. Biol. Chem.* 285:8290–8301. http://dx.doi.org/10.1074/jbc.M109.083196

Cejka, P., E. Cannavo, P. Polaczek, T. Masuda-Sasa, S. Pokharel, J.L. Campbell, and S.C. Kowalczykowski. 2010. DNA end resection by Dna2-Sgs1-RPA and its stimulation by Top3-Rmi1 and Mre11-Rad50-Xrs2. *Nature*. 467:112–116. http://dx.doi.org/10.1038/nature09355

Cotta-Ramusino, C., D. Fachinetti, C. Lucca, Y. Doksani, M. Lopes, J. Sogo, and M. Foiani. 2005. Exo1 processes stalled replication forks and counteracts fork reversal in checkpoint-defective cells. *Mol. Cell*. 17:153–159. http://dx.doi.org/10.1016/j.molcel.2004.11.032

Couch, F.B., C.E. Bansbach, R. Driscoll, J.W. Luzwick, G.G. Glick, R. Bétous, C.M. Carroll, S.Y. Jung, J. Qin, K.A. Cimprich, and D. Cortez. 2013. ATR phosphorylates SMARCAL1 to prevent replication fork collapse. *Genes Dev.* 27:1610–1623. http://dx.doi.org/10.1101/gad.214080.113

Courcelle, J., J.R. Donaldson, K.H. Chow, and C.T. Courcelle. 2003. DNA damage-induced replication fork regression and processing in Escherichia coli. *Science*. 299:1064–1067. http://dx.doi.org/10.1126/science.1081328

Crabbe, L., R.E. Verdun, C.I. Haggblom, and J. Karlseder. 2004. Defective telomere lagging strand synthesis in cells lacking WRN helicase activity. *Science*. 306:1951–1953. http://dx.doi.org/10.1126/science.1103619

Duxin, J.P., H.R. Moore, J. Sidorova, K. Karanja, Y. Honaker, B. Dao, H. Piwnica-Worms, J.L. Campbell, R.J. Monnat Jr., and S.A. Stewart. 2012. Okazaki fragment processing-independent role for human Dna2 enzyme during DNA replication. *J. Biol. Chem.* 287:21980–21991. http://dx.doi.org/10.1074/jbc.M112.359018

Franchitto, A., L.M. Pirzio, E. Prosperi, O. Sapora, M. Bignami, and P. Pichierri. 2008. Replication fork stalling in WRN-deficient cells is overcome by prompt activation of a MUS81-dependent pathway. *J. Cell Biol.* 183:241–252. http://dx.doi.org/10.1083/jcb.200803173

Franken, N.A., H.M. Rodermond, J. Stap, J. Haveman, and C. van Bree. 2006. Clonogenic assay of cells in vitro. *Nat. Protoc.* 1:2315–2319. http://dx.doi.org/10.1038/nprot.2006.339

Gari, K., C. Décaillet, M. Delannoy, L. Wu, and A. Constantinou. 2008. Remodeling of DNA replication structures by the branch point translocase FANCM. *Proc. Natl. Acad. Sci. USA*. 105:16107–16112. http://dx.doi.org/10.1073/pnas.0804777105

Gravel, S., J.R. Chapman, C. Magill, and S.P. Jackson. 2008. DNA helicases Sgs1 and BLM promote DNA double-strand break resection. *Genes Dev.* 22:2767–2772. http://dx.doi.org/10.1101/gad.503108

Hanada, K., M. Budzowska, S.L. Davies, E. van Drunen, H. Onizawa, H.B. Beverloo, A. Maas, J. Essers, I.D. Hickson, and R. Kanaar. 2007. The structure-specific endonuclease Mus81 contributes to replication restart by generating double-strand DNA breaks. *Nat. Struct. Mol. Biol.* 14:1096–1104. http://dx.doi.org/10.1038/nsmb1313

Hashimoto, Y., F. Puddu, and V. Costanzo. 2012. RAD51- and MRE11-dependent reassembly of uncoupled CMG helicase complex at collapsed replication forks. *Nat. Struct. Mol. Biol.* 19:17–24. http://dx.doi.org/10.1038/nsmb.2177

Henricksen, L.A., C.B. Umbricht, and M.S. Wold. 1994. Recombinant replication protein A: expression, complex formation, and functional characterization. *J. Biol. Chem.* 269:11121–11132.

Hu, J., L. Sun, F. Shen, Y. Chen, Y. Hua, Y. Liu, M. Zhang, Y. Hu, Q. Wang, W. Xu, et al. 2012. The intra-S phase checkpoint targets Dna2 to prevent stalled replication forks from reversing. *Cell*. 149:1221–1232. http://dx.doi.org/10.1016/j.cell.2012.04.030

Kantake, N., T. Sugiyama, R.D. Kolodner, and S.C. Kowalczykowski. 2003. The recombination-deficient mutant RPA (rfa1-t11) is displaced slowly from single-stranded DNA by Rad51 protein. *J. Biol. Chem.* 278:23410–23417. http://dx.doi.org/10.1074/jbc.M302995200

Karanja, K.K., S.W. Cox, J.P. Duxin, S.A. Stewart, and J.L. Campbell. 2012. DNA2 and EXO1 in replication-coupled, homology-directed repair and in the interplay between HDR and the FA/BRCA network. *Cell Cycle*. 11:3983–3996. http://dx.doi.org/10.4161/cc.22215

Karanja, K.K., E.H. Lee, E.A. Hendrickson, and J.L. Campbell. 2014. Preventing over-resection by DNA2 helicase/nuclease suppresses repair defects in Fanconi anemia cells. *Cell Cycle*. 13:1540–1550. http://dx.doi.org/10.4161/cc.28476

Kumar, S., and P.M. Burgers. 2013. Lagging strand maturation factor Dna2 is a component of the replication checkpoint initiation machinery. *Genes Dev.* 27:313–321. http://dx.doi.org/10.1101/gad.204750.112

Kuo, C., H. Nuang, and J.L. Campbell. 1983. Isolation of yeast DNA replication mutants in permeabilized cells. *Proc. Natl. Acad. Sci. USA*. 80:6465–6469. http://dx.doi.org/10.1073/pnas.80.21.6465

Levikova, M., D. Klaue, R. Seidel, and P. Cejka. 2013. Nuclease activity of *Saccharomyces cerevisiae* Dna2 inhibits its potent DNA helicase activity. *Proc. Natl. Acad. Sci. USA*. 110:E1992–E2001. http://dx.doi.org/10.1073/pnas.1300390110

Liao, S., T. Toczylowski, and H. Yan. 2008. Identification of the Xenopus DNA2 protein as a major nuclease for the 5′->3′ strand-specific processing of DNA ends. *Nucleic Acids Res.* 36:6091–6100. http://dx.doi.org/10.1093/nar/gkn616

Machwe, A., R. Karale, X. Xu, Y. Liu, and D.K. Orren. 2011. The Werner and Bloom syndrome proteins help resolve replication blockage by converting (regressed) holliday junctions to functional replication forks. *Biochemistry*. 50:6774–6788. http://dx.doi.org/10.1021/bi2001054

Masuda-Sasa, T., O. Imamura, and J.L. Campbell. 2006. Biochemical analysis of human Dna2. *Nucleic Acids Res.* 34:1865–1875. http://dx.doi.org/10.1093/nar/gkl070

Mendoza-Maldonado, R., V. Faoro, S. Bajpai, M. Berti, F. Odreman, M. Vindigni, T. Ius, A. Ghasemian, S. Bonin, M. Skrap, et al. 2011. The human RECQ1 helicase is highly expressed in glioblastoma and plays an important role in tumor cell proliferation. *Mol. Cancer*. 10:83. http://dx.doi.org/10.1186/1476-4598-10-83

Mimitou, E.P., and L.S. Symington. 2008. Sae2, Exo1 and Sgs1 collaborate in DNA double-strand break processing. *Nature*. 455:770–774. http://dx.doi.org/10.1038/nature07312

Murfuni, I., A. De Santis, M. Federico, M. Bignami, P. Pichierri, and A. Franchitto. 2012. Perturbed replication induced genome wide or at common fragile sites is differently managed in the absence of WRN. *Carcinogenesis*. 33:1655–1663. http://dx.doi.org/10.1093/carcin/bgs206

Neelsen, K.J., A.R. Chaudhuri, C. Follonier, R. Herrador, and M. Lopes. 2014. Visualization and interpretation of eukaryotic DNA replication intermediates in vivo by electron microscopy. *Methods Mol. Biol.* 1094:177–208. http://dx.doi.org/10.1007/978-1-62703-706-8_15

Nicolette, M.L., K. Lee, Z. Guo, M. Rani, J.M. Chow, S.E. Lee, and T.T. Paull. 2010. Mre11-Rad50-Xrs2 and Sae2 promote 5′ strand resection of DNA double-strand breaks. *Nat. Struct. Mol. Biol.* 17:1478–1485. http://dx.doi.org/10.1038/nsmb.1957

Nimonkar, A.V., J. Genschel, E. Kinoshita, P. Polaczek, J.L. Campbell, C. Wyman, P. Modrich, and S.C. Kowalczykowski. 2011. BLM-DNA2-RPA-MRN and EXO1-BLM-RPA-MRN constitute two DNA end resection machineries for human DNA break repair. *Genes Dev.* 25:350–362. http://dx.doi.org/10.1101/gad.2003811

Niu, H., W.H. Chung, Z. Zhu, Y. Kwon, W. Zhao, P. Chi, R. Prakash, C. Seong, D. Liu, L. Lu, et al. 2010. Mechanism of the ATP-dependent DNA end-resection machinery from *Saccharomyces cerevisiae*. *Nature*. 467:108–111. http://dx.doi.org/10.1038/nature09318

Peng, G., H. Dai, W. Zhang, H.J. Hsieh, M.R. Pan, Y.Y. Park, R.Y. Tsai, I. Bedrosian, J.S. Lee, G. Ira, and S.Y. Lin. 2012. Human nuclease/helicase DNA2 alleviates replication stress by promoting DNA end resection. *Cancer Res.* 72:2802–2813. http://dx.doi.org/10.1158/0008-5472.CAN-11-3152

Pirzio, L.M., P. Pichierri, M. Bignami, and A. Franchitto. 2008. Werner syndrome helicase activity is essential in maintaining fragile site stability. *J. Cell Biol.* 180:305–314. http://dx.doi.org/10.1083/jcb.200705126

Ray Chaudhuri, A., Y. Hashimoto, R. Herrador, K.J. Neelsen, D. Fachinetti, R. Bermejo, A. Cocito, V. Costanzo, and M. Lopes. 2012. Topoisomerase I poisoning results in PARP-mediated replication fork reversal. *Nat. Struct. Mol. Biol.* 19:417–423. http://dx.doi.org/10.1038/nsmb.2258

Schlacher, K., N. Christ, N. Siaud, A. Egashira, H. Wu, and M. Jasin. 2011. Double-strand break repair-independent role for BRCA2 in blocking stalled replication fork degradation by MRE11. *Cell*. 145:529–542. http://dx.doi.org/10.1016/j.cell.2011.03.041

Schlacher, K., H. Wu, and M. Jasin. 2012. A distinct replication fork protection pathway connects Fanconi anemia tumor suppressors to RAD51-BRCA1/2. *Cancer Cell*. 22:106–116. http://dx.doi.org/10.1016/j.ccr.2012.05.015

Seigneur, M., V. Bidnenko, S.D. Ehrlich, and B. Michel. 1998. RuvAB acts at arrested replication forks. *Cell*. 95:419–430. http://dx.doi.org/10.1016/S0092-8674(00)81772-9

Sidorova, J.M., N. Li, A. Folch, and R.J. Monnat Jr. 2008. The RecQ helicase WRN is required for normal replication fork progression after DNA damage or replication fork arrest. *Cell Cycle*. 7:796–807. http://dx.doi.org/10.4161/cc.7.6.5566

Sidorova, J.M., N. Li, D.C. Schwartz, A. Folch, and R.J. Monnat Jr. 2009. Microfluidic-assisted analysis of replicating DNA molecules. *Nat. Protoc.* 4:849–861. http://dx.doi.org/10.1038/nprot.2009.54

Sturzenegger, A., K. Burdova, R. Kanagaraj, M. Levikova, C. Pinto, P. Cejka, and P. Janscak. 2014. DNA2 cooperates with the WRN and BLM RecQ helicases to mediate long-range DNA end resection in human cells. *J. Biol. Chem.* 289:27314–27326. http://dx.doi.org/10.1074/jbc.M114.578823

Thangavel, S., R. Mendoza-Maldonado, E. Tissino, J.M. Sidorova, J. Yin, W. Wang, R.J. Monnat Jr., A. Falaschi, and A. Vindigni. 2010. Human RECQ1 and RECQ4 helicases play distinct roles in DNA replication initiation. *Mol. Cell. Biol.* 30:1382–1396. http://dx.doi.org/10.1128/MCB.01290-09

Wawrousek, K.E., B.K. Fortini, P. Polaczek, L. Chen, Q. Liu, W.G. Dunphy, and J.L. Campbell. 2010. Xenopus DNA2 is a helicase/nuclease that is found in complexes with replication proteins And-1/Ctf4 and Mcm10 and DSB response proteins Nbs1 and ATM. *Cell Cycle*. 9:1156–1166. http://dx.doi.org/10.4161/cc.9.6.11049

Wu, L., and I.D. Hickson. 2003. The Bloom's syndrome helicase suppresses crossing over during homologous recombination. *Nature*. 426:870–874. http://dx.doi.org/10.1038/nature02253

Yata, K., J. Lloyd, S. Maslen, J.Y. Bleuyard, M. Skehel, S.J. Smerdon, and F. Esashi. 2012. Plk1 and CK2 act in concert to regulate Rad51 during DNA double strand break repair. *Mol. Cell*. 45:371–383. http://dx.doi.org/10.1016/j.molcel.2011.12.028

Yeo, J.E., E.H. Lee, E.A. Hendrickson, and A. Sobeck. 2014. CtIP mediates replication fork recovery in a FANCD2-regulated manner. *Hum. Mol. Genet.* 23:3695–3705. http://dx.doi.org/10.1093/hmg/ddu078

Yin, J., Y.T. Kwon, A. Varshavsky, and W. Wang. 2004. RECQL4, mutated in the Rothmund-Thomson and RAPADILINO syndromes, interacts with ubiquitin ligases UBR1 and UBR2 of the N-end rule pathway. *Hum. Mol. Genet.* 13:2421–2430. http://dx.doi.org/10.1093/hmg/ddh269

Ying, S., F.C. Hamdy, and T. Helleday. 2012. Mre11-dependent degradation of stalled DNA replication forks is prevented by BRCA2 and PARP1. *Cancer Res.* 72:2814–2821. http://dx.doi.org/10.1158/0008-5472.CAN-11-3417

Zellweger, R., D. Dalcher, K. Mutreja, R. Herrador, M. Berti, A. Vindigni, and M. Lopes. 2015. Rad51-mediated replication fork reversal is a global response to genotoxic treatments in human cells. *J. Cell Biol.* 208:563–579.

Zeman, M.K., and K.A. Cimprich. 2014. Causes and consequences of replication stress. *Nat. Cell Biol.* 16:2–9. http://dx.doi.org/10.1038/ncb2897

Zhu, Z., W.H. Chung, E.Y. Shim, S.E. Lee, and G. Ira. 2008. Sgs1 helicase and two nucleases Dna2 and Exo1 resect DNA double-strand break ends. *Cell*. 134:981–994. http://dx.doi.org/10.1016/j.cell.2008.08.037

3. Discussion.

Replication fork reversal was first proposed long time ago as a mechanism for DNA damage bypass in mammalian cells (Higgins N.P., et al., 1976). The concept, initially largely ignored, found some support from genetic and biochemical data in bacteria in the 80s-90s (Atkinson and McGlynn, NAR 2009). More recently, studies in yeast (*S. cerevisiae* and *S. pombe*) proved that indeed these structures can be formed, but they only accumulate in checkpoint-deficient yeast cells and under specific DNA damaging conditions (Sogo et al., 2002; Bermejo et al., Cell 2011; Hu et al., Cell 2012). These yeast findings challenged the importance and physiological significance of these structures in eukaryotic cells. However, it was recently shown that in different eukaryotic systems – yeast (*S. cerevisiae*), *Xenopus laevis* egg extracts, mouse embryonic fibroblasts and human osteosarcoma cell line – reversed forks readily accumulate, even in checkpoint proficient cells, in response to treatments with Topoisomerase I inhibitors (Ray Chaudhuri A, et al., 2012). Later on it was shown that replication fork reversal is more general response to cancer relevant conditions of replication stress (Neelsen et al., 2013a and b), to repetitive DNA sequence prone to form secondary structures (Follonier et al., 2013) and to a wide variety of genotoxic agents (Zellweger R, et al., 2015), bringing further support to its proposed function in the protection of replication forks challenged by genotoxic stress (Neelsen and Lopes, 2015).

In this project, we wanted to investigate in vivo the potential role of the newly discovered class of proteins named annealing helicases (focusing on two of them: ZRANB3 and HARP), that are able to re-anneal RPA coated ssDNA strands into dsDNA and can drive replication fork reversal in vitro (Yusufzai and Kadonaga, 2008; Yusufzai and Kadonaga, 2010; Ciccia A, et al., 2012; Weston R, et al., 2012; Yuan J, et al., 2012; Betous R, et al., 2011; Betous R, et al., 2012; Betous R, et al., 2013; Carrol C, et al., 2014).

In parallel, we wanted to test if proteins involved in error-free branch of post replicative repair (PRR), play a direct role in replication fork reversal upon DNA damage. Published data suggest that error-free PRR repair entails template switching strategy for DNA damage tolerance, either using fork reversal to bypass the lesion, or - after replication restart by re-priming - promoting recombinational bypass of the damage behind the fork. A crucial replication factor playing a role in these processes is the polymerase clamp PCNA, via its posttranslational modifications by mono- and poly-ubiquitination at lysine K164. For the template switching events, yeast studies proposed a key role for PCNA polyubiquitination at K164, via K63-linked ubiquitin chains (Ghosal and Chen, 2013).

To investigate if these factors could be involved in replication fork regression in vivo, we decided to focus on two major techniques: 1) DNA fiber spreading, described in detail in other chapters, to assess replication fork speed, which is expected to decrease upon DNA damage, by active promotion of fork remodelling; 2) electron microscopic analysis of replication intermediates (also described previously), to assess reversed replication fork frequency upon different genotoxic treatments.

Using these techniques, we could conclude that ZRANB3 plays a crucial role in mediating replication fork slow down upon at least two different genotoxic treatments - camptothecin (CPT) and mitomycin C (MMC). We could also show that ZRANB3-defective cells failed to accumulate reversed forks upon both of these treatments (over the slightly increased basal level observed in untreated cells), implicating this protein in effective fork slowing and reversal upon treatment with genotoxic agents. We initially tested the role of ZRANB3 in fork slow down and reversal, coupling siRNA-mediated protein depletion with DNA fiber assays or EM visualization. To possibly strengthen our observations, and to exclude the possibility of off-target effects or insufficient downregulation of the protein, we performed the same assays on ZRANB3 knock out cells. The key results were remarkably similar by

both strategies of gene inactivation. Importantly, although ZRANB3 defective cells fail to significantly induce fork reversal upon exogenous damage, we repeatedly observed elevated basal levels of reversed replication forks upon ZRANB3 inactivation. We attribute this to mild replication stress accumulating in these cells, luckily as a consequence of impaired fork reversal in face of endogenous lesions, possibly stimulating ZRANB3-independent mechanisms of fork remodelling. Overall, we can confidently conclude that, in agreement with previous in vitro data on plasmid substrates (Ciccia A, et al., 2012), ZRANB3 annealing helicase has a crucial role in inducing reversed replication fork formation, and that its function is required to minimize replication stress during unperturbed S phase.

As described previously in the text, ZRANB3 has several domains, mediating its biochemical activities and its interaction with other factors. After producing mutant cell lines and performing the experiments described above, we could determine that fork reversal in vivo strictly depends on ZRANB3 helicase activity and on its interaction with PCNA (PIP and APIM domains), at least upon the two tested genotoxic treatments (CPT and MMC). Mutations in these domains phenocopied complete absence of the protein upon these treatments, as they impaired active fork slowdown and reversed fork accumulation above basal levels. We could also show that cells harbouring mutations in ZRANB3 nuclease domain behave identically to wild type cells in our assays, i.e. they display replication fork slow down and high frequency of reversed replication forks upon CPT or MMC treatment. This implies that ZRANB3 nuclease domain does not have a direct role in replication fork reversal upon genotoxic treatment, and may well play a role in some other, yet unrecognized, function of ZRANB3, related or not to replication fork metabolism. The results obtained so far on the NZF domain – which still require experimental confirmation - suggest a role for this domain in delaying replication fork progression, but not in inducing efficient replication fork reversal. Indeed, mutations in the NZF domain lead to unrestrained replication fork

progression upon genotoxic treatments, but do not seem to impair accumulation of reversed replication forks in the same experimental conditions. If confirmed, this apparent discrepancy may be explained by the different sensitivity and the different read-out of the two assays. While the fibers assay is a "dynamic" approach that measures the rate of replication fork progression over a period of time in different genetic backgrounds and upon different treatments, our electron microscopy approach is providing a "static" snapshot of the replication intermediates present in the cells at a given time point. it is thus possible that – upon certain genetic manipulations (e.g. mutations in ZRANB3 NZF domain) - replication forks can progress at accelerated rates upon genotoxic treatments, while still retaining their propensity to transit through a regressed state in a similar proportion of the forks, by possibly restarting reversed forks at a higher rate than in wild type cells. A study (Ciccia A, et al., 2012) has shown that PIP&APIM domains are necessary for recruitment to damage site via interaction with PCNA, and NZF domain is important for retention at the damage site via interaction with polyubiqitinated PCNA. It could well be that initial recruitment via interaction with PCNA is necessary for prompt and efficient replication fork reversal, while retention at the damage sites may play role in abovementioned unrecognized functions of ZRANB3 (where nuclease domain could be crucial). What shall also be considered is that mutations in the particular domain (NZF) in the full length protein could give rise to different phenotypes than mutation in individual domains tested individually. Further investigations will be required to possibly confirm this discrepancy and to clarify its molecular determinants.

Importantly, a second genetic perturbation completely impairing fork slowing, but having only partial effects on fork reversal, is HARP downregulation (see below), further suggesting that the penetrance of a fork progression phenotype may not necessarily be mirrored by

equivalent defects in the efficiency of fork reversal. Conversely, differently from genetic ablation of UBC13, which has complete DNA fiber and EM phenotypes, its partial siRNA-mediated downregulation of UBC13 leads to partial effects on fork progression upon damage, but drastic impairment of replication fork reversal upon CPT and MMC treatments. Elucidating the mechanisms leading to detectable effects by each of these approach will likely require detailed investigation of several other genetic perturbations.

Ubc13 is an E2 conjugating enzyme, involved in many processes in the cell, and thus its function on fork slowing and reversal may result from inactivation of various ubiquitin-regulated pathways. However, several additional lines of evidence in this thesis strongly suggest that its function on fork progression and remodelling stems from its role in polyubiquitination of PCNA via K63 linked ubiquitin chains.

Using a previously described system, where the endogenous ubiquitin can be replaced by WT ubiquitin or its K63 mutant, we could show that cells expressing the K63 ubiquitin mutant display defective fork slowing (data not shown) and only marginal induction of fork reversal upon genotoxic treatments. A very similar phenotype was observed when we applied the same techniques to mouse embryonic fibroblasts bearing a point mutation on the PCNA residue (K164) which is the acceptor of both mono- or poly- ubiquitination. Altogether these results strongly suggest that PCNA polyubiquitination is strictly required to enable replication fork remodelling and effective fork slowing upon mild treatments with genotoxic stress.

Our preliminary investigations on a second annealing helicase (HARP/SMARCAL1) showed promising effects on the regulation of fork progression (DNA fibers), but only partial effects on the efficiency of replication fork reversal (EM analysis). However, it should be noted that this analysis was uniquely performed upon CPT treatment. In light of the

abundance of replication fork reversal in response to different sources of genotoxic stress (Zellweger et al., 2015; Neelsen and Lopes, 2015), it is conceivable that different cellular factors may promote fork remodelling in response to different drugs, possibly because of the accumulation of different molecular precursors (e.g. amount and/or distribution of ssDNA regions at stalled forks) or different chromatin marks around forks challenged by different sources of stress. It will thus be important to extend our analysis on annealing helicases – as well as other candidate cellular factors in fork remodelling – to different genotoxic treatments, including for example HU and UV treatments, that challenge the replication process by rather different mechanisms, in respect to CPT or MMC.

Other important areas that will require further investigation and protocol optimization include: 1) methods to directly detect endogenous levels of polyubiquitinated PCNA; being able to follow directly the putative effects on this specific post-translational modification would possibly provide additional confidence in the interpretation of a subset of data in this thesis; 2) optimized iPOND protocol to directly detect binding to forks of relatively large (>100kDa) proteins, such as the annealing helicases HARP and ZRANB3. We have been as of yet unsuccessful in detecting ZRANB3 by the standard iPOND approach coupled to western blotting. However, testing protocols optimized for the detection of large proteins by iPOND would possibly enable assessing whether different effects on fork slowing and reversal closely mirror defects in having these proteins recruited to the fork, via defective binding to PCNA and/or to its polyubiquitinated form.

4. Materials and Methods.

4.1 Cell culture and cell lines.

Human U2OS osteosarcoma cells were cultivated at 37°C (10% CO2) in Dulbecco's Modified Eagle's Medium (DMEM, Gibco) supplemented with 10% Fetal Bovine Serum (FBS, Gibco), 100 U/ml penicillin and 100 μg/ml streptomycin. Cells were treated with different cancer chemotherapeutics and DNA damaging agents at indicated time points, trypsinized and collected for Western blot analysis, PFGE and EM extraction.

Human U2OS wild type or ZRANB3 knock out cells were cultivated at 37°C (10% CO2) in Dulbecco's Modified Eagle's Medium (DMEM, Gibco) supplemented with 7.5%Fetal Bovine Serum (FBS, Gibco), 100 U/ml penicillin and 100 μg/ml streptomycin.

Human HEK293T cells were cultivated at 37°C (10% CO2) in Dulbecco's Modified Eagle's Medium (DMEM, Gibco) supplemented with 10% Fetal Bovine Serum (FBS, Gibco), 100 U/ml penicillin and 100 μg/ml streptomycin.

Human HCT116 cell line were cultivated at 37°C (10% CO2) in McCoy's (5A) Modified Medium (26600-023, Gibco) supplemented with 10% Fetal Bovine Serum (FBS, Gibco), 100 U/ml penicillin and 100 μg/ml streptomycin.

Human U20S cells with inducible ubiquitin mutant expression were kept in media without tetracycline until the expression was needed. Then

4.2 Transfections.

For knockdown experiments, cells were transfected 48-60 h with the indicated siRNA using RNAiMax transfection reagent (Invitrogen), according to the manufacturer's instructions: siLuc (40nM; 5′-CGUACGCGGAAUACUUCGAdTdT-3'), siHARP (40nM; 5'-

GCUUUGACCUUCUUAGCAAdTdT-3'), siUbc13 (40nM; 5'AAUGGCAGCCCCUAAAGUAdTdT-3'), siRad18 (40nM; 5'AUGGUUGUUGCCCGAGGUUAAdTdT-3'), siHLTF (40nM; 5'-GGUGCUUUGGCCUAUAUCAdTdT-3'), siUSP1 (40nM; 5'-UCGGCAAUACUUGCUAUCUUAdTdT-3'), all purchased from Microsynth. The two ZRANB3 oligos were siGENOME siRNA D-010025-03-005 (84083) and siGENOME siRNA J-010025-10 purchased from Dharmacon (60nM final concentration for transfection).

4.3. Drugs and reagents.

Camptothecin (C9911, Sigma-Aldrich) was dissolved in dimethyl sulfoxide (DMSO) to yield freshly made 20 mM stock (7 mg/ml). Mitomycin C (M0503, Sigma-Aldrich) was prepared in ddH2O to obtain freshly made 3 mM stock (1 mg/ml). UV 254 nm was measured with digital radiometer (UVP. Inc. Upland. CA), 20 mW/cm2, cells were irradiated with Camag UV lamp dual wavelength, 254/366 (V 220; A 0.2). Cells were UV-irradiated and utilized for analysis after 12 or 4 h recovery.

EDTA-free protease inhibitor cocktail (Roche) and N-ethylmaleimide (Sigma-Aldrich) were freshly added to immunoprecipitation buffers.

4.3 Western blotting.

Intracellular protein level and protein expression after knockdown experiments were determined by Western blot analysis of cell extracts. Mammalian cells were collected and lysed using 2xLaemmli buffer (4% SDS, 20% glycerol, 120 mM Tris-HCl pH 6.8). Protein amounts were normalized using known BSA (Bovine Serum Albumin) concentrations and protein absorbance was measured using Agilent Technologies Cary60 UV-Vis 115pectrophotometer technology. Proteins (20-60 μg) were resolved on 6-12% casted SDS-

gels, or gradient 4-15% SDS-gels. SDS-gels were run at 12 mA-18 mA (voltage/gel). Proteins were then wet-blotted on nitrocellulose blotting membranes (GE Healthcare) in buffer containing 20% methanol and 80% 1x transfer buffer (transfer buffer 10x: 25 mM Tris, 192 mM glycine, 10% methanol), either for 2 h (100 V, 4°C) or overnight (30 V, 4°C). Membranes were blocked for at least 30 min in 2% ECL (GE Healthcare) in 0.1% TBST (1x Tris-Buffered Saline supplemented with 0.1% Tween-20), 5% milk or 5% BSA dissolved in 0.1% TBST (different proteins demanded different blocking solutions). Afterwards, membranes were incubated with primary antibodies, either overnight at 4°C or for 3-4h at RT. Secondary antibodies were added in blocking solution for 1h at RT. Membranes were washed 3 times with 0.1% TBST (10 min each) after incubation with primary and secondary antibodies. Membranes were detected with ECL detection reagents (GE Healthcare) using Fusion SOLO chemiluminescence imaging system (Vilber Lourmat).

4.4 Detection of chromatin-bound PCNA.

To prepare nuclear extracts cells were washed once with ice-cold 1× PBS and incubated 5 min on ice with pre-extraction buffer (25 mM HEPES pH 7.4, 100 mM NaCl, 1 mM EDTA, 3 mM MgCl2, 300 mM sucrose and 0.2% Triton X-100). Pre-extraction buffer was removed and cells were harvested by scraping with 2× Laemmli buffer. Nuclear fractions were incubated 5 min at RT and sonicated 2 times for 15sec each (30%). Absorbance of chromatin-bound proteins was measured using Agilent Technologies Cary60 UV-Vis spectophotometer technology and proteins (20-60 μg) were separated by 8% SDS-gels and incubated with antibodies. Membranes were blocked for at least 30 min in 5% milk in 0.1% TBST (1× TBS supplemented with 0.1% Tween-20) and washed 5 times with 0.1% TBST (10 min each) after incubation with primary and secondary antibodies. Membranes were

immunoblotted with anti-PCNA (PC10) or anti-Ubiquitin antibodies and visualized with SuperSignal West-Femto (Thermo Scientific) or ECL detection reagents (GE Healthcare). Images were acquired using Fusion SOLO chemiluminescence imaging system (Vilber Lourmat).

4.5 Immunoprecipitation.

To prepare nuclear extracts cells were trypsinized and resuspended in pre-extraction buffer (25 mM HEPES pH 7.4, 50 mM NaCl, 1 mM EDTA, 3 mM MgCl2, 300 mM sucrose, 0.5% Triton X-100, EDTA-free protease-inhibitor cocktail, 20 mM N-ethylmaleimide). Cells were kept on ice for 15 min and centrifugated at 400 rpm for 15 min (4°C). Protein pellet was resuspended in lysis buffer (1% SDS, 50 mM Tris-HCl pH 8.0, 10 mM EDTA pH 8.0, EDTA-free protease inhibitor cocktail, 20 mM N-ethylmaleimide), sonicated once for 20sec (30%) and centrifugated at maximal speed for 10 min (4°C). Protein absorbance was measured by Nanodrop technology and 200-500 μg of total protein was utilized for immunoprecipitation. Protein lysate volume was adjusted with IP buffer (1.2 mM EDTA, 1.1% Triton X-100, 16.7 mM Tris-HCl pH 8.0, 300 mM NaCl, EDTA-free protease inhibitor cocktail, 20 mM N-ethylmaleimide) and incubated with 1 μg of anti-PCNA monoclonal antibody (PC10) for 3-4 h at 4°C. Subsequently, the lysates were incubated with protein G Sepharose beads (GE Healthcare) for 2-4 h at 4°C. Beads were centrifugated for 1 min at 2000 rpm (4°C) and washed 3-5 times with washing buffer (0.1% SDS, 1% Triton X-100, 2 mM EDTA, 20 mM Tris-HCl pH 8.0, 500 mM NaCl, EDTA-free protease inhibitor cocktail, 20 mM N-ethylmaleimide). Proteins were eluted by boiling at 95°C in 2× Laemmli buffer for 5-10 min. Proteins absorbance was measured by Nanodrop technology and anti-PCNA immunoprecipitates were separated by 8% SDS-gels, transferred onto nitrocellulose blotting

membranes (GE Healthcare) and detected with anti-PCNA (PC10) or anti-Ubiquitin monoclonal antibodies.

4.6 Antibodies.

The following primary antibodies were used for Western blotting: ZRANB3 (A303-033A, Bethyl laboratories; 23111-1-AP, Proteintech), Beta tubulin (sc-9104, Santa Cruz Biotechnology, Inc.), GAPDH (MAB374, Millipore), Ub K164 PCNA (13439S, Cell Signalling), Harp (SMARCAL1) (ab69900, Abcam), Ubc13 (#4919; Cell Signaling Technology), Rad18 (provided by J. Jiricny, IMCR, Zurich), USP1 (provided by S.Ferrari, IMCR, Zurich), PCNA (sc-56; Santa Cruz Biotechnology, Inc.), TFIIH (sc-293; Santa Cruz Biotechnology, Inc.), GAPDH (provided by A. Sartori, IMCR, Zurich). Secondary antibodies used for Western blotting were anti-rabbit and anti-mouse ECL (GE Healthcare). Primary antibodies used for DNA fibers spreading were mouse anti-BrdU/IdU (347580; Becton Dickinson) and rat anti-BrdU/CldU (ab6326; Abcam). Secondary antibodies used for DNA fibers spreading were anti-mouse Alexa Fluor 488 (Molecular Probes) and anti-rat Cy3 (Jackson Immuno Research).

4.7 Pulse-field gel electrophoresis.

Asynchronous subconfluent (40-70% confluency) mammalian U2OS cells were treated with defined concentration of specific DNA damaging agent for 4 h. Cells were harvested by trypsinization and embedded in 0.8% agarose plugs (3x105 cells/plug). Plugs were digested for 36-72 h at 37°C in lysis buffer (100 mM EDTA pH 8.0, 1% [wt/vol] sodium lauryl sarcosyne, 0.2% [wt/vol] sodium deoxycholate, and 1 mg/ml proteinase K) and washed 3-4

times (30 min each) in 20 mM Tris-HCl pH 8.0 and 50 mM EDTA. Electrophoresis was performed at 14°C in 0.9% [wt/vol] Pulsed Field Certified Agarose (Bio-Rad) containing 0.5× TBE buffer (Tris/Borate/EDTA) in CHEF DR III apparatus (Block I: 9 h, 120°, 5.5 V/cm, 30-18 s switch time; Block II: 6 h, 117°, 4.5 V/cm, 18-19 s switch time; Block III: 6 h, 112°, 4 V/cm, 9-5 s switch time). The gel was stained with ethidium bromide and imaged on an Alpha Innotech Imager.

4.8 DNA fiber spreading.

Asynchronously growing U2OS cells (40-60% confluency) were pulse-labelled for 30 min with 30 μM CldU, washed 3 times with warm 1x PBS and labelled 30 min with 250 μM IdU. DNA damaging agents or chemotherapeutics were optionally added with the second labelling (30 min). Cells were trypsinized and resuspended in ice-cold 1xPBS to 2.5*105 cells/mL. Labelled cells were mixed 1:5 with unlabelled cells and cell suspension was mixed by stirring with lysis buffer (200 mM Tris-HCl pH 7.4, 50 mM EDTA, 0.5% SDS) on glass slides. After 9 min at RT the slides were tilted manually (30°-45°) to allow the DNA to spread down the slide. Slides were air-dried and fixed with methanol/acetic acid 3:1 overnight at 4°C. DNA fibers were denaturated with 2.5 M HCl, washed 5 times (3 min each) with 1xPBS and blocked for 40 min with 2% BSA (Bovine Serum Albumin) in 0.1% PBST (1xPhosphate-Buffered Saline supplemented with 0.1% Tween-20). Slides were incubated in dark for 2.5h at RT with anti-BrdU antibodies recognizing CldU (ab6326; Abcam, rat) and IdU (347580; BD, mouse). Slides were washed 5 times (3 min each) in 0.2% PBST (0.2% Tween-20) and incubated in dark for 1h at RT with appropriate secondary antibodies; anti-mouse Alexa 488 (Molecular Probes) and anti-rat Cy3 (Jackson Immuno Research). After washing 5 times (3 min each) in 0.2% PBST, the slides were air-dried, coverslip mounted with 20 μL/slide

Antifade Gold (Invitrogen) and sealed with transparent nail polish. Slides were stored at 4°C. Images were acquired with either Olympus IX81 fluorescence microscope equipped with CCD camera (Orca AG, Hamamatsu) or Leica DMRB equipped with a camera (model DFC360 FX, Leica). Images were processed with CellR software (Olympus) or Leica Application Suite 3.3.0. CldU and IdU tract lengths were measured using ImageJ (National Institutes of Health). Mann-Whitney test was utilized to assess if differences in tract length were significant using Prism (GraphPad Software).

4.9 Electron microscopic analysis of genomic DNA.

In vivo psoralen cross-linking, isolation of total genomic DNA, enrichment of replication intermediated and EM visualization were performed as described in (Neelsen et al., 2014). Asynchronous sub confluent U2OS cells were treated with defined concentration of specific DNA damaging agent for 1 h. Cells were harvested by trypsinization and washed with ice-cold 1xPBS. Genomic DNA was cross-linked by two rounds of incubation (5 min each) with 10 μM 4,5', 8- trimethylpsoralen (TMP) followed by irradiation pulses of 3 min with 366 nm UV light (Stratagene UV Stratlinker 1800). Cell suspension was washed 2 times with ice-cold 1xPBS and and cells were lysed with lysis buffer (1.28 M sucrose, 40 mM Tris-HCl pH 7.5, 20 mM MgCl2, 4% Triton X-100) and incubated on ice for 10 min. After a brief centrifugation step, the lysed cells were resuspended in ice-cold 1xPBS. DNA was isolated from nuclei by incubation at 50°C with digestion buffer (800 mM guanidine-HCl, 30 mM Tris-HCl pH 8.0, 30 mM EDTA pH 8.0, 5% Tween-20, 0.5% Triton X-100) and proteinase K (stock 20 mg/mL in ddH2O) until the solution became clear (1-2 h). Samples were cooled down to room temperature and mixed with chlorophorm/isoamylalcohol. Samples were centrifugated for 20 min at 8000 rpm, the upper phase was removed and isopropanol was

added to precipitate DNA. DNA was washed with 70% ethanol, air-dried and resuspended in 1xTE buffer (Tris/EDTA). Purified mammalian DNA was digested for 4-5 h with PvuII HF restriction enzyme. Replication intermediates were enriched on BND cellulose chromatography columns (Bio-Rad, BND cellulose granules 0.1 g/mL dissolved in 10 mM Tris-HCl pH 8.0, 300 mM NaCl). Columns were washed 6 times with 10 mM Tris-HCl pH 8.0, 1 M NaCl and subsequently washed 6 times with 10 mM Tris-HCl pH 8.0, 300 mM NaCl to equilibrate cellulose. Samples were loaded on the columns and incubated for 30 min at RT. The columns were washed 2 times with 10 mM Tris-HCl pH 8.0, 1 M NaCl and incubated for 10 min with 10 mM Tris-HCl pH 8.0, 1 M NaCl, 1.8% caffeine. The flow-troughs, enriched in replication intermediates, were collected in microcentrifuge tubes and DNA was purified and enriched using Amicon size-exclusion filters (EMD Millipore). EM samples were prepared by spreading the DNA on carbon-coated grids and visualized by platinum rotary shadowing. Images were acquired on a transmission electron microscope (CM100, Philips) and analysed with ImageJ (National Institutes of Health).

4.10 Chromatin enrichment.

Cells were scraped in buffer A (100 mM NaCl, 300 mM sucrose, 3 mM MgCl2, 10 mM Pipes (pH 6.8), 1 mM EGTA, 0.2% Triton X-100, 100 μM NaVO4, 50 mM NaF, and protease inhibitors (Roche Applied Science) + DUB inhibitors, then incubated for 5 min on ice with gentle inverting. The supernatants were recovered as the soluble fraction after centrifugation (e.g. 5 min 5000 rpm 4C). This was followed by washing with the same volume of buffer A, the pellet was resuspended in buffer B (50 mM Tris-HCl (pH 7.5), 150 mM NaCl, 5 mM EDTA, 1% Triton X-100, 0.1% SDS, 100 μM NaVO4, 50 mM NaF, and protease inhibitors+ DUB inhibitors) for immunoblotting. Next was a 10-min incubation on

ice, then the samples were sonicated (bioruptor with cycles 30s sonication, 30s pause for 10 min) and then incubated for another 10 min on ice before centrifugation (full speed (approximately 10min, 4°C) to isolate the chromatin-bound fraction (supernatant). Protein concentrations were measured (using Lowry or Bradford methods). Lastly, Laemmli buffer supplemented with DTT (1M for 2X Laemmli) was added.

4.11 Creation of stable cell lines.

Phoenix retrovirus producer cells were transfected (grown in DMEM media with 10% FBS and 1% Glutamine) with plasmids that were carrying the corresponding retroviruses (the mutants that were produced had mutations in following domains: mutants in annealing helicase domain (HD, aspartic acid at position 157 and glutamic acid at position 158 changed to alanine), in endonuclease domain (ND, histidine at position 1045 changed to leucine in the domain responsible for interaction with polyubiquitinated PCNA (NZF, threonine at position 631 changed to leucine, and tyrosine at position 632 changed to valine), and domains responsible for interaction with PCNA (PIP, where glutamine at position 519 was changed to alanine, and isoleucine at position 522 was changed to alanine; APIM, where phenylalanines at position 525 and 526 were changed to alanines, and a stop codon was introduced instead of threonine at position 1073)). 1h before transfection we added Chloroquine (final concentration of 20 μm), and then added the transfection mixture (H_2O, 10 μg plasmid DNA and 2 M $CaCl_2$). 8h post transfection fresh media was added. 48h post transfection supernatant from Phoenix cells containing viruses was collected. Polybrene (8mg/ml) was added to the supernatant, and it was used as a media for target cells (in this case ZRANB3 knock out cells), that were supposed to be infected. 3h later the infection procedure was

repeated. After second infection procedure, the media was changed to usual growth media (DMEM, 7.5% FBS, 100 U/ml penicillin and 100 μg/ml streptomycin).

48h post infection cells were kept in selection media containing puromycin (3 μg/ml) for few days until cells from control group without resistance died out. If the integration took place in the infected cells, they were supposed to survive, while the cells with no integration should die, as control uninfected cells. Two different strategies for collecting surviving cells expressing the protein were used. The first strategy was included collection of all the surviving cells from particular mutant. The second strategy included growing different dilutions of particular mutant cell line in an attempt to obtain individual colonies, which were then further propagated. After obtaining stable cell lines, protein levels were assessed using Western Blot

5. References.

Akbari, M., and Krokan, H.E. (2008). Cytotoxicity and mutagenicity of endogenous DNA base lesions as potential cause of human aging. Mech Ageing Dev *129*, 353-365.

Andressoo, J.O., Hoeijmakers, J.H., and de Waard, H. (2005). Nucleotide excision repair and its connection with cancer and ageing. Adv Exp Med Biol *570*, 45-83.

Bansbach, C.E., Betous, R., Lovejoy, C.A., Glick, G.G., and Cortez, D. (2009). The annealing helicase SMARCAL1 maintains genome integrity at stalled replication forks. Genes & development *23*, 2405-2414.

Bell S.P., S.B. (1992). ATP-dependent recognition of eukaryotic origins of DNA replication by a multiprotein complex. Nature *357*, 128-134.

Berti, M., Chaudhuri, A.R., Thangavel, S., Gomathinayagam, S., Kenig, S., Vujanovic, M., Odreman, F., Glatter, T., Graziano, S., Mendoza-Maldonado, R.*, et al.* (2013). Human RECQ1 promotes restart of replication forks reversed by DNA topoisomerase I inhibition. Nat Struct Mol Biol *20*, 347-354.

Betous, R., Couch, F.B., Mason, A.C., Eichman, B.F., Manosas, M., and Cortez, D. (2013). Substrate-selective repair and restart of replication forks by DNA translocases. Cell Rep *3*, 1958-1969.

Bienko M, G.C., Crosetto N, Rudolf F, Zapart G, Coull B, Kannouche P, Wider G, Peter M, Lehmann AR, Hofmann K, Dikic I. (2005). Ubiquitin-binding domains in Y-family polymerases regulate translesion synthesis. Science *310*, 1821-1824.

Blastyak A., P.L., Unk I., Prakash L., Prakash S., Haracska L. (2007). Yeast Rad5 protein required for postreplication repair has a DNA helicase activity specific for replication fork regression. Mol Cell *28*, 167-175.

Boerkoel, C.F., O'Neill, S., Andre, J.L., Benke, P.J., Bogdanovic, R., Bulla, M., Burguet, A., Cockfield, S., Cordeiro, I., Ehrich, J.H.*, et al.* (2000). Manifestations and treatment of Schimke immuno-osseous dysplasia: 14 new cases and a review of the literature. Eur J Pediatr *159*, 1-7.

Branzei D, e.a. (2004). Rad18/Rad5/Mms2-mediated polyubiquitination of PCNA is implicated in replication completion during replication stress. Genes Cells *9*, 1031-1042.
Branzei D, F.M. (2010). Maintaining genome stability at the replication fork. Nat Rev Mol Cell Biol *11*, 208-219.

Brooks PJ, Z.S. (2014). Acetaldehyde and the genome: beyond nuclear DNA adducts and carcinogenesis. Environ Mol Mutagen *55*, 77-91.

Broomfield S, H.T., Xiao W. (2001). DNA postreplication repair and mutagenesis in Saccharomyces cerevisiae.
Mutat Res *486*, 167-184.
Calzada, A., Hodgson, B., Kanemaki, M., Bueno, A., and Labib, K. (2005). Molecular anatomy and regulation of a stable replisome at a paused eukaryotic DNA replication fork. Genes Dev *19*, 1905-1919.

Carroll, C., Badu-Nkansah, A., Hunley, T., Baradaran-Heravi, A., Cortez, D., and Frangoul, H. (2013). Schimke Immunoosseous Dysplasia associated with undifferentiated carcinoma and a novel SMARCAL1 mutation in a child. Pediatr Blood Cancer *60*, E88-90.
Cayrou C, C.P., Mechali M (2010). Programming DNA replication origins and chromosome organization. Chromosome Res *18*, 137-145.

Centore R.C., Y.S.A., Tse A., Zou L. (2012). Spartan/C1orf124, a reader of PCNA ubiquitylation and a regulator of UV-induced DNA damage response. Mol Cell *46*, 625-635.
Champoux, J.J. (2001). DNA topoisomerases: structure, function, and mechanism. Annu Rev Biochem *70*, 369-413.

Chang DJ, C.K. (2009). DNA damage tolerance: when it's OK to make mistakes. Nat Chem Biol *5*, 82-90.

Chikahide Masutani, R.K., Shigenori Iwai and Fumio Hanaoka (2000). Mechanisms of accurate translesion synthesis by human DNA polymerase η. EMBO J *19*, 3100-3109.
Ciccia, A., Nimonkar, A.V., Hu, Y., Hajdu, I., Achar, Y.J., Izhar, L., Petit, S.A., Adamson, B., Yoon, J.C., Kowalczykowski, S.C.*, et al.* (2012). Polyubiquitinated PCNA recruits the ZRANB3 translocase to maintain genomic integrity after replication stress. Mol Cell *47*, 396-409.

Couch, F.B., Bansbach, C.E., Driscoll, R., Luzwick, J.W., Glick, G.G., Betous, R., Carroll, C.M., Jung, S.Y., Qin, J., Cimprich, K.A.*, et al.* (2013). ATR phosphorylates SMARCAL1 to prevent replication fork collapse. Genes & development *27*, 1610-1623.
Daigaku Y, D.A., Ulrich HD. (2010). Ubiquitin-dependent DNA damage bypass is separable from genome replication.. Nature *465*, 951-955.
De Bont R, v.L.N. (2004). Endogenous DNA damage in humans: a review of quantitative data. Mutagenesis *19*, 169-185.

Delmolino LM, S.N.a.C.J.J. (2001). COP-1, a member of the CCN family, is a heparin-induced growth arrest speci®c gene in vascular smooth muscle cells. J Cell Physiol *188*, 45-55.
Drury LS, P.G., Diffley JF. (2000). The cyclin-dependent kinase Cdc28p regulates distinct modes of Cdc6p proteolysis during the budding yeast cell cycle. Curr Biol *10*, 231-240.
Durando, M.e.a. (2013). A non-catalytic role of DNA polymerase η in recruiting Rad18 and promoting PCNA monoubiquitination at stalled replication forks. Nucleic Acids Res *41*, 3079-3093.

Edenberg HJ, H.J. (1975). Eukaryotic chromosome replication. Annu Rev Genet *9*, 245-284.

Fachinetti, D., Bermejo, R., Cocito, A., Minardi, S., Katou, Y., Kanoh, Y., Shirahige, K., Azvolinsky, A., Zakian, V.A., and Foiani, M. (2010). Replication termination at eukaryotic chromosomes is mediated by Top2 and occurs at genomic loci containing pausing elements. Mol Cell *39*, 595-605.

Fien, K., Cho, Y.S., Lee, J.K., Raychaudhuri, S., Tappin, I., and Hurwitz, J. (2004). Primer utilization by DNA polymerase alpha-primase is influenced by its interaction with Mcm10p. J Biol Chem *279*, 16144-16153.

Friedman KL, D.J., Ferguson BM, Nyland SV, Brewer BJ, Fangman WL. (1996). Multiple determinants controlling activation of yeast replication origins late in S phase. Genes & Dev *10*, 1595–1607.

Gambus, A., Jones, R.C., Sanchez-Diaz, A., Kanemaki, M., van Deursen, F., Edmondson, R.D., and Labib, K. (2006). GINS maintains association of Cdc45 with MCM in replisome progression complexes at eukaryotic DNA replication forks. Nat Cell Biol *8*, 358-366.

Garg P, B.P. (2005). DNA polymerases that propagate the eukaryotic DNA replication fork. Crit Rev Biochem Mol Biol *40*, 115-128.

Ghosal G, C.J. (2013). DNA damage tolerance: a double-edged sword guarding the genome. Transl Cancer Res *2*, 107-129.

Ghosal G., L.J.W., Nair B.C., Fong K.W., Chen J. (2012). Proliferating cell nuclear antigen (PCNA)-binding protein C1orf124 is a regulator of translesion synthesis. J Biol Chem *287*.
Giannattasio M, e.a. (2014). Visualization of recombination-mediated damage bypass by template switching. Nat Struct Mol Biol *21*, 884-892.

Gregan J , L.K., Brimage L , Franklin R , Namdar M , Hart EA , Aves SJ , Kearsey SE . (2003). Fission yeast Cdc23/Mcm10 functions after pre-replicative complex formation to promote Cdc45 chromatin binding. Mol Biol Cell *14*, 3876-3887.

Guo C, F.P., Luk-Paszyc MJ, Masuda Y, Zhou J, Kamiya K, Kisker C, Friedberg EC (2003). Mouse Rev1 protein interacts with multiple DNA polymerases involved in translesion DNA synthesis. EMBO J *22*.

Hashimoto, Y., Puddu, F., and Costanzo, V. (2012). RAD51- and MRE11-dependent reassembly of uncoupled CMG helicase complex at collapsed replication forks. Nat Struct Mol Biol *19*, 17-24.

Hoege C, P.B., Moldovan GL, Pyrowolakis G, Jentsch S. (2002). RAD6-dependent DNA repair is linked to modifi
cation of PCNA by ubiquitin and SUMO.
Nature *419*, 135-141.

Hoeijmakers (2009). DNA damage, aging, and cancer. N Engl J Med.

Holm, C., Covey, J.M., Kerrigan, D., and Pommier, Y. (1989). Differential requirement of DNA replication for the cytotoxicity of DNA topoisomerase I and II inhibitors in Chinese hamster DC3F cells. Cancer Res *49*, 6365-6368.

Homesley L1, L.M., Kawasaki Y, Sawyer S, Christensen T, Tye BK. (2000). Mcm10 and the MCM2-7 complex interact to initiate DNA synthesis and to release replication factors from origins. Genes Dev *14*, 913-926.

Houtgraaf, J.H., Versmissen, J., and van der Giessen, W.J. (2006). A concise review of DNA damage checkpoints and repair in mammalian cells. Cardiovasc Revasc Med *7*, 165-172.
Huang TT, D.A.A. (2006). Regulation of DNA repair by ubiquitylation. Nat Rev Mol Cell Biol *7*, 323-334.

Ilves, I., Petojevic, T., Pesavento, J.J., and Botchan, M.R. (2010). Activation of the MCM2-7 helicase by association with Cdc45 and GINS proteins. Mol Cell *37*, 247-258.
Kanemaki M, L.K. (2006). Distinct roles for Sld3 and GINS during establishment and progression of eukaryotic DNA replication forks.
EMBO J *25*, 1753-1763.

Kannouche, P., and Stary, A. (2003). Xeroderma pigmentosum variant and error- prone DNA polymerases. Biochimie *85*, 1123-1132.

Kannouche, P.e.a. (2001). Localization of DNA polymerases and to the replication machinery is tightly co-ordinated in human cells. . EMBO J *21*, 6246-6256.

Kannouche, P.L., Wing, J., and Lehmann, A.R. (2004). Interaction of Human DNA Polymerase eta with Monoubiquitinated PCNA; A Possible Mechanism for the Polymerase Switch in Response to DNA Damage. Mol Cell Biol *14*, 491-500.

Karras GI, J.S. (2010). The RAD6 DNA damage tolerance pathway operates uncoupled from the replication fork and is functional beyond S phase.
Cell *141*, 255-267.

Kile AC, C.D., Bacal J, Eldirany S, Korzhnev DM, Bezsonova I, Eichman BF, Cimprich KA. (2015). HLTF's Ancient HIRAN Domain Binds 3' DNA Ends to Drive Replication Fork Reversal. Mol Cell *58*, 1090-1100.

Koster, D.A., Crut, A., Shuman, S., Bjornsti, M.A., and Dekker, N.H. (2010). Cellular strategies for regulating DNA supercoiling: a single-molecule perspective. Cell *142*, 519-530.
Kubota, Y., and Takisawa, H. (2003). Block to DNA replication in meiotic maturation: a unified view for a robust arrest of cell cycle in oocytes and somatic cells. Bioessays *25*, 313-316.

Labib, K.G., Agnieszka. (2007). A key role for the GINS complex at DNA replication forks. Trends in Cell Biology *17*, 271-278.

Lee, J.K., Seo, Y.S., and Hurwitz, J. (2003). The Cdc23 (Mcm10) protein is required for the phosphorylation of minichromosome maintenance complex by the Dfp1-Hsk1 kinase. Proc Natl Acad Sci U S A *100*, 2334-2339.

Lee KY, M.K. (2008). PCNA modifications for regulation of post-replication repair pathways. Mol Cells *26*, 5-11.

Lehmann, A.R. (2003). DNA repair-deficient diseases, xeroderma pigmentosum, Cockayne syndrome and trichothiodystrophy. Biochimie *85*, 1101-1111.

Lehmann, T.O.A.R. (2006). The Y-family DNA polymerase κ (pol κ) functions in mammalian nucleotide-excision repair. Nature Cell Biology *8*, 640-642.
Lindahl, T. (1993). Instability and decay of the primary structure of DNA. . Nature *362*, 709-715.

Marinsek, N., Barry, E.R., Makarova, K.S., Dionne, I., Koonin, E.V., and Bell, S.D. (2006). GINS, a central nexus in the archaeal DNA replication fork.
EMBO Rep *7*, 539-545.

McCulloch SD, K.T. (2008). The fidelity of DNA synthesis by eukaryotic replicative and translesion synthesis polymerases. Cell Res *18*, 148-161.
Mosbech A., G.-S.I., Kagias K., Thorslund T., Beli P., Povlsen L., Nielsen S.V., Smedegaard S., Sedgwick G., Lukas C., et al. (2012). DVC1 (C1orf124) is a DNA damage-targeting p97

adaptor that promotes ubiquitin-dependent responses to replication blocks. Nat Struct Mol Biol *19*, 1084-1092.

Motegi A, L.H., Lee KY, Roest HP, Maas A, Wu X, Moinova H, Markowitz SD, Ding H, Hoeijmakers JH, Myung K. (2008). Polyubiquitination of proliferating cell nuclear antigen by HLTF and SHPRH prevents genomic instability from stalled replication forks.
Proc Natl Acad Sci U S A *105*, 12411-12416.

Narottam Acharyaa, J.-H.Y., Himabindu Galib, Ildiko Unkb, Lajos Haracskab, Robert E. Johnsona,, and Jerard Hurwitzc, L.P., and Satya Prakasha (2008). Roles of PCNA-binding and ubiquitin-binding domains
in human DNA polymerase in translesion
DNA synthesis. PNAS *105*, 17724-17729.

Neelsen KJ, L.M. (2015). Replication fork reversal in eukaryotes: from dead end to dynamic response. Nat Rev Mol Cell Biol *16*, 207-220.

Noguchi, A.R.L.a.E. (2013). The Replication Fork: Understanding the Eukaryotic Replication Machinery and the Challenges to Genome Duplication. Genes *4*, 1-32.

Paixao S, C.I., Cubells M, et al. (2004). Modular structure of the human lamin B2 replicator. . Molecular Cell Biology *24*, 2958-2967.
Parker JL, U.H. (2009). Mechanistic analysis of PCNA poly-ubiquitylation by the ubiquitin protein ligases Rad18 and Rad5.
EMBO J *28*, 3657-3666.

Patricia Kannouche, A.R.F.d.H., Barry Coull,1 Antonio E. Vidal,Colin Gray, Daniel Zicha, Roger Woodgate, and Alan R. Lehmann (2003). Localization of DNA polymerases η and ι to the replication machinery is tightly co-ordinated in human cells. EMBO J *22*, 1223-1233.
Pommier, Y. (2006). Topoisomerase I inhibitors: camptothecins and beyond. Nat Rev Cancer *6*, 789-802.

Postow, L., Woo, E.M., Chait, B.T., and Funabiki, H. (2009). Identification of SMARCAL1 as a component of the DNA damage response. J Biol Chem *284*, 35951-35961.

Povlsen L.K., B.P., Wagner S.A., Poulsen S.L., Sylvestersen K.B., Poulsen J.W., Nielsen M.L., Bekker-Jensen S., Mailand N., Choudhary C. (2012). Systems-wide analysis of ubiquitylation dynamics reveals a key role for PAF15 ubiquitylation in DNA-damage bypass. . Nat Cell Biol *14*, 1089-1098.
Prelich, G., Kostura, M., Marshak, D.R., Mathews, M.B., and Stillman, B. (1987). The cell-cycle regulated proliferating cell nuclear antigen is required for SV40 DNA replication in vitro. Nature *326*, 471-475.

Pursell, Z.F., Isoz, I., Lundstrom, E.B., Johansson, E., and Kunkel, T.A. (2007). Yeast DNA polymerase epsilon participates in leading-strand DNA replication. Science *317*, 127-130.
Ray Chaudhuri, A., Hashimoto, Y., Herrador, R., Neelsen, K.J., Fachinetti, D., Bermejo, R., Cocito, A., Costanzo, V., and Lopes, M. (2012). Topoisomerase I poisoning results in PARP-mediated replication fork reversal. Nat Struct Mol Biol *19*, 417-423.

Remus D, B.F., Tolun G, Griffith JD, Morris EP, Diffley JF. (2009). Concerted loading of Mcm2-7 double hexamers around DNA during DNA replication origin licensing. Cell *139*, 719-730.

San Filippo J, C.P., Sehorn MG, Etchin J, Krejci L, Sung P. (2006). Recombination mediator and Rad51 targeting activities of a human BRCA2 polypeptide. J Biol Chem *281*, 11649-11657.

Sawyer, S.L., Cheng, I.H., Chai, W., and Tye, B.K. (2004). Mcm10 and Cdc45 cooperate in origin activation in Saccharomyces cerevisiae. J Mol Biol *340*, 195-202.

Shrivastav M, D.H.L., Nickoloff JA. (2008). Regulation of DNA double-strand break repair pathway choice. Cell Res *18*, 134-147.

Stelter P1, U.H. (2003). Control of spontaneous and damage-induced mutagenesis by SUMO and ubiquitin conjugation. Nature *425*, 188-191.
Stillman, B. (2008). DNA polymerases at the replication fork in eukaryotes. Mol Cell *30*, 259-260.
Symington, L.S., and Gautier, J. (2011). Double-strand break end resection and repair pathway choice. Annu Rev Genet *45*, 247-271.

T. Ogi, Y.S., K. Tanaka, H. Ohmori (2002). Polkappa protects mammalian cells against the lethal and mutagenic effects of benzo[a]pyren. PNAS *99*, 15548-15553.

Takayama Y, K.Y., Okawa M, Muramatsu S, Sugino A, Araki H (2003). GINS, a novel multiprotein complex required for chromosomal DNA replication in budding yeast. . Genes Dev *17*, 1153-1165.

Takeda DY, D.A. (2005). DNA replication and progression through S phase.
Oncogene *24*, 2827-2843.

Thomas J. Kelly, G.W.B. (2000). Regulation of Chromosome Replication. Annual Review of Biochemistry *69*, 829-880.

Umar, A. (2004). Lynch syndrome (HNPCC) and microsatellite instability. Dis Markers *20*, 179-180.

Unk, I., Hajdu, I., Blastyak, A., and Haracska, L. (2010). Role of yeast Rad5 and its human orthologs, HLTF and SHPRH in DNA damage tolerance. DNA Repair (Amst) *9*, 257-267.
Unk I, H.I., Blastyák A, Haracska L. (2010). Role of yeast Rad5 and its human orthologs, HLTF and SHPRH in DNA damage tolerance.
DNA Repair (Amst) *9*, 257-267.

Vashee, S., Cvetic, C., Lu, W., Simancek, P., Kelly, T.J., and Walter, J.C. (2003). Sequence-independent DNA binding and replication initiation by the human origin recognition complex. Genes & Dev *17*, 1894-1908.

Wang L, L.C.M., Brooks S, Cimbora D, Groudine M, Aladjem M.I. (2004). The human beta-globin replication initiation region consists of two modular independent replicators. Mol Cell Biol *24*, 3373-3386.

Wu, Y. (2012). Unwiding and Rewinding: Double Faces of Helicase? Journal of Nucleic Acids Volume *2012*.

Xiao W, e.a. (2000). The Saccharomyces cerevisiae RAD6 group is composed of an error-prone and two error-free postreplication repair pathways. Genetics 155(4):1633-41. Genetics *155*, 1633-1641.

Yasuo Kawasaki, S.-i.H.a.A.S. (2001). Interactions between Mcm10p and other replication factors are required for proper initiation and elongation of chromosomal DNA replication in Saccharomyces cerevisiae. Genes to Cells *5*, 975-989.

Yuan, J., Ghosal, G., and Chen, J. (2012). The HARP-like domain-containing protein AH2/ZRANB3 binds to PCNA and participates in cellular response to replication stress. Mol Cell *47*, 410-421.

Yusufzai, T., and Kadonaga, J.T. (2010). Annealing helicase 2 (AH2), a DNA-rewinding motor with an HNH motif. Proc Natl Acad Sci U S A *107*, 20970-20973.

Yusufzai, T., Kadonaga, JT. (2008). HARP Is an ATP-Driven Annealing Helicase. . Science *31*, 748-750.

Yusufzai, T., Kong, X., Yokomori, K. and Kadonaga, JT. (2009). The annealing helicase HARP is recruited to DNA repair sites via an interaction with RPA. Genes and Development *23*, 2400-2404.

Zellweger R, D.D., Mutreja K, Berti M, Schmid JA, Herrador R, Vindigni A, Lopes M. (2015). Rad51-mediated replication fork reversal is a global response to genotoxic treatments in human cells. J Cell Biol *208*, 563-579.

Zeman MK, C.K. (2014). Causes and consequences of replication stress. Nat Cell Biol *16*, 2-9.

Zhu Z, C.W., Shim EY, Lee SE, Ira G (2008). Sgs1 helicase and two nucleases Dna2 and Exo1 resect DNA double-strand break ends. . Cell *134*, 981-994.